Government of Western Australia

Department of
Mines and Petroleum

REPORT
152

DETERMINING CRUSTAL ARCHITECTURE IN THE EAST ALBANY–FRASER OROGEN FROM GEOLOGICAL AND GEOPHYSICAL DATA

by LI Brisbout

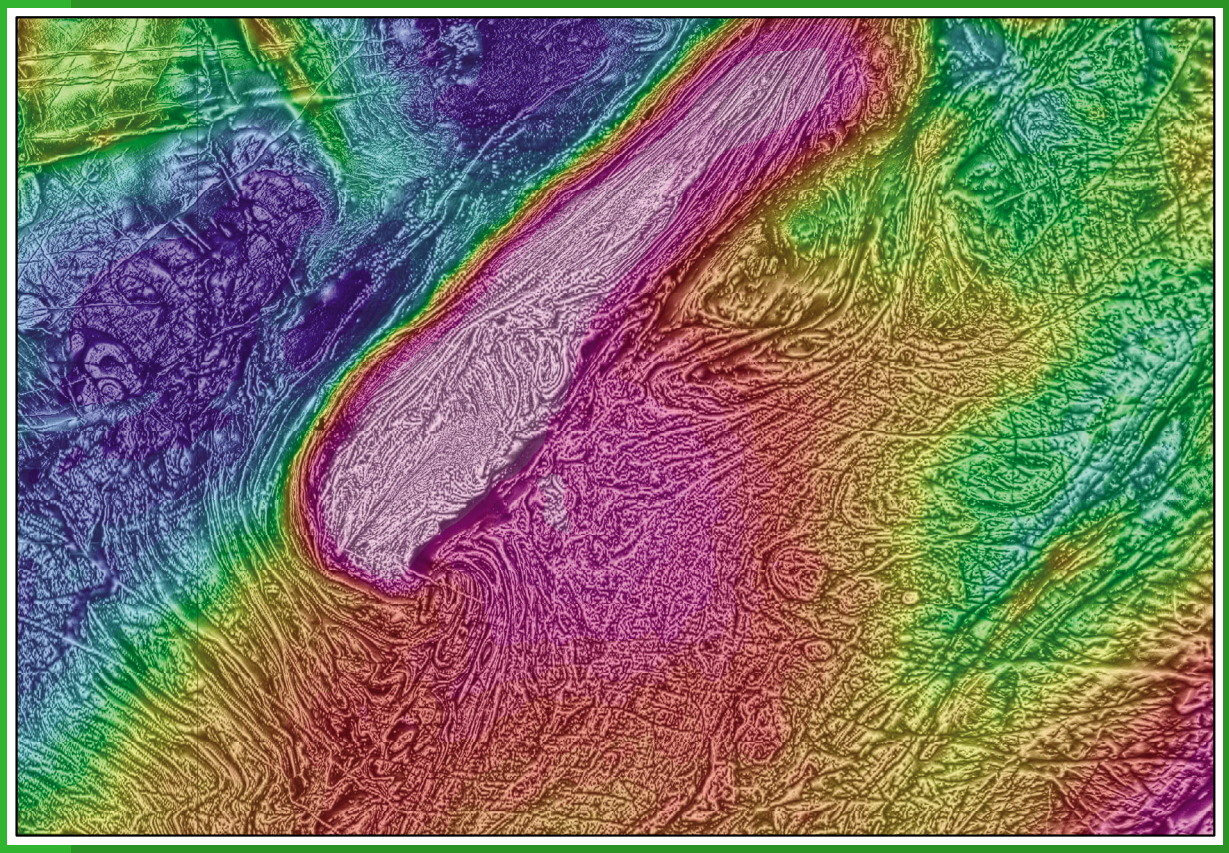

Geological Survey of Western Australia

Government of **Western Australia**
Department of **Mines and Petroleum**

REPORT 152

DETERMINING CRUSTAL ARCHITECTURE IN THE EAST ALBANY–FRASER OROGEN FROM GEOLOGICAL AND GEOPHYSICAL DATA

by
LI Brisbout

Perth 2015

Geological Survey of Western Australia

REFERENCE
The recommended reference for this publication is:
Brisbout, LI, 2015 Determining crustal architecture in the east Albany–Fraser Orogen from geological and geophysical data: Geological Survey of Western Australia, Report 152, 52p.

National Library of Australia Cataloguing-in-Publication entry:

Creator:	Brisbout, L.I., author.
Title:	Determining crustal architecture in the East Albany–Fraser Orogen from geological and geophysical data / LI Brisbout.
ISBN:	9781741686326 (ebook)
Subjects:	Geology, Structural--Western Australia--Albany Region. Orogeny--Western Australia--Albany Region.
Dewey Decimal Classification:	551.82

ISSN 1834–2280

Grid references in this publication refer to the Geocentric Datum of Australia 1994 (GDA94). Locations mentioned in the text are referenced using Map Grid Australia (MGA) coordinates, Zone 51. All locations are quoted to at least the nearest 100 m.

Copy editor: K Hawkins
Cartographer: A Symonds and M Prause
Desktop publisher: RL Hitchings

Published 2015 by Geological Survey of Western Australia
This Report is published in digital format (PDF) and is available online at <www.dmp.wa.gov.au/GSWApublications>.

Further details of geological publications and maps produced by the Geological Survey of Western Australia are available from:
Information Centre | Department of Mines and Petroleum | 100 Plain Street | EAST PERTH | WESTERN AUSTRALIA 6004
Telephone: +61 8 9222 3459 Facsimile: +61 8 9222 3444 **www.dmp.wa.gov.au/GSWApublications**

Cover photograph: Coloured Bouguer gravity image draped on grey-scale tilt-angle magnetic image, showing the southwest Fraser Zone

Contents

Appendices

Figures

Tables

Determining crustal architecture in the east Albany–Fraser Orogen from geological and geophysical data

by

LI Brisbout

Abstract

Structural analysis and forward modelling in the east Albany–Fraser Orogen has led to new interpretations of regional-scale structure and crustal architecture. The regional-scale map-view structures in the Mesoproterozoic, metagabbro-dominated Fraser Zone have been interpreted primarily from aeromagnetic data and include: (1) regional-scale, northeast-trending tight to isoclinal folds (~1.6 – 4.5 km in width); (2) regional-scale, north- to north-northwest-trending, tight to isoclinal folds (~6 km in width); (3) isoclinal folds (~500 m in width) truncated by northeast-trending shear zones; and (4) eye-shaped magnetic features, which can be interpreted either as doubly plunging antiforms or synforms, or as 'magnetic porphyroclasts'. Some of the structures that have been mapped in the Paleoproterozoic to Mesoproterozoic Nornalup Zone include: (1) north- and northeast-trending folds (~10 km in width); (2) tight folds (~3–6 km in width) truncated by northeast-trending shears; and (3) variably magnetic subcircular anomalies interpreted as plutons of the Esperance Supersuite. The results presented here suggest that in the study area, the regional structure of the Fraser and Nornalup Zones is dominated by northeast-trending folds and shear zones.

Two crustal-scale geologically and petrophysically constrained magnetic and gravity forward models were constructed along two northwest-trending profiles that traverse the east Albany–Fraser Orogen. Of these two profiles, only profile 2 traverses the mapped area described above. The Fraser Zone has been modelled with the median specific gravity of the Fraser Zone petrophysical samples (3 g/cm^3) and is interpreted as near-triangular, extending to depths of 12.4 km in profile 1 and 15.4 km in profile 2. The long wavelength Bouguer gravity anomaly to the southeast of the Fraser Zone in profile 2 is interpreted as a subhorizontal body of mafic–ultramafic material located in the middle crust. This body is possibly associated with the intrusion of the Fraser Zone gabbros and granites (1305–1290 Ma) during Stage I of the Albany–Fraser Orogeny, given that this is the only regional mafic intrusive event recognized in the Albany–Fraser Orogen. Where it is attributed the same density as the Fraser Zone, the interpreted mid-crustal body has a maximum thickness of 14.5 km. The near-triangular geometry of the Fraser Zone is consistent with the intrusion of the Fraser Zone gabbros and granites into a graben or half-graben, formed by the southeast-dipping Fraser Shear Zone and the northwest-dipping Newman Shear Zone. This is consistent with recent tectonic models of Stage I of the Albany–Fraser Orogeny, which suggest that gabbros and granites of the Fraser Zone were emplaced in an extensional tectonic setting, possibly an intracontinental rift or a distal back-arc.

KEYWORDS: crustal structure, geophysical interpretation, geophysical models, structural terranes

Introduction

This study uses the integrated analysis of aeromagnetic, gravity, and geological data to provide new interpretations (map-view and section-view) of crustal architecture in the east Albany–Fraser Orogen. The east Albany–Fraser Orogen lends itself to an integrated geological–geophysical method for several reasons: (1) large parts of the east Albany–Fraser Orogen are not exposed, making geophysical interpretation necessary; (2) despite this lack of outcrop, the study area is one of the better exposed parts of the eastern orogen, which allows some geological and petrophysical constraints for geophysical interpretations; (3) high-resolution aeromagnetic (<400 m line spacing) and gravity (~2.5 km gravity station spacing) data are available; and (4) the tectonic zones of the Albany–Fraser Orogen contain considerable magnetic and density variations. More specifically, the diverse magnetic properties of the Paleoproterozoic to Mesoproterozoic Nornalup and Fraser Zones allow the regional structural trends of the Fraser Zone and the regional structural and magmatic trends of the Nornalup Zone to be mapped from aeromagnetic images. The metagabbro-dominated Fraser Zone also forms a distinct gravity high, which allows the geometry of this zone in section-view to be determined from geologically and petrophysically constrained forward modelling of magnetic and gravity data. The structures and geometries presented in this study, particularly in the Fraser and Nornalup Zones, will contribute to improving structural and tectonic models of the Albany–Fraser Orogen.

Regional geology

The Albany–Fraser Orogen is a Proterozoic orogenic belt that lies along the southern and southeastern margin of the Archean Yilgarn Craton (Fig. 1). The orogen is divided into two tectonic components: the dominantly Archean Northern Foreland and the dominantly Proterozoic Kepa Kurl Booya Province. This province is further subdivided into the dominantly Paleoproterozoic Biranup and Nornalup Zones, and the Mesoproterozoic Fraser Zone (Fig. 1). The Albany–Fraser Orogen contains two recognized Mesoproterozoic supersuites, the Recherche and Esperance Supersuites, which dominantly intrude the Nornalup Zone. The orogen also contains metasedimentary rocks from the Paleoproterozoic Barren Basin and the Mesoproterozoic Arid and Ragged Basins (Spaggiari et al., 2011).

Tectonic units

The Northern Foreland is an east- to northeast-trending unit that is separated from the Yilgarn Craton by the linked Jerdacuttup–Cundeelee Fault (Fig. 1) and is defined as the southern portion of the Yilgarn Craton that has been reworked during the Biranup and Albany–Fraser Orogenies (Myers, 1990a; Spaggiari et al., 2009; Spaggiari et al., 2011). The Northern Foreland is composed of greenschist to granulite facies Archean granites and greenstones that have been extensively intruded by the Gnowangerup–Fraser Dyke Suite (Myers, 1990b; Wingate et al., 2000; Spaggiari et al., 2009). The Northern Foreland also contains several intrusions of Paleoproterozoic granite, and one known intrusion of Mesoproterozoic Recherche Supersuite (Nelson et al., 1995; Spaggiari and Pawley, 2012).

The Barren Basin is composed of metasedimentary rocks that were deposited in the Paleoproterozoic, prior to and during the Biranup Orogeny (Spaggiari et al., 2014a). The Barren Basin units in the study area include the Woodline and Fly Dam Formations. The Woodline Formation comprises lower greenschist facies, quartz-rich sandstone interbedded with siltstone, and unconformably overlies the Yilgarn Craton basement (Hall et al., 2008). The Fly Dam Formation comprises amphibolite to granulite facies, interlayered psammitic to semipelitic gneiss, and forms part of the Biranup Zone (Spaggiari and Pawley, 2012). In addition to these named units, rafts of metasedimentary rocks exist throughout the Biranup and Nornalup Zones and are interpreted as remnants of a previously continuous basin that formed on the Yilgarn Craton margin during the Paleoproterozoic (Hall et al., 2008).

The Biranup Zone (Fig. 1) forms an east- to northeast-trending unit that in the east of the orogen is separated from the Northern Foreland by the Frog Dam Shear Zone. The Paleoproterozoic Biranup Zone is dominated by intensely deformed amphibolite to granulite facies orthogneiss, paragneiss, and metagabbro (Spaggiari et al., 2011). Igneous rocks of the Biranup Zone have Paleoproterozoic magmatic crystallization ages (1815–1650 Ma), with the majority emplaced during the 1710–1650 Ma Biranup Orogeny (Kirkland et al., 2011a,b; Spaggiari et al., 2011). The presence of Archean rocks within the Biranup Zone (Spaggiari et al., 2011) and magmatic zircon hafnium isotope data (Kirkland et al., 2011b) suggest that magmas of the Biranup Zone intruded the Yilgarn Craton crust.

The Fraser Zone (Fig. 1) forms a distinct, 425 km-long by 50 km-wide gravity high in the east Albany–Fraser Orogen (Spaggiari et al., 2011). To the northwest, the Fraser Zone is separated from the Biranup Zone by the Fraser Shear Zone, and to the southeast it is separated from the Nornalup Zone by the Newman Shear Zone. The Fraser Zone includes the 1305–1290 Ma Fraser Range Metamorphics, which outcrop in the southwest of the Fraser Zone and which comprise sheeted amphibolite to granulite facies metagabbro, metagranite, and metasedimentary rocks (Spaggiari et al., 2011). Fraser Zone metasedimentary rocks comprise pelitic, semipelitic, and locally, calc-silicate gneisses (Oorschot, 2011; Spaggiari et al., 2011). The metasedimentary rocks of the Fraser Zone are part of the Mesoproterozoic Arid Basin and were deposited between c. 1450 and 1305 Ma, just prior to and during Stage I of the Albany–Fraser Orogeny (Clark et al., 2014). Other units of the Arid Basin include the Malcolm Metamorphics, which comprise mafic amphibolitic schists and minor calc-silicate rocks that may have volcanic precursors, and the Gwynne Creek Gneiss, which comprises psammitic and semipelitic gneisses and minor metagranitic, metamafic, and meta-ultramafic rocks (Spaggiari et al., 2011).

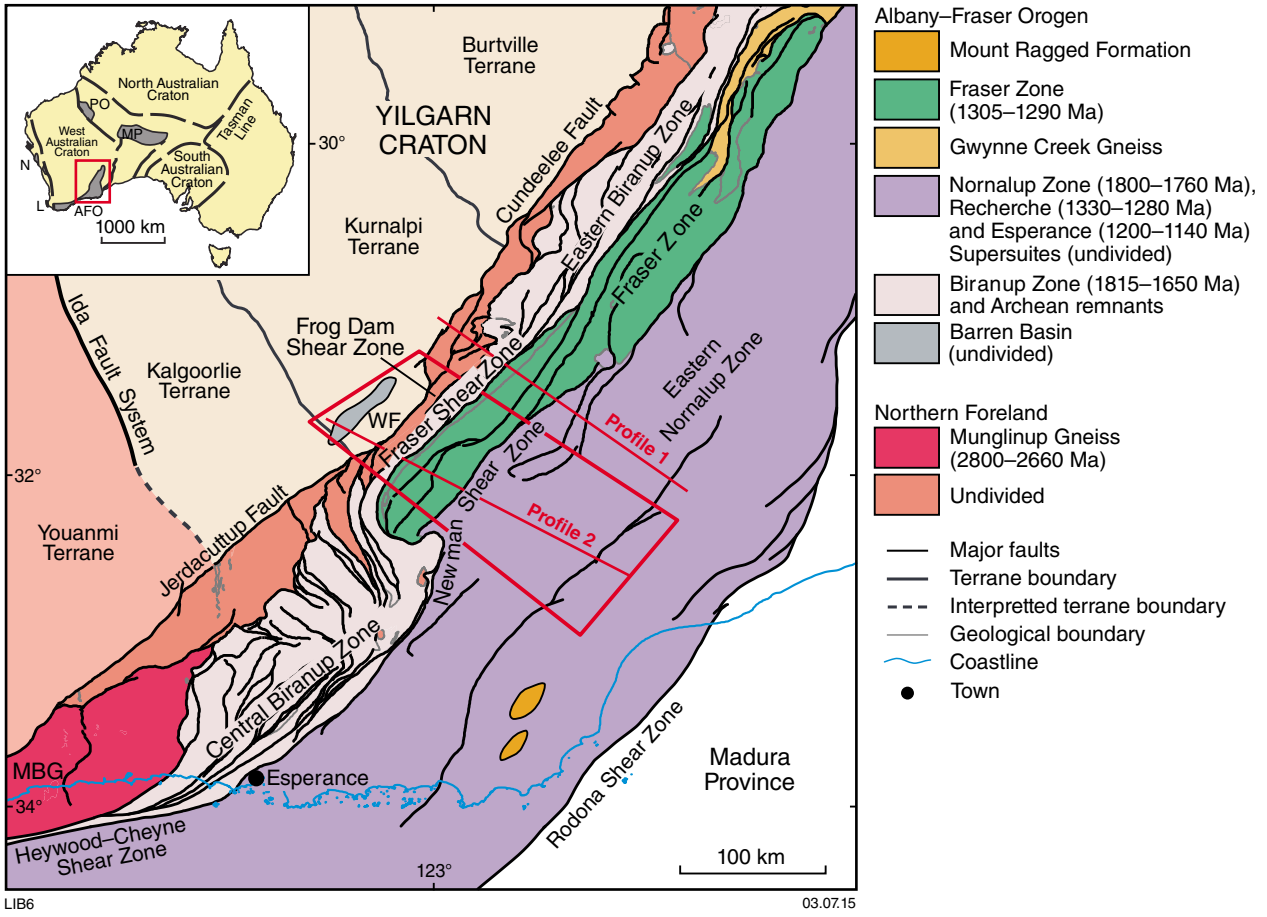

Figure 1. Simplified bedrock geology of the east Albany–Fraser Orogen (AFO) (after Spaggiari et al., 2011) showing the study area and locations of forward modelled profiles 1 and 2. MBG, Mount Barren Group; WF, Woodline Formation; PO, Paterson Orogen; MP, Musgrave Province; N, Northampton Province; L, Leeuwin Province

During Stage I of the Albany–Fraser Orogeny, metasedimentary rocks of the Fraser Zone were intruded by mafic and felsic igneous rocks (Spaggiari et al., 2011; Fig. 2). The metasedimentary rocks of the Fraser Zone preserve c. 1290 Ma (Stage I) peak metamorphic conditions of 800–850°C and 8–9 kbar, equivalent to depths of 22–25 km (Clark et al., 2014). The high-temperature metamorphism of the Arid Basin metasedimentary rocks is attributed to a regional thermal anomaly produced by the Fraser Zone mafic magmatism (Clark et al., 2014). A Fraser Zone gabbronorite is reported to have cooled beneath the Rb–Sr biotite closure temperature (~400°C) late in Stage I (1268 ± 30 Ma) (Fletcher et al., 1991), suggesting that sediment deposition, burial, high-temperature metamorphism, and cooling below the solidus occurred in less than 25 Ma (Fletcher et al., 1991; Clark et al., 1999, 2014).

Hafnium isotope data and trace element geochemistry suggest that the Fraser Zone intruded into a basement that included a Sr-depleted component of Archean or reworked Archean crust (Kirkland et al., 2011b; Smithies et al., 2013).

The Nornalup Zone is the most southerly unit of the Albany–Fraser Orogen and extends as far east as the Madura Province, which it is separated from by the Rodona Shear Zone (Spaggiari et al., 2011, 2012). The Nornalup Zone contains Paleoproterozoic granites that have been extensively intruded by the Mesoproterozoic Recherche and Esperance Supersuites (Spaggiari et al., 2011). The Recherche Supersuite (1330–1280 Ma) was emplaced during Stage I of the Albany–Fraser Orogeny and is dominated by amphibolite–granulite facies syenogranite, monzogranite, and granodiorite, and lesser amounts of comagmatic intermediate and mafic intrusives (Myers, 1995; Nelson et al., 1995; Spaggiari et al., 2011; Smithies et al., 2013, 2014). The Esperance Supersuite (1200–1140 Ma) was emplaced during Stage II of the Albany–Fraser Orogeny and is dominated by greenschist–amphibolite facies metagranite that includes highly magnetic phases (Myers, 1995; Spaggiari et al., 2011, 2014c). Distinguishing Paleoproterozoic metagranites from Recherche Supersuite metagranites without geochronology is difficult because both have potentially undergone high-temperature metamorphism and deformation during either or both Stages I and II of the Albany–Fraser Orogeny.

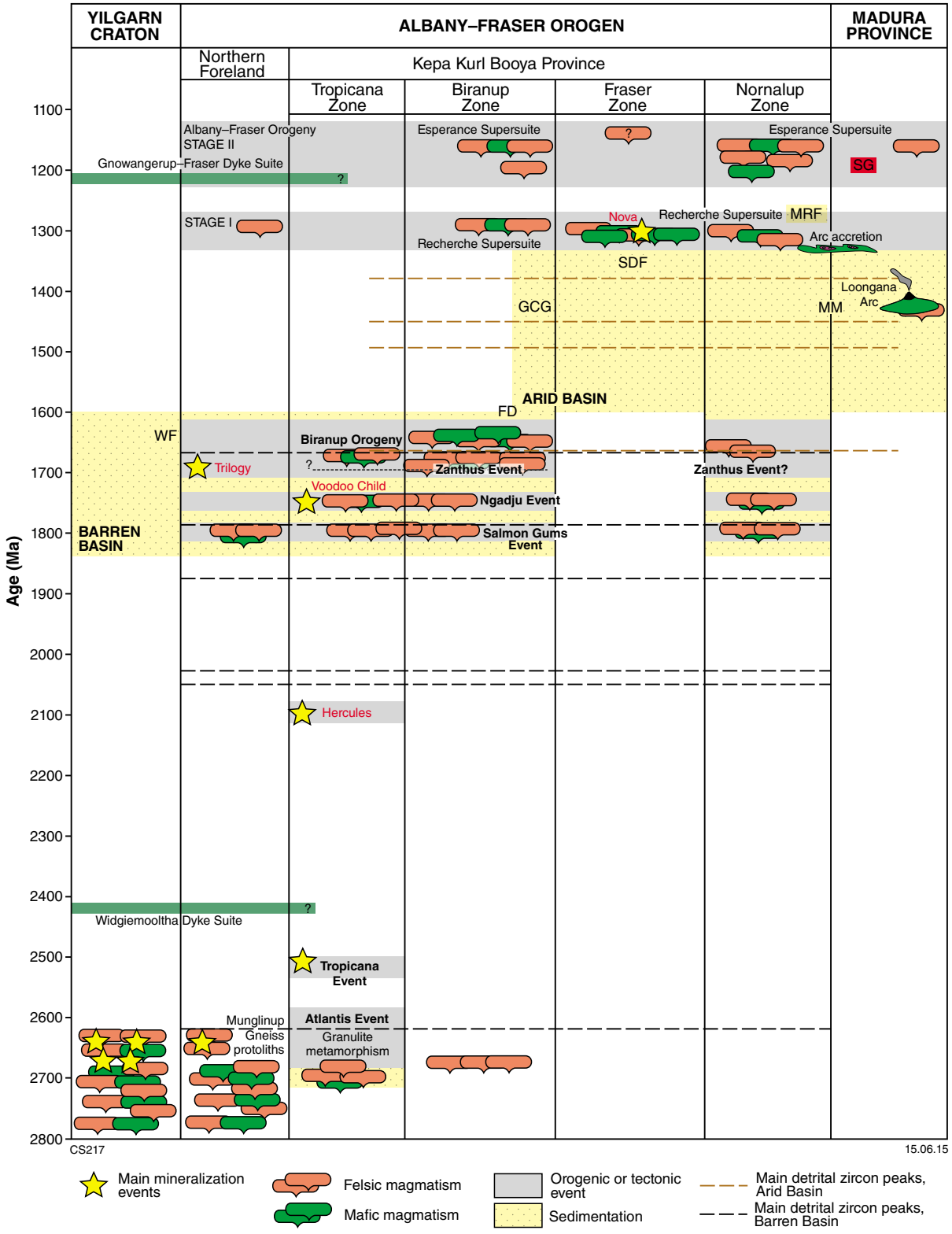

Figure 2. Time–space plot of the Albany–Fraser Orogen and Madura Province (from Spaggiari et al., 2014c). SG, Salisbury Gneiss; MM, Malcolm Metamorphics, MRF, Mount Ragged Formation; SDF, Snowys Dam Formation; GCG, Gwynne Creek Gneiss; FD, Fly Dam Formation

Tectonic events

In the Albany–Fraser Orogen, magmatism and basin formation are closely related to the recognized tectonic events. The earliest orogenic event recognized in the Albany–Fraser Orogen is the Paleoproterozoic Biranup Orogeny (1710–1650 Ma), which occurred shortly after the magmatic Salmon Gums (1815–1800 Ma) and Ngadju Events (1780–1760 Ma) (Spaggiari et al., 2014a). The Biranup Orogeny was accompanied by the magmatism that formed the majority of the Biranup Zone and includes the compressional Zanthus Event (c. 1680 Ma; Fig. 2), which produced northwest-trending isoclinal folds (Kirkland et al., 2011a, b). Given the presence of Archean rocks in the Biranup Zone (Spaggiari et al., 2011) and magmatic zircon hafnium isotope data that suggest the Biranup Zone contains both Yilgarn Craton-like and juvenile craton crust (Kirkland et al., 2011b), the Biranup Zone is provisionally interpreted to have formed in a continental rift or back-arc setting (Kirkland et al., 2011b).

The Mesoproterozoic Albany–Fraser Orogeny is divided into Stage I (1345–1260 Ma) and Stage II (1215–1140 Ma) (Clark et al., 2000; Kirkland et al., 2011a, b) (Fig. 2). Stage I was accompanied by the mafic and felsic magmatism that formed the igneous rocks of the Fraser Zone and Recherche Supersuite (Fig. 2). Clark et al. (2000) report that Stage I deformation in the eastern Nornalup Zone included: (1) 1330–1310 Ma recumbent folds and an axial planar foliation, produced under granulite facies conditions; and (2) late Stage I, or possibly early Stage II, open folds with steeply southeast-dipping axial planes that formed under amphibolite facies conditions. In the central Nornalup Zone, within the Coramup Shear Zone, Stage I deformation included: (1) c. 1300 Ma planar gneissic layering that was produced under granulite facies conditions and interpreted to have formed in an extensional setting; and (2) c. 1290 Ma tight, recumbent folds, with shallowly southeast-dipping axial planes, interpreted to indicate northwest-directed thrusting, and an axial planar foliation (Bodorkos and Clark, 2004).

Stage I of the Albany–Fraser Orogeny has previously been interpreted to record continent–continent collision between the West Australian Craton and the Mawson Craton (Myers et al., 1996; Clark et al., 2000; Bodorkos and Clark, 2004). In a recent tectonic model, Spaggiari et al. (2014a) proposed that Stage I marked the end of east-dipping ocean–ocean subduction beneath the c. 1410 Ma Loongana oceanic–magmatic arc, and the soft collision and westward accretion of the Loongana arc onto the passive margin of the Albany–Fraser Orogen. Following the accretion of the Loongana oceanic–magmatic arc, it has been proposed that the Albany–Fraser Orogen continued to converge with the western Madura Province, accommodated by the west-dipping subduction of oceanic crust of the western Madura Province (Spaggiari et al., 2014a). West-dipping subduction beneath the Albany–Fraser Orogen – Madura Province resulted in slab rollback and the formation of an extensional back-arc in the Albany–Fraser Orogen (c. 1300 Ma), into which the Fraser Zone gabbros and granites, and the Recherche Supersuite intruded (Spaggiari et al., 2014a).

Stage II of the Albany–Fraser Orogeny (1215–1140 Ma) is the dominant high-temperature metamorphic event preserved in all tectonic units of the Albany–Fraser Orogen, with the exception of the Fraser Zone (Fig. 2; Clark et al., 2000; Bodorkos and Clark, 2004; Kirkland et al., 2011a, b). In the eastern orogen, Stage II deformation in the Recherche Supersuite is reported to include northeast-trending southeast side-up thrust zones that have been reactivated by dextral shearing under greenschist to amphibolite facies conditions (Clark et al., 2000). Similar Stage II kinematics have been reported within the Coramup Shear Zone. In the central Nornalup Zone, dextral transpression under granulite facies conditions is interpreted to have been compartmentalized into pure shear, characterized by subvertical, southeast-dipping fold axial planes, and dextral simple shear, characterized by subvertical, southeast-dipping shear zones parallel to fold axial planes (Bodorkos and Clark, 2004). At c. 1180 Ma, in the eastern Biranup Zone, Stage II shortening and shear-related folding are reported to alternate with mid- to lower crustal, bidirectional, northwest and northeast extension (Bodorkos and Clark, 2004; Barquero-Molina, 2010).

Stage II of the Albany–Fraser Orogeny has been interpreted to record the intracratonic reactivation of the orogen (Clark et al., 2000; Bodorkos and Clark, 2004) or final continent–continent collision which, because of the asymmetrically shaped ocean between the West Australian and Mawson Cratons, is interpreted to have occurred in the east during Stage I and in the west during Stage II (Bodorkos and Clark, 2004; Barquero-Molina, 2010).

Petrophysical data

Method

Specific gravity and magnetic susceptibility data have been collected for the east Albany–Fraser Orogen. This dataset has been used to constrain map-view interpretations of aeromagnetic and gravity data and, in particular, the physical properties assigned to magnetic and gravity forward models.

The density of samples was determined by calculating the specific gravity, a unitless ratio of the density of the sample to the density of water. Specific gravity, which does not account for rock porosity, is considered a reasonable measure of the density of the dominantly crystalline Albany–Fraser Orogen samples. Specific gravity samples include hand and drillcore samples retrieved from the GSWA archive and hand samples collected during fieldwork. The specific gravity (SG) values of 231 samples from the east Albany–Fraser Orogen were calculated using the equation:

$$SG = weight_{dry} / (weight_{dry} - weight_{wet})$$

Dry samples were weighed on a bench-top balance to a precision of 0.1g. Wet weights were obtained by placing the samples in a wire basket and weighing the sample while submerged in water.

In addition to specific gravity data, 464 magnetic susceptibility measurements were compiled. Susceptibility data collected during this study include measurements made on archived GSWA hand and drillcore samples, and measurements made on outcrop during fieldwork. This dataset has been compiled with susceptibility data collected from outcrop by other GSWA workers.

All magnetic susceptibilities were measured with a handheld GMS-2 magnetic susceptibility meter to a precision of 1×10^{-5} SI. The average susceptibility of outcrop and hand samples was calculated as the average of five measurements made on five apparently representative and relatively unweathered surfaces. Susceptibilities are reported in units of (1×10^{-5}) $\log_{10}$ SI.

For analysis, petrophysical data were divided into the following tectonic units: Northern Foreland, eastern Biranup Zone, Fraser Zone, eastern Nornalup Zone (which includes Paleoproterozoic rocks and the Mesoproterozoic Recherche Supersuite), Esperance Supersuite, and Barren Basin. Because of the low number of Northern Foreland samples in the east Albany–Fraser Orogen, 14 susceptibility samples and 13 specific gravity samples from the central part of the orogen were included in the analysis. Because of the difficulty in distinguishing the eastern Nornalup Zone Paleoproterozoic metagranites from Recherche Supersuite metagranites, with the exception of a few dated samples, these samples are considered together. Included in the Barren Basin are samples from the Eddy Suite, Fly Dam Formation, and Woodline Formation.

Data for each tectonic unit are further divided into five lithological groups: (1) mafic intrusive; (2) intermediate intrusive; (3) felsic intrusive; (4) metasedimentary rocks; and (5) felsic rocks of unknown protolith. Petrophysical data are presented in stacked histograms, with different lithological groups represented by different colours (Fig. 3). Data are summarized in box and whisker plots, which show the minimum, maximum, lower quartile, upper quartile, and median values for specific gravity (Fig. 4) and magnetic susceptibility (Fig. 5). Specific gravity and magnetic susceptibility data statistics, which are used to constrain forward modelling, are presented in Table 1. A summary of the petrophysical data is given below, and detailed descriptions are in Appendix 1.

Summary of results

Specific gravity

In the east Albany–Fraser Orogen petrophysical dataset, specific gravity is typically determined by rock type (felsic, mafic, and metasedimentary rock) regardless of tectonic unit. Overall, mafic intrusives have higher specific gravities than felsic intrusives and metasedimentary rocks, and intermediate intrusives and hybridized metagabbroic–metagranitic rocks occupy the lower tail of the mafic intrusive distribution (Fig. 3). An exception to this general trend includes a sample of serpentinized schist from the Northern Foreland, which has an exceptionally low specific gravity, lower even than the felsic intrusives (Fig. 3a). Other exceptions from the Fraser Zone include a high-density metagranite sample, which is most likely hybridized (Fig. 3k), and a low-density mafic pegmatite (Fig. 3m). The Fraser Zone also contains several mafic amphibolite and metagabbro samples with very high specific gravity (Fig. 3m).

Metasedimentary rocks of the Barren (Paleoproterozoic) and Arid (Mesoproterozoic) Basins have similar specific gravity distributions (Fig. 3c and k respectively). The distribution of metasedimentary rocks overlaps considerably with the distributions of felsic intrusives although typically, metasedimentary rocks have higher mean specific gravities and greater variability than felsic intrusives. Both the Barren and Arid Basin distributions contain several samples with very high specific gravity. The Barren Basin samples include a metamorphic iron formation and a metasandstone (Fig. 3c). Arid Basin samples include a semipelitic gneiss and an iron-rich metasedimentary rock (Fig. 3k). In both the Barren and Arid Basins there is no clear relationship between the type of metasedimentary rock and specific gravity.

Given that specific gravity is largely determined by rock type, the average specific gravity of a tectonic unit is largely determined by the proportion of mafic and felsic samples (Fig. 4). For example, the Fraser Zone contains more mafic intrusive samples than the eastern Biranup and Nornalup Zones and therefore has a higher specific gravity (Fig. 4b). The eastern Nornalup Zone, which includes the dominantly felsic Recherche Supersuite samples, has a lower specific gravity than the eastern Biranup Zone (Fig. 4b).

Magnetic susceptibility

In the east Albany–Fraser Orogen petrophysical dataset most lithological groups have bimodal magnetic susceptibility distributions, which contain susceptible and non-susceptible subpopulations (Fig. 3). For analysis the mean and median of these bimodal populations have been determined (Table 1). Although the mean and median are not representative of either of these subpopulations, they do provide values that can be used to constrain the susceptibilities used in forward modelling. Some of the characteristics of the magnetic susceptibility dataset are described below.

The Northern Foreland has a small number of felsic intrusive samples that form roughly equal subpopulations of non-susceptible and weakly to moderately susceptible samples (Fig. 3b). The Barren Basin samples are divided where possible into formations. Of these, the Fly Dam Formation and the undivided Barren Basin samples have bimodal subpopulations. The three samples of Woodline Formation and the one sample of the Eddy Suite are non-susceptible (Fig. 3d). This dataset suggests that it might be possible to distinguish the units of the Barren Basin by their susceptibility. Mapping rafts of Barren Basin metasedimentary rocks in the Biranup and Nornalup Zones, however, is complicated by the presence of susceptible and non-susceptible mafic and felsic intrusives in both of these zones.

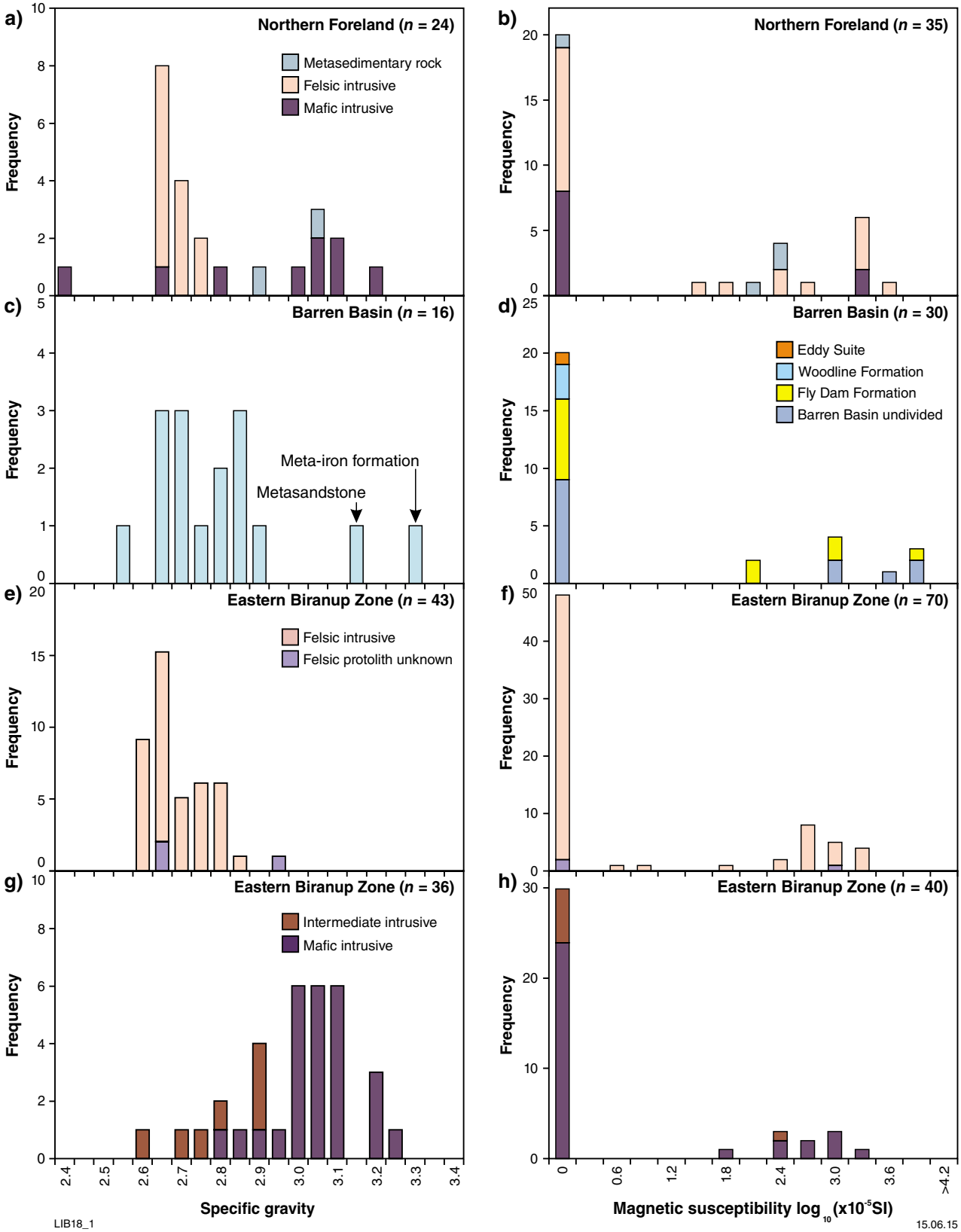

Figure 3. Northern Foreland petrophysical data: a) specific gravity; b) magnetic susceptibility. Barren Basin: c) specific gravity; d) magnetic susceptibility. Eastern Biranup Zone: e) felsic intrusive and metasedimentary rock specific gravity data; f) felsic intrusive and metasedimentary rock magnetic susceptibility data; g) mafic and intermediate intrusive specific gravity data; h) mafic and intermediate intrusive magnetic susceptibility data. Nornalup Zone and Recherche Supersuite: i) specific gravity; j) magnetic susceptibility. Fraser Zone: k) felsic intrusive and metasedimentary rock specific gravity data; l) felsic intrusive and metasedimentary rock magnetic susceptibility data; m) mafic intrusive and hybridized mafic intrusive specific gravity data; n) mafic intrusive and hybridized mafic intrusive magnetic susceptibility data. Esperance Supersuite: o) specific gravity; p) magnetic susceptibility (continued p. 8)

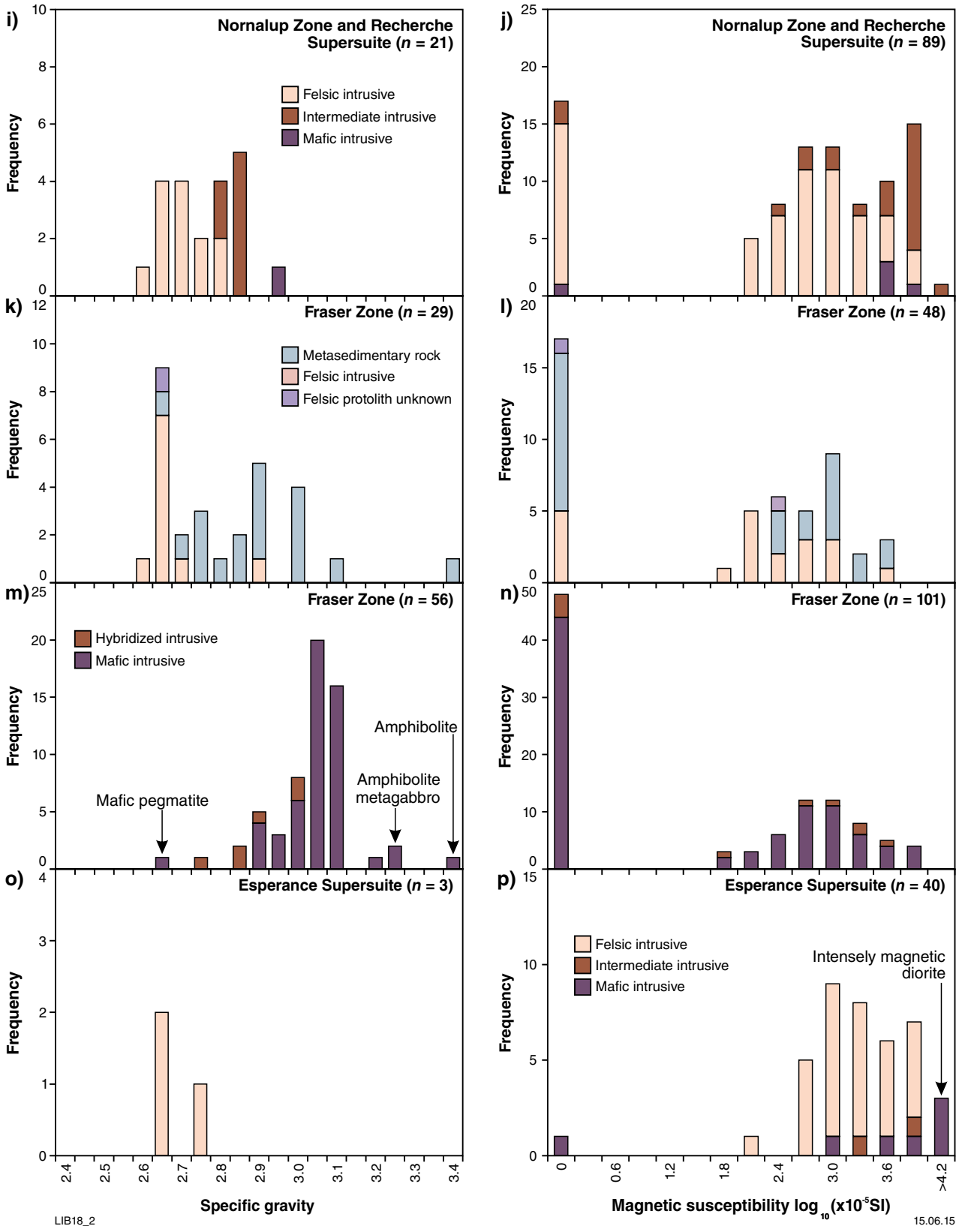

Figure 3. continued

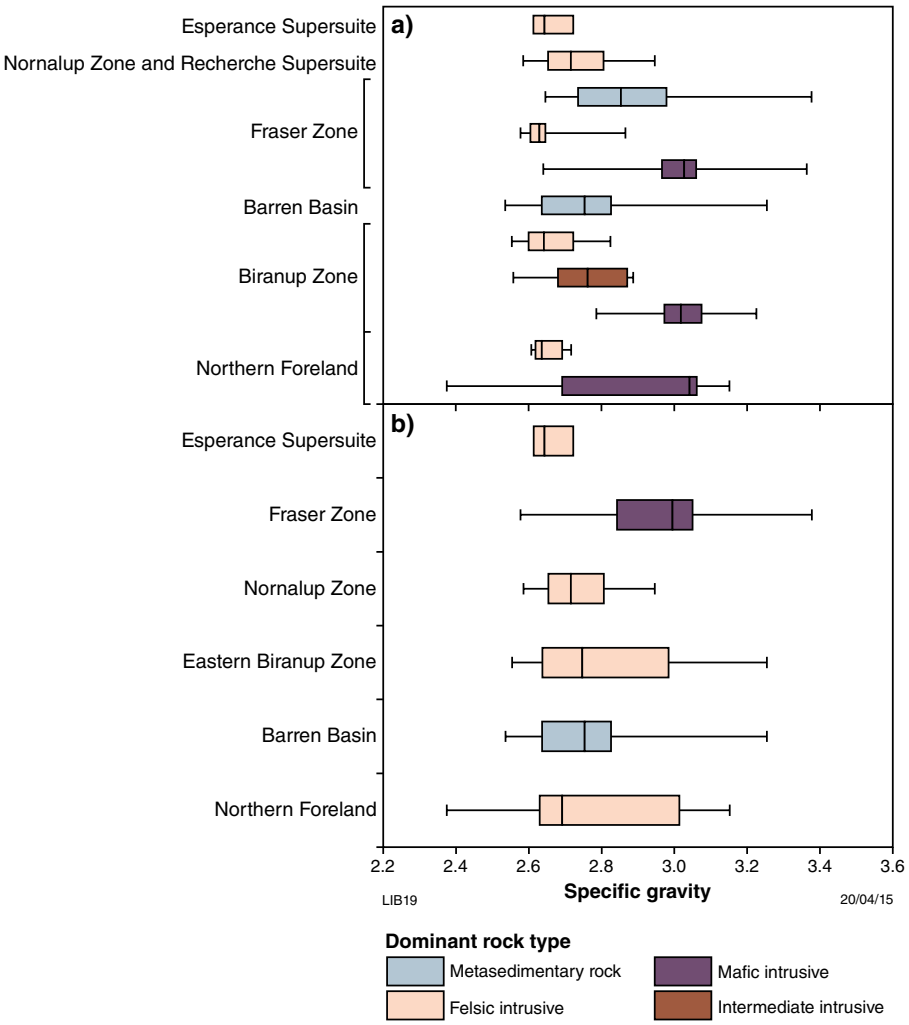

Figure 4. Box and whisker plots showing the minimum, lower quartile, median, upper quartile, and maximum specific gravity for: a) lithological groups in tectonic units; b) tectonic units

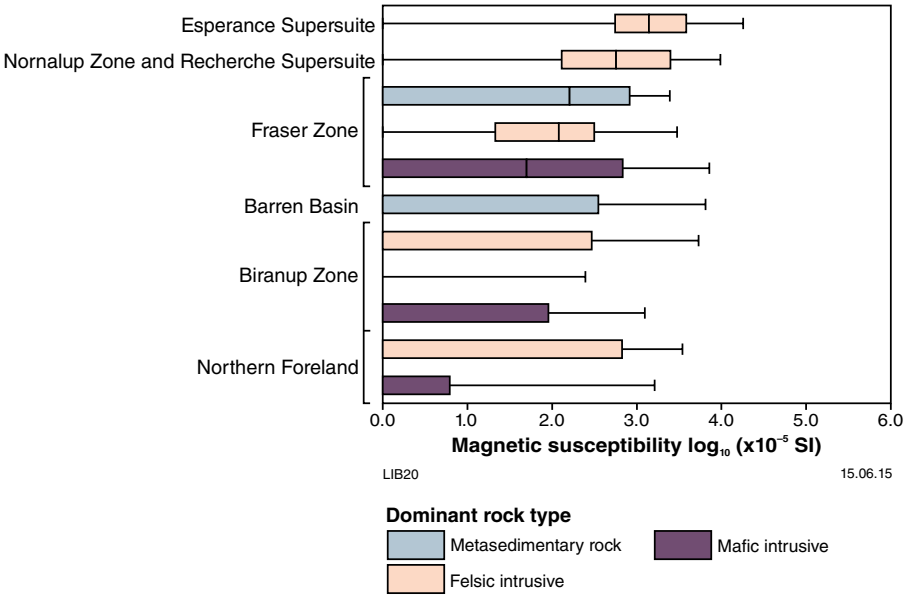

Figure 5. Box and whisker plot showing the minimum, lower quartile, median, upper quartile and maximum magnetic susceptibility for tectonic units

Table 1. Summary of magnetic susceptibility and specific gravity measurements by tectonic unit and rock type

Tectonic unit or basin	*Lithology*	*Specific gravity*			*Magnetic susceptibility (×10^{-5})*					
		Number	*Mean ± SD*	*Median*	*Number*	*Mean ± SD*	*Median*	*Geometric mean (log_{10})*	*Min.*	*Max.*
Northern Foreland	Mafic intrusives	9	2.901 ± 0.259	3.042	10	309.6 ± 654	0	0.638	0	1623
	Felsic intrusives	13	2.653 ± 0.037	2.636	21	505.1 ± 930	0	1.258	0	3463
	All samples (incl. metasedimetary rocks)	24	2.770 ± 0.204	2.692	35	403.2 ± 801	0	1.118	0	3463
Barren Basin	Metasedimentary rocks	16	2.771 ± 0.187	2.754	30	753.8 ± 1717	0	0.005	0	6500
Eastern Biranup Zone	Mafic intrusives	26	3.023 ± 0.102	3.018	33	145.1 ± 314	0	0.702	0	1250
	Intermediate intrusives	7	2.763 ± 0.122	2.762	7	35.2 ± 93	0	0.342	0	246.4
	Felsic intrusives	40	2.664 ± 0.074	2.642	67	184.4 ± 395	0	0.776	0	1750
	All samples (incl. metamorphic rocks of unknown protolith)	76	2.799 ± 0.188	2.747	110	163.3 ± 357	0	0.730	0	1750
Nornalup Zone and Recherche Suite	Felsic, mafic, and intermediate intrusives	21	2.733 ± 0.091	2.716	89	1732.1 ± 2725	678	2.405	0	9721
	All samples (incl. Esperance Supersuite)	24	2.723 ± 0.090	2.714	129	1933 ± 2635	875	2.625	0	18050
Fraser Zone	Mafic intrusives (including hybrids)	60	3.010 ± 0.111	3.027	101	642.2 ± 1366	50	1.453	0	7224
	Felsic intrusives	10	2.646 ± 0.081	2.629	20	328.8 ± 659	120	1.774	0	3000
	Arid Basin metasedimentary rocks	18	2.872 ± 0.173	2.853	26	486.1 ± 652	164	1.608	0	2454
	All samples (incl. metamorphic rocks of unknown protolith)	89	2.937 ± 0.173	2.995	149	565.4 ± 1185	100	1.519	0	7224
Esperance Supersuite	Felsic and intermediate intrusives	3	2.660 ± 0.056	2.643	40	2823.8 ± 3541	1406	3.115	0	18050

The eastern Biranup Zone dataset is dominated by non-susceptible samples, although it does contain a small number of mafic and felsic samples with weak to moderate susceptibilities (Fig. 3f,h). The Nornalup Zone samples are composed largely of metagranitic Recherche Supersuite samples, and have a susceptibility distribution dominated by moderately to highly susceptible samples (Fig. 3j). The two known Paleoproterozoic samples are both migmatitic gneisses, one sampled from the Newman Rock in the Newman Shear Zone and the other east of Boingaring Rocks, and both have high specific gravities and moderate susceptibilities. Based on this very small sample set, it might be possible, in the Nornalup Zone, to distinguish Paleoproterozoic metagranites by their higher density and susceptibility.

The felsic, mafic, and metasedimentary rocks of the Fraser Zone have almost equal numbers of susceptible and non-susceptible samples and the susceptible populations have very similar distributions (Fig. 3l,n). Aeromagnetic images of the Fraser Zone typically show linear, high-, and low-intensity magnetic horizons. The susceptibility data compiled here suggest that the source of the magnetic highs in the Fraser Zone could be felsic, mafic, or metasedimentary rocks. In the metasedimentary rocks of the Fraser Zone (Arid Basin) there is no clear relationship between rock type (e.g. psammitic gneiss vs semipelitic gneiss) and susceptibility.

The Esperance Supersuite is the only geological unit to have a near-unimodal distribution of moderately to highly susceptible samples (Fig. 3p). This distribution is very similar to the distribution of Nornalup Zone samples, with the exception of an intensely magnetic diorite, intersected in diamond drillcore and reverse circulation chips by Enterprise Metals NL (Fig. 3p).

Data used for mapping and modelling

Geological information

Geological information used in this study includes a 1:250 000 scale interpreted bedrock geology map of the east Albany–Fraser Orogen (Spaggiari and Pawley, 2012), 1:100 000 scale surface geology maps (Erayinia, Yardilla, and Yardina), which are available in the northwest of the study area, 1:250 000 scale surface geology maps (Widgiemooltha, Norseman, Balladonia, and Zanthus), which cover the entire study area, and the GSWA field observation database (WAROX), which includes lithological and structural information. In addition to these maps and datasets are new field observations made during this study. The interpreted bedrock geology map of Spaggiari and Pawley (2012; Fig. 6) forms the framework of this study and has been used to provide information on the surface locations of tectonic units and major structures. The surface geology maps and WAROX data have been used primarily to provide structural information, which has been used to constrain the orientations of regional-scale structures interpreted from aeromagnetic images.

Aeromagnetic and gravity data

The geophysical datasets used in this study include high-resolution aeromagnetic data downloaded from GSWA's MAGIX database. Aeromagnetic data used in this study comprise 16 airborne surveys with flight line spacing of 50–400 m (Fig. 7a). Aeromagnetic surveys have flight line-directions of 90 to 180°, with the majority at 90° (aeromagnetic survey details are provided in Appendix 2). Total magnetic intensity datasets have been merged in Intrepid software and gridded to a cell size of 75 m. Gridded aeromagnetic data were reduced to the pole (RTP) (Baranov, 1957) to locate magnetic anomalies above their causative bodies, and enhanced by geophysical filters including the first vertical derivative (1VD), horizontal derivative, tilt derivative, analytic signal, and upward continuation (images of some of these geophysical datasets are shown in Fig. 8a–c).

Gravity data were downloaded from the Geophysical Archive Data Delivery System at <www.geoscience.gov.au/gadds> and comprise several land- and helicopter-based surveys. Gravity surveys cover the study area in approximately 2.5 and 5 km-spaced grids and include several higher resolution surveys and transects (Fig. 7b). Bouguer gravity data (Fig. 8d) have been terrain corrected by applying the spherical cap approximation, gridded to 400 m cell size and enhanced by application of 1VD and upward continuation.

Map-view structural interpretation

Method

Aeromagnetic and gravity image interpretation along with field-based structural observations were used to construct a regional-scale map-view structural interpretation of the study area (Fig. 9). Where possible, the tectonic subdivisions of Spaggiari and Pawley (2012) have been divided into structural domains that define regions with distinct structural and magmatic trends and which are typically bound by major structures (Fig. 10a). Where domains contain internal structural variation they have been further divided into subdomains, some separated by structures and others with more continuous boundaries. Some of the structures that have been mapped are described in more detail below (Fig. 10b).

In this study, aeromagnetic images form the primary dataset used to interpret regional-scale structural and magmatic trends. Aeromagnetic images provide information on the lateral magnetization contrasts in the top approximately 20 km of crust. The texture of magnetic images (e.g. mottled, smooth) commonly reflects the distribution of magnetite in rocks (Betts et al., 2003). The distribution of magnetite in rocks is influenced by both primary (e.g. in igneous rocks, primary fractionation and cooling history) and secondary processes (e.g. metamorphism) (Isles and Rankin, 2013).

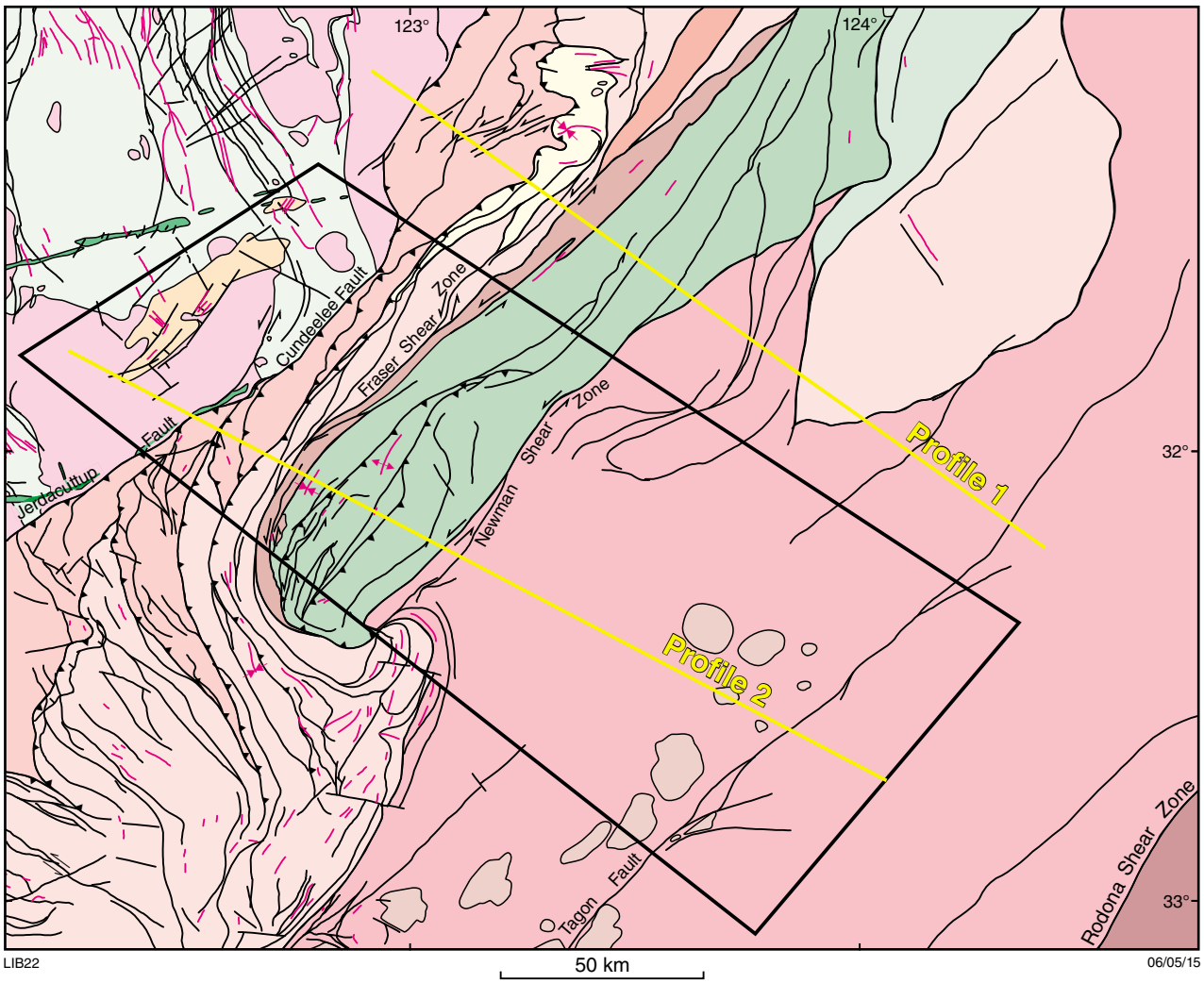

Figure 6. Interpreted bedrock geology map with simplified Yilgarn Craton geology (from Spaggiari and Pawley, 2012) showing the location of the study area and forward modelled profiles

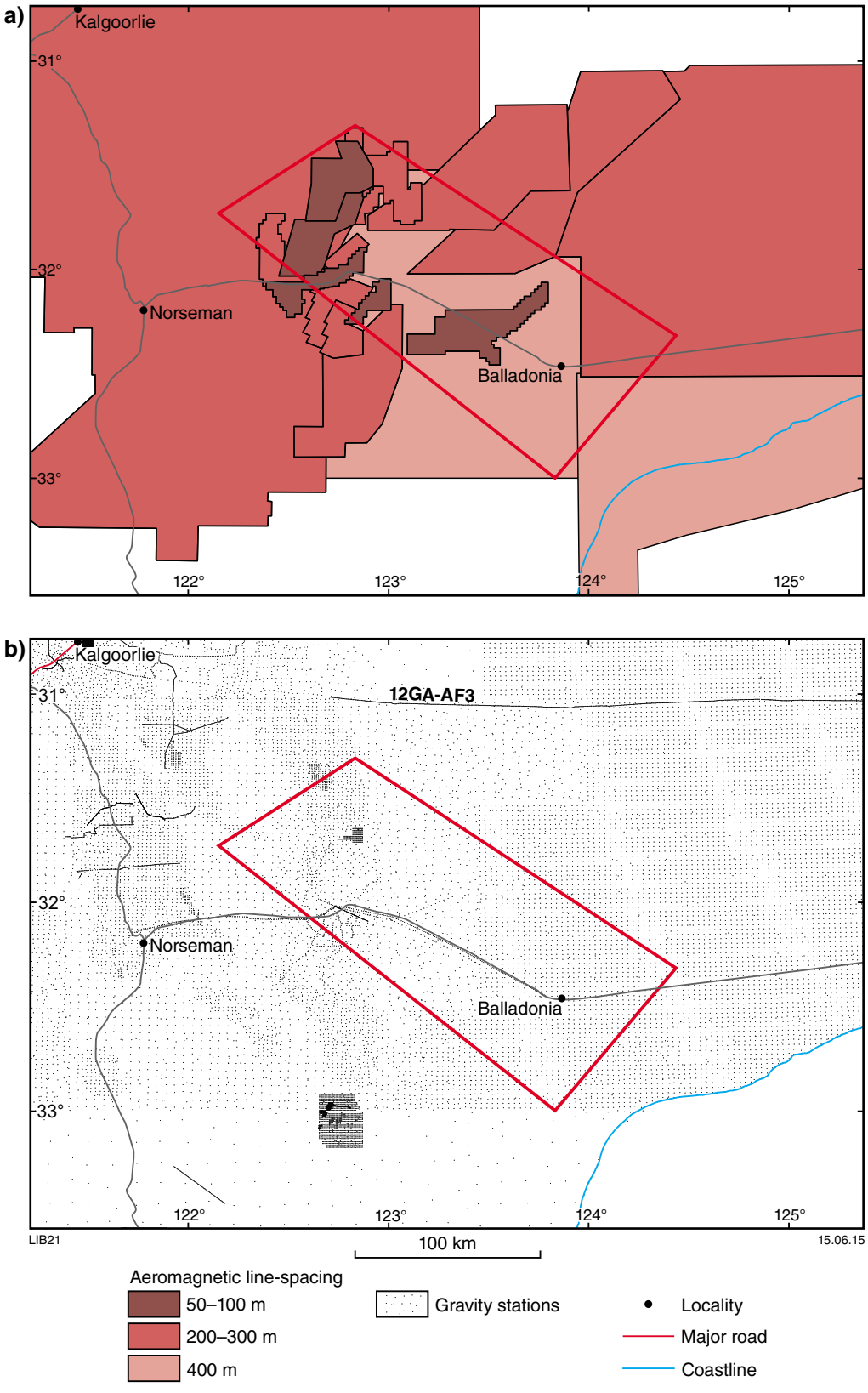

Figure 7. **Resolution of the geophysical data used to construct the structural domain map and forward models: a) aeromagnetic surveys, coloured by flight line spacing; b) gravity stations in the study area**

In high-grade metamorphic terranes, such as the Fraser Zone and parts of the Nornalup Zone, magnetite is considered to have been produced and redistributed during the secondary processes of metamorphism and deformation. In the lower metamorphic grade parts of the Nornalup Zone (for example the Esperance Supersuite), the distribution of magnetite appears dominated by magmatic processes. Where possible the interpreted aeromagnetic trends are related to features (e.g. structures) that can be observed in outcrop. However, because of differences in scale between aeromagnetic features and outcrop observations, it is not usually possible to directly correlate the two.

In this study, aeromagnetic trend lines have been drawn to trace magnetization contrasts in RTP 1VD images. Aeromagnetic trend lines, which are treated similarly to form-lines in structural geology, provide a framework within which faults, shear zones, and folds can be interpreted. Faults and shear zones can be interpreted where aeromagnetic trend lines are offset, regions of different magnetic character are juxtaposed, and structures have undergone magnetite creation or destruction (Betts et al., 2003). Folds can commonly be interpreted where aeromagnetic horizons show recognizable fold geometries. The magnetic gradients of folded horizons can in places provide information on the dip of the fold axial plane and the plunge of the fold axis.

Bouguer gravity images, which have a lower resolution than aeromagnetic data, have also been used to provide information on lateral density contrasts in the crust and upper mantle. The density contrasts in gravity images are commonly major lithological contacts or large-scale structures that juxtapose units of contrasting density.

The orientations of faults, shear zones, and folds mapped in aeromagnetic and gravity images in places can be broadly constrained from asymmetries in magnetic and gravity gradients. Kinematic information can also be obtained from aeromagnetic images; for example, the rotation of magnetic anomalies towards a structure and the offset of magnetic marker horizons can provide information on the movement direction and displacement along a faults and shear zones (Betts et al., 2003).

Northern Foreland

In the study area, the northeast-trending Cundeelee Fault is the boundary between the Kurnalpi Terrane of the Yilgarn Craton and the Northern Foreland (Spaggiari and Pawley, 2012). The Cundeelee Fault truncates the northwest-trending magnetic horizons and coincident gravity high of the Kurnalpi Terrane greenstone belt (Spaggiari and Pawley, 2012). The gravity high of the greenstone belt appears to continue, subdued and slightly offset, across the Cundeelee Fault and is possibly the continuation of the Kurnalpi Terrane greenstone belt beneath the Northern Foreland and Biranup Zone (Fig. 11a). Alternatively, the source of this anomaly may be unrelated to the Kurnalpi Terrane and may be simply a dense body in the Northern Foreland or Biranup Zone.

The magnetic fabric of the Northern Foreland is characterized by a low-intensity and smooth texture with regions containing discontinuous, northeast- to north-northeast-trending, moderately magnetic horizons (Fig. 11b). This dominantly subdued magnetic fabric expresses structures poorly. The sparse outcrop in the Northern Foreland has a dominant steeply southeast-dipping foliation (YARDILLA) parallel to the magnetic horizons. The Kurnalpi Terrane of the Yilgarn Craton, adjacent to the Northern Foreland, has a dominant northwest-vergent fold and thrust geometry (WAROX; this study).

Biranup Zone

Like the Northern Foreland, the magnetic fabric of the Biranup Zone is characterized by low-intensity and smooth texture that expresses structures poorly (Fig. 11b). The Biranup Zone contains several northeast- to north-northeast-trending moderately magnetic horizons (~400 m in width). The higher magnetic intensity horizons have been interpreted as shear zones (Spaggiari and Pawley 2012). The limited Biranup Zone outcrop in the study area has a northeast-trending, steeply southeast-dipping gneissic foliation (~1 cm layering) and a shallowly northeast-plunging mineral lineation (YARDILLA). The northeast-trending magnetic horizons are parallel to the foliation.

Fraser Zone

The magnetic fabric of the Fraser Zone is characterized by variably continuous, high- to low-intensity magnetic horizons (~200 m in width) (e.g. Fig. 12a). Based on different structural trends, the Fraser Zone is divided into six subdomains (Fig. 10a), some interpreted to be separated by structures and others with more continuous boundaries. Magnetic horizons have not been directly correlated with features observed in outcrop although they most likely comprise a combination of lithological variations and subparallel shear zones. Magnetic horizons (Fig. 12a) are parallel to the dominantly northeast-striking, steeply dipping gneissic layering that is defined by sheets of metagranite, metagabbro, and metasedimentary rocks that are approximately 10 cm to 1 m wide (Clark et al., 1999; Jones and Hall, 2004; Spaggiari et al., 2011; Fig. 12b). The bimodal magnetic susceptibility distributions of the metagabbro, metagranite, and metasedimentary rocks of the Fraser Zone (Fig. 12c,d) suggest that the high- or low-intensity magnetic horizons could be any of these lithologies. Magnetic horizons are also truncated by low-intensity northeast-trending features (~500 m in width), which are interpreted as demagnetized shear zones (Fig. 12a).

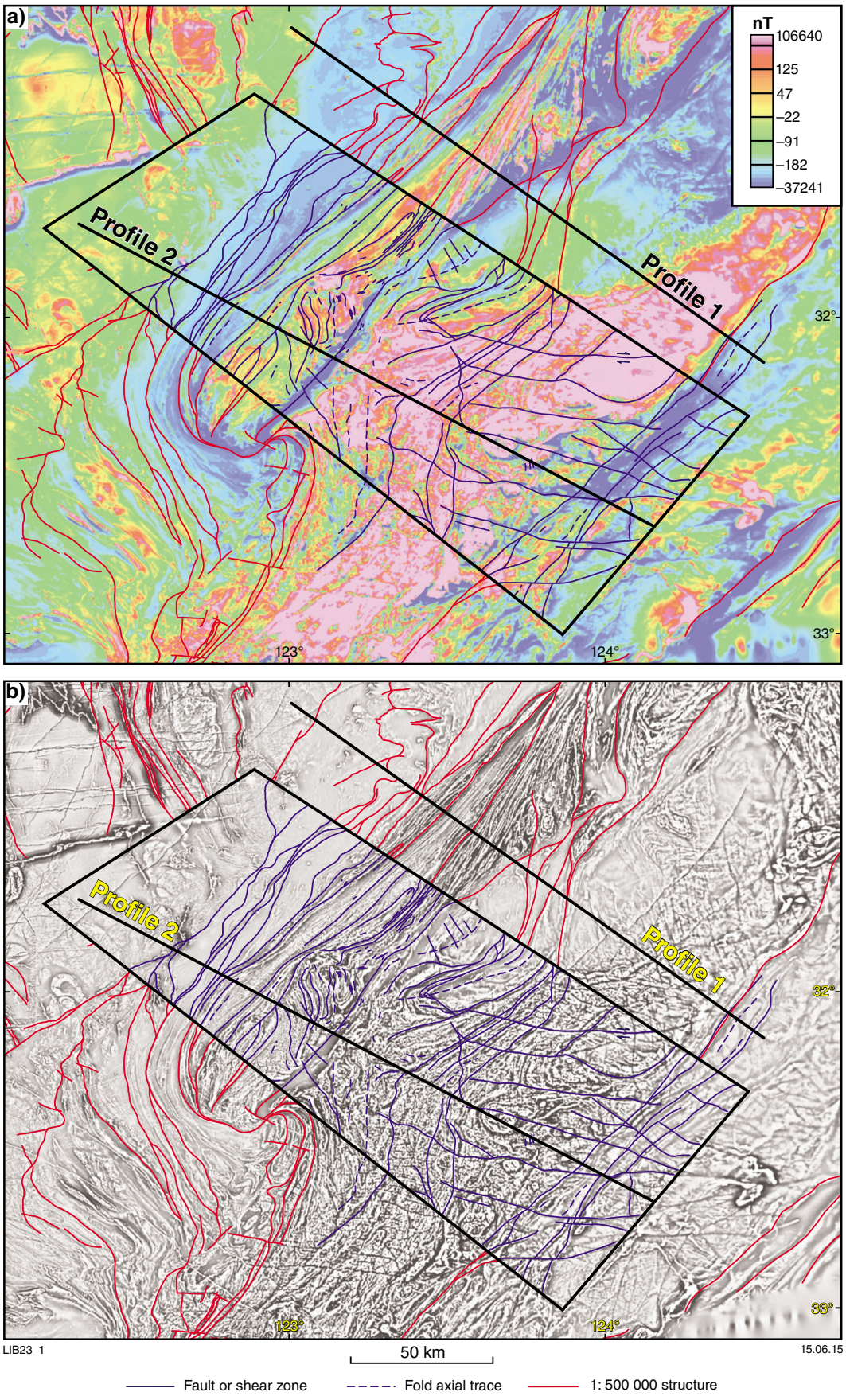

Figure 8. Structural interpretation of the study area overlain on geophysical images and 1:500 000 scale structures (Geological Survey of Western Australia, 2014): a) reduced to the pole (RTP) aeromagnetic image; b) RTP first vertical derivative (1VD) aeromagnetic image; c) RTP tilt derivative aeromagnetic image; d) Bouguer gravity image (continued p. 16)

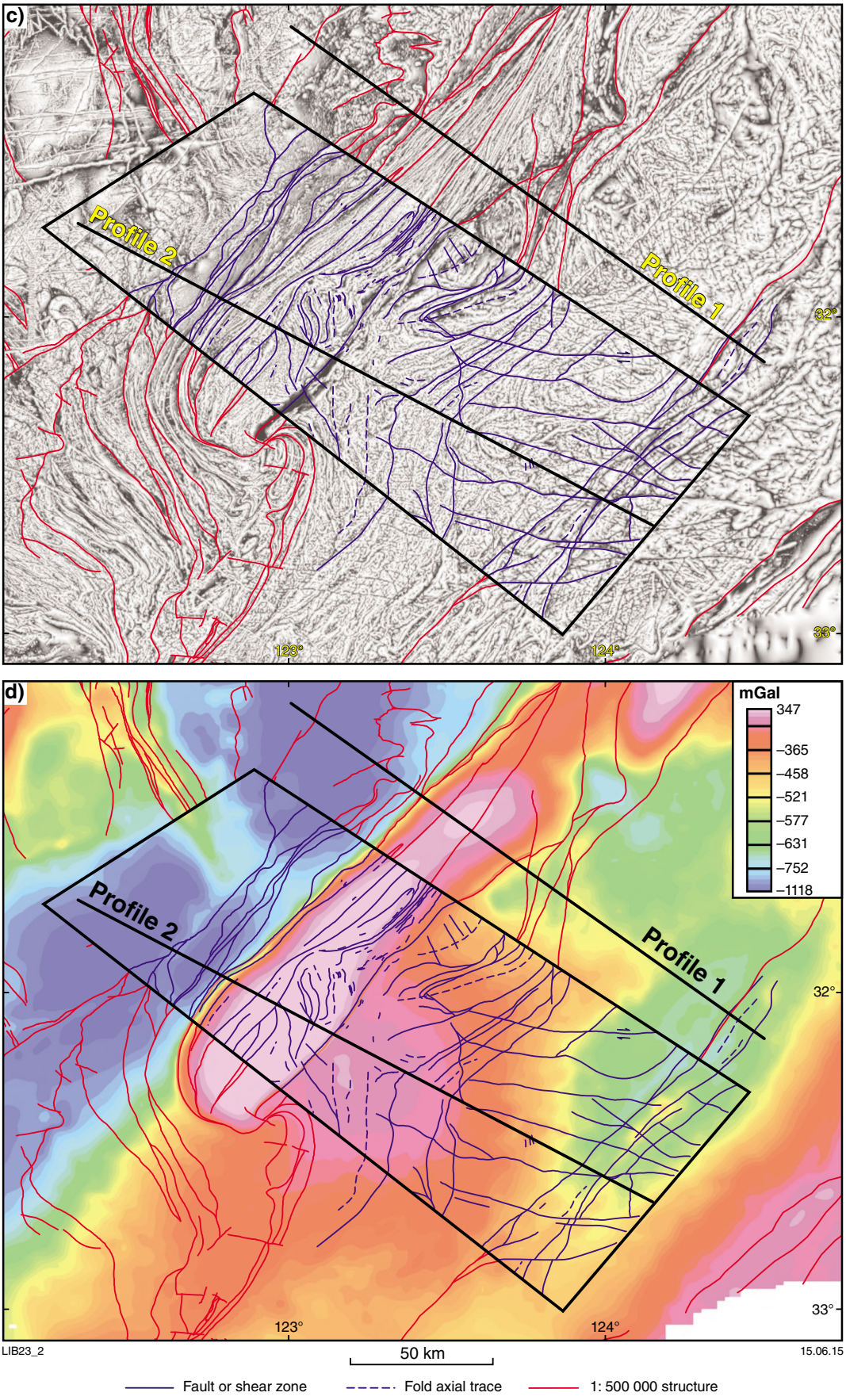

Figure 8. continued

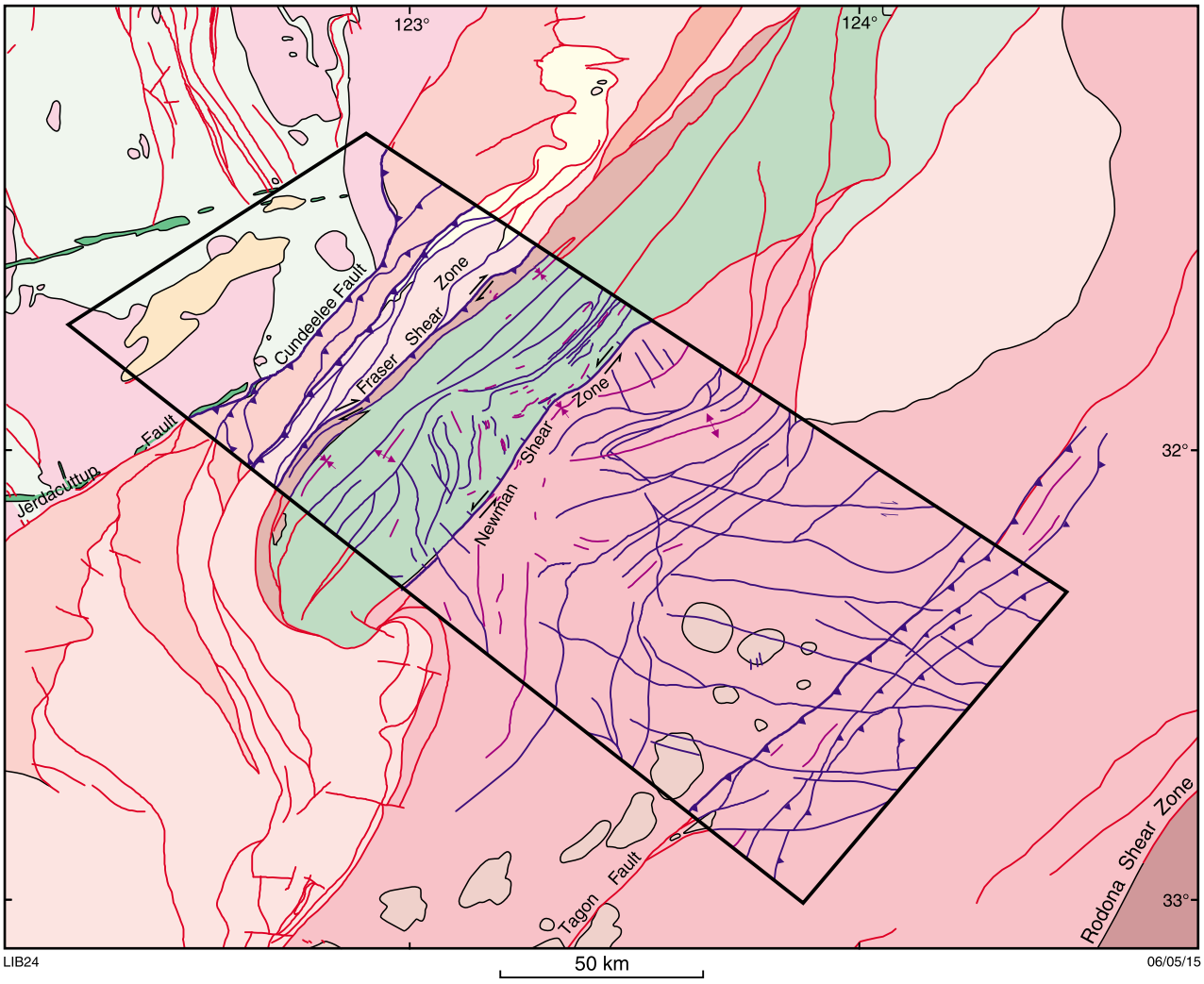

Figure 9. Structural interpretation of the study area overlain on interpreted bedrock geology (Spaggiari and Pawley, 2012) and 1:500 000 structures (Geological Survey of Western Australia, 2014)

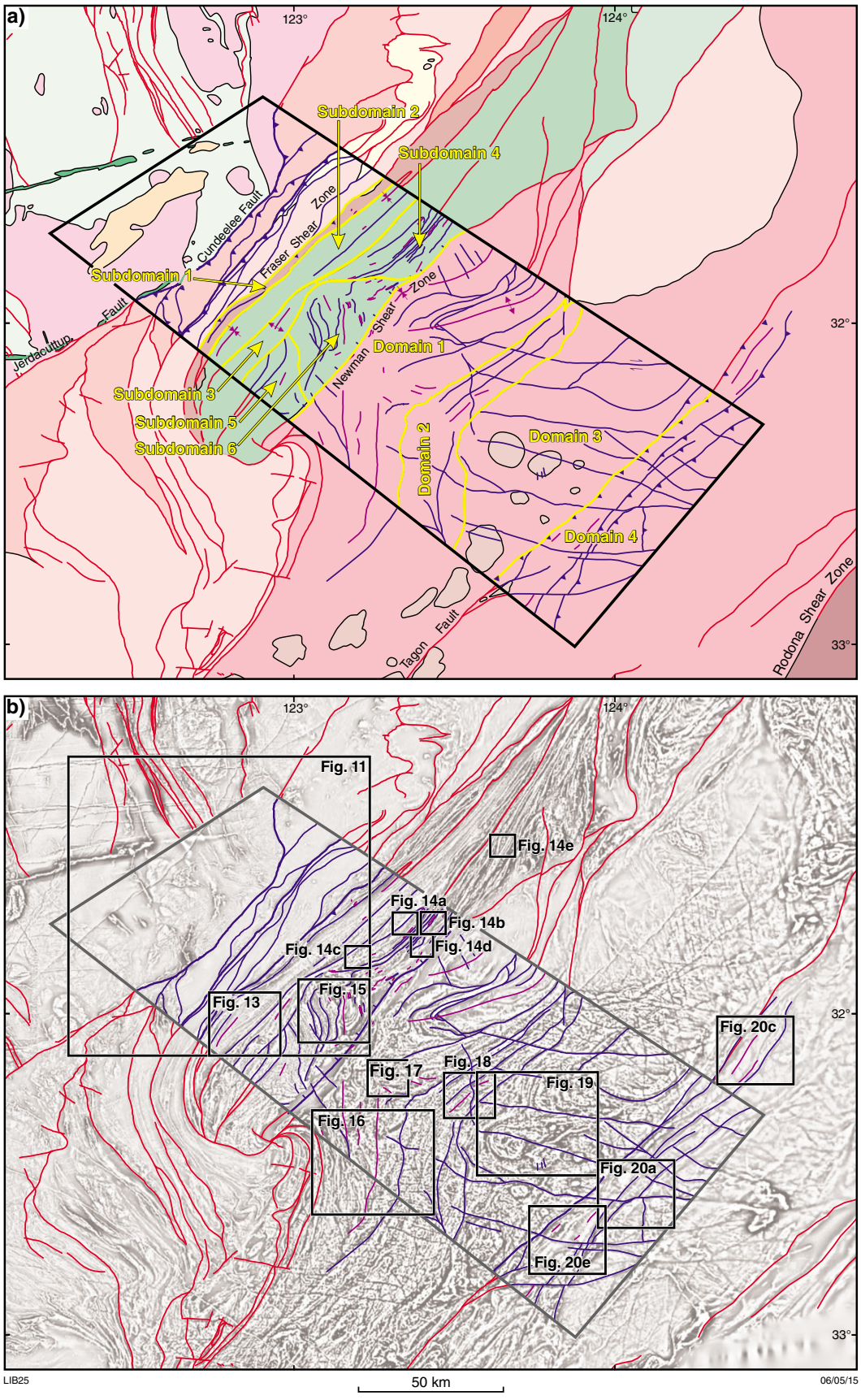

Figure 10. **a) Interpreted structures and structural domains and subdomains overlain on interpreted bedrock geology (Spaggiari and Pawley, 2012) and 1:500 000-scale structures (Geological Survey of Western Australia, 2014); b) interpreted structures and structural domains, subdomains, and locations of detailed study sites overlain on reduced to the pole first vertical derivative (RTP 1VD) image and 1:500 000 scale structures (Geological Survey of Western Australia, 2014)**

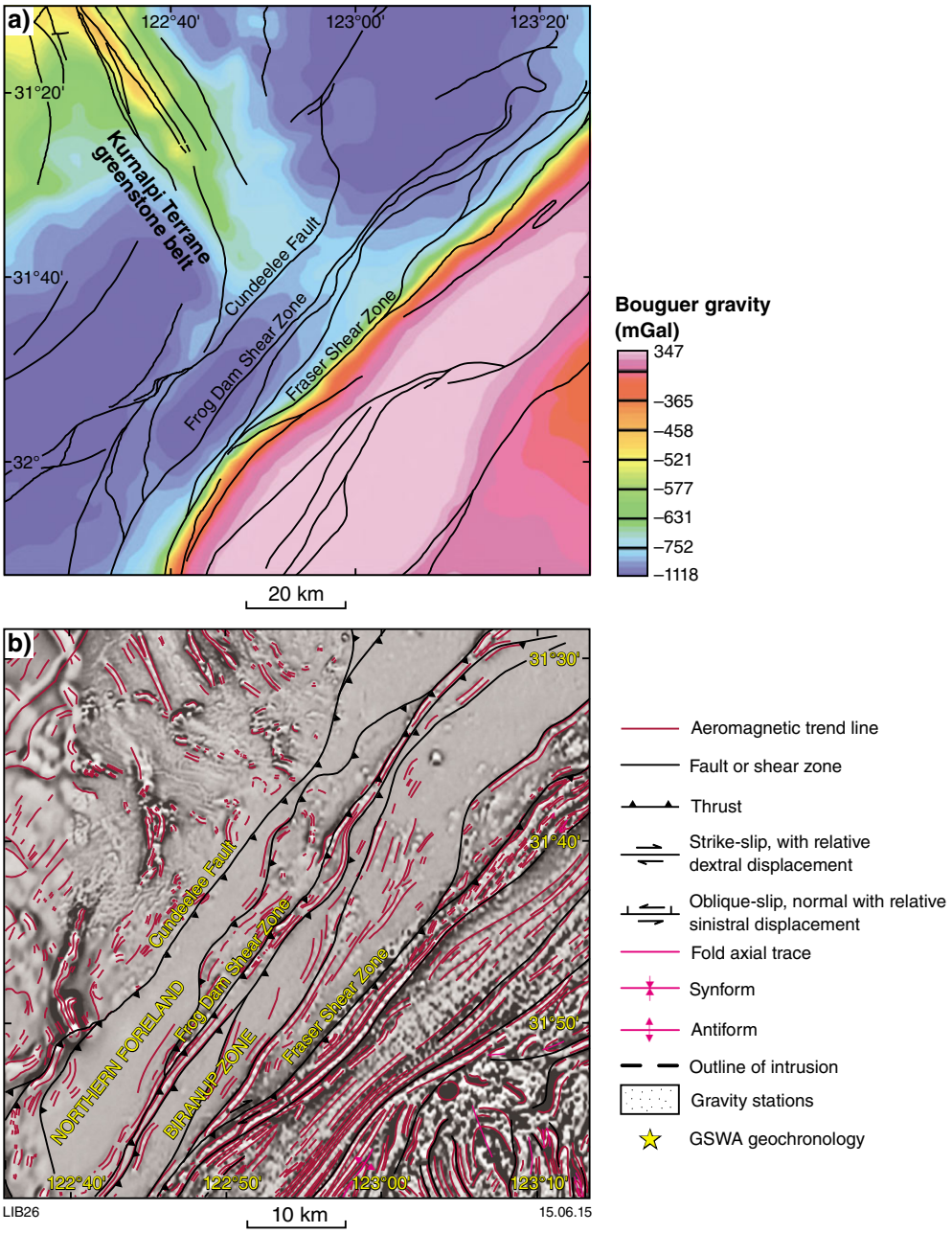

Figure 11. a) Bouguer gravity image and 1:500 000 scale structures (Geological Survey of Western Australia, 2014) showing the gravity anomaly associated with the greenstone belt of the Yilgarn Craton's Kurnalpi Terrane, and the apparent continuation of this anomaly into the Northern Foreland and Biranup Zone; b) reduced to the pole first vertical derivative (RTP 1VD) showing the smooth magnetic texture of the Northern Foreland and Biranup Zone; key applies to subsequent figures

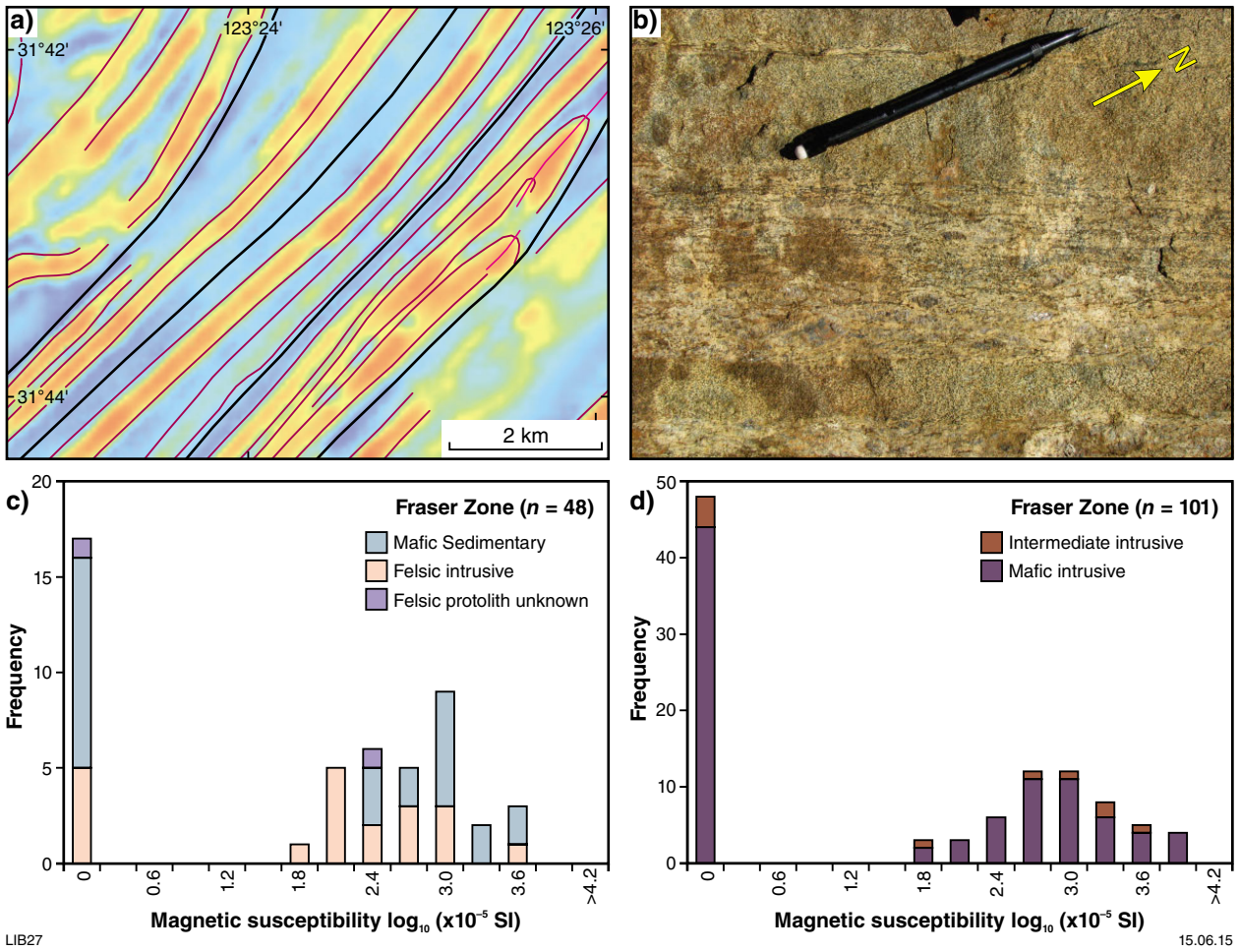

Figure 12. Fraser Zone: a) reduced to the pole (RTP) aeromagnetic image showing northeast-trending high- and low-intensity horizons; b) interlayered metagabbro and metagranite with northeast-trending gneissic foliation. Bimodal Fraser Zone magnetic susceptibility data: c) metagranitic and metasedimentary rocks; d) metagabbroic and hybridized metagabbroic rocks; key for a) shown in Figure 11b

In subdomains 1 to 4 of the Fraser Zone (Fig. 10) the magnetic fabric is characterized by northeast-trending magnetic horizons of varying continuity and intensity. In subdomain 1, which is equivalent to the metasedimentary-dominated component of the Fraser Range Metamorphics (the Snowys Dam Formation; Spaggiari et al., 2014a), the northeast-trending magnetic horizons are discontinuous, most likely reflecting both the primary and secondary magnetic properties of the metasedimentary rocks. This magnetic fabric is parallel to the northeast-trending, steeply dipping gneissic to mylonitic foliation observed in outcrop (Myers, 1985; Clark et al., 1999; Jones and Hall, 2004; Spaggiari et al., 2011).

In subdomains 2 and 3, magnetic horizons define northeast-trending, tight to isoclinal folds (1.6 to 4.5 km in width) (Spaggiari and Pawley, 2012) (Fig. 13a,b). The magnetic horizons in subdomains 2 and 3, as in subdomain 1, are parallel to the northeast-trending, steeply dipping gneissic to mylonitic foliation that is defined by layers of metagabbro, metagranite, and metasedimentary rocks (Spaggiari et al., 2011). Locally, outcrop contains tight to isoclinal intrafolial folds (Fig. 13d) that have a similar orientation and style to the regional-scale, northeast-trending folds observed in aeromagnetic images in subdomains 2 and 3.

In subdomain 4, which is completely under cover, magnetic horizons are locally isoclinally folded around northeast-trending fold axial traces (approximately 500 m wide). Folds are truncated by demagnetized zones interpreted as northeast-trending shears (Fig. 14a,b). Subdomain 4 of the Fraser Zone also contains several eye-shaped magnetic features (Fig. 14c–e) including the ‘eye’ anomaly at the Nova–Bollinger Ni–Cu deposit (Fig. 14c). The long axes of the eyes are parallel to the northeast-trending magnetic fabric. Further interpretation of these features is hindered by the lack of outcrop and therefore structural constraint. Additional field observations, for example lineations and associated kinematic indicators, might provide information on the direction of movement and sense of shear at an outcrop scale, which might be used to understand the direction of movement at a larger scale.

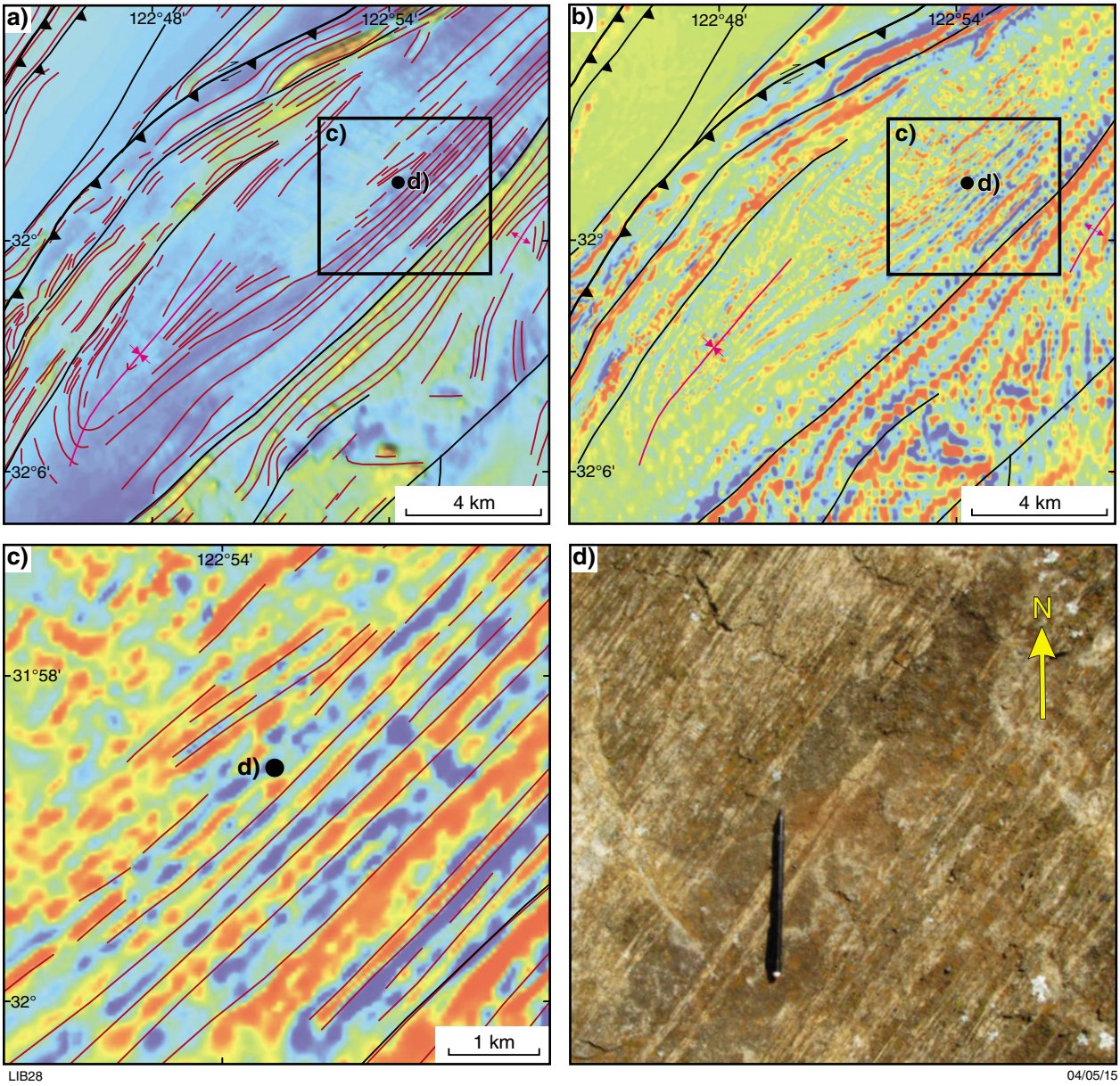

Figure 13. Fraser Zone: a) reduced to the pole (RTP) aeromagnetic image showing the synform interpreted by Spaggiari and Pawley (2012); b) RTP first vertical derivative (1VD) aeromagnetic image of the area shown in a); c) RTP 1VD aeromagnetic image, showing northeast-trending magnetic horizons in the southeast limb of the synform; d) outcrop photo from the southeast limb of the synform, showing interlayered metagabbro and metagranite with northeast-trending mylonitic foliation and intrafolial isoclinal fold; key for a)–c) shown in Figure 11b

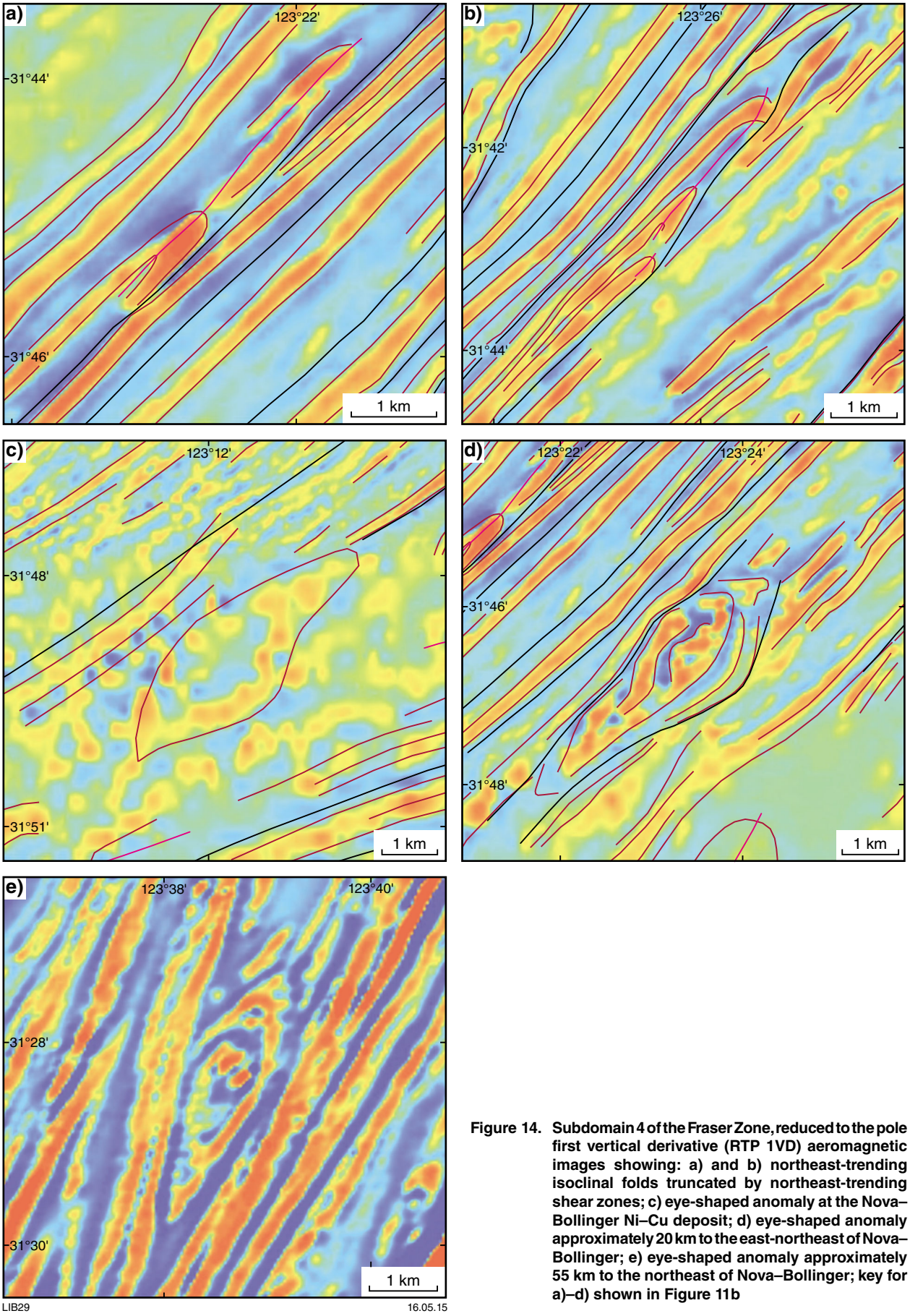

Figure 14. Subdomain 4 of the Fraser Zone, reduced to the pole first vertical derivative (RTP 1VD) aeromagnetic images showing: a) and b) northeast-trending isoclinal folds truncated by northeast-trending shear zones; c) eye-shaped anomaly at the Nova–Bollinger Ni–Cu deposit; d) eye-shaped anomaly approximately 20 km to the east-northeast of Nova–Bollinger; e) eye-shaped anomaly approximately 55 km to the northeast of Nova–Bollinger; key for a)–d) shown in Figure 11b

In the centre of the study area, in subdomain 6 of the Fraser Zone, magnetic horizons appear to trend to the north-northwest, almost orthogonal to the dominant northeasterly trend (Figs 10 and 15a). Outcrop in subdomain 6 is dominated by metagabbro (Doepel and Lowry, 1970a; Myers, 1985; this study) that commonly appears unfoliated (Myers, 1985). Where foliation measurements are available, for example at southern Cullinia Rocks (Fig. 15c), they are subparallel to the magnetic horizons (Fig. 15d). Locally, for example, at southern Cullinia Rocks, the foliation is folded by north-trending isoclinal folds that appear truncated by north-trending shears (Fig. 15b; MGA 514293E 6459608N). The northeast of subdomain 6 contains an outcrop of psammitic gneiss at northern Cullinia Rocks (MGA 515529E 6461108N), which suggests this subdomain might contain some lithological variability.

Nornalup Zone

In the study area the magnetic fabric of the Nornalup Zone is characterized by variably continuous, moderately to intensely magnetic horizons that define structural and magmatic trends (Fig. 10). Based on differences in these trends, the Nornalup Zone is divided into four domains interpreted to be separated by major shear zones. In the northwest of the Nornalup Zone, domains 1 and 2 are characterized by magnetic horizons that define regional-scale folds. To the southeast, domain 3 is characterized by magnetic horizons that define regional-scale magmatic features, and southeast of the Tagon Shear Zone, domain 4 is characterized by a northeast-trending, low- to moderate-intensity magnetic fabric. Magnetic horizons have not been correlated directly with features observed in outcrop although they are typically subparallel to foliation measurements shown on the 1:250 000 map sheets. It is possible that the magnetic horizons represent the dominant layering of the gneissic, migmatitic, and magmatic rocks present in this domain.

Domain 1 is characterized by weakly to moderately continuous magnetic horizons that define regional-scale folds (~10 km wide) with east-northeast and northerly trending axial traces (Fig. 10). From east to west the fold axial traces change in trend from east-northeast to north. In the hinge of the northeast-trending, southwest-closing fold, the magnetic gradient shallows to the southwest, which suggests this fold is an antiform. The north-trending folds contain circular aeromagnetic trends, along-strike of the axial trace, which are interpreted to be caused by the non-cylindrical nature of the folding (Fig. 16). Domain 1 contains very little outcrop and few structural measurements. The lack of outcrop and therefore structural information in this region, and the indistinct magnetic gradients caused by complex overlapping magnetic anomalies (see next section), make it difficult to constrain the dip direction of shears or the orientations of the axial plane and plunge of folds.

Where detailed structural information is available, for example at Harms Lake, it is commonly not possible to correlate structures observed in outcrop with magnetic features. Harms Lake is between the east-northeast and north-trending axial traces of the regional-scale folds described above. This region has a complex magnetic fabric that contains northwest, northeast, and easterly magnetic trends (Fig. 17a,b). A migmatitic metagranite with a west-striking, steeply north-dipping foliation and folds with axial planes subparallel to the foliation are exposed near Harms Lake (MGA 526423E 6436421N; Fig. 17c,d). Approximately 2 km to the northeast of Harms Lake (MGA 527259E 6438248N), a migmatitic metagranite of similar composition has a northeast-striking foliation and a steep northwest dip. It is possible that the complex, variably orientated magnetic fabrics in domain 1 of the Nornalup Zone are a result of migmatization, a process that has been associated with irregular patches of flat or fuzzy magnetic texture (Isles and Rankin, 2013).

Within domain 1 the Bouguer gravity data are dominated by a long wavelength gravity anomaly (~150 km) that is elliptical in map-view (Fig. 8d). The maxima of this long wavelength anomaly coincide with the chaotic magnetic fabric between the east-northeast and north-trending axial traces of the regional-scale folds.

The magnetic fabric of domain 2, particularly in the southwest, is dominated by a mottled, moderately to highly magnetic fabric and an absence of continuous linear trends (Fig. 10). The very limited outcrop in domain 2 suggests that this region is dominated by a migmatite unit, described as a complex of leucocratic granite and gneisses (Doepel and Lowry, 1970b). The dominance of migmatitic metagranite is possibly the source of the mottled, fuzzy magnetic fabric. Locally, some of the more continuous magnetic horizons are folded into approximately 3 km-wide tight folds that are truncated by demagnetized zones interpreted as northeast-trending shears (Fig. 18a). The lack of outcrop and therefore structural information in this region (Fig. 18b), and indistinct magnetic gradients caused by the complex overlapping magnetic anomalies, make it difficult to constrain the dip direction of shear zones or the axial plane and plunge of folds. Elliptical magnetic horizons along-strike of the north-trending fold axial trace are interpreted as non-cylindrical folds, although it is also possible these anomalies are plutons (Fig. 18a).

In domain 3 (Fig. 10) the northeast-trending to variably orientated, highly magnetic fabric is crosscut by circular and subcircular, highly to intensely magnetic anomalies (Spaggiari and Pawley, 2012) (Fig. 19a). The subcircular magnetic horizons are interpreted as magmatic fabrics that are defined by magnetite. The intensely magnetic subcircular anomalies are coincident with gravity highs (Fig. 19a,b). Five of the coincident magnetic and gravity anomalies have been drilled by Enterprise Metals NL, which reported intersecting magnetite-rich, intermediate intrusive rocks (Williams and Robertson, 2011). Given their circular to subcircular shape, truncation of other magnetic fabrics and weak to absent deformation (Williams and Robertson, 2011), the intermediate intrusive rocks are interpreted as a mafic variety of the Esperance Supersuite.

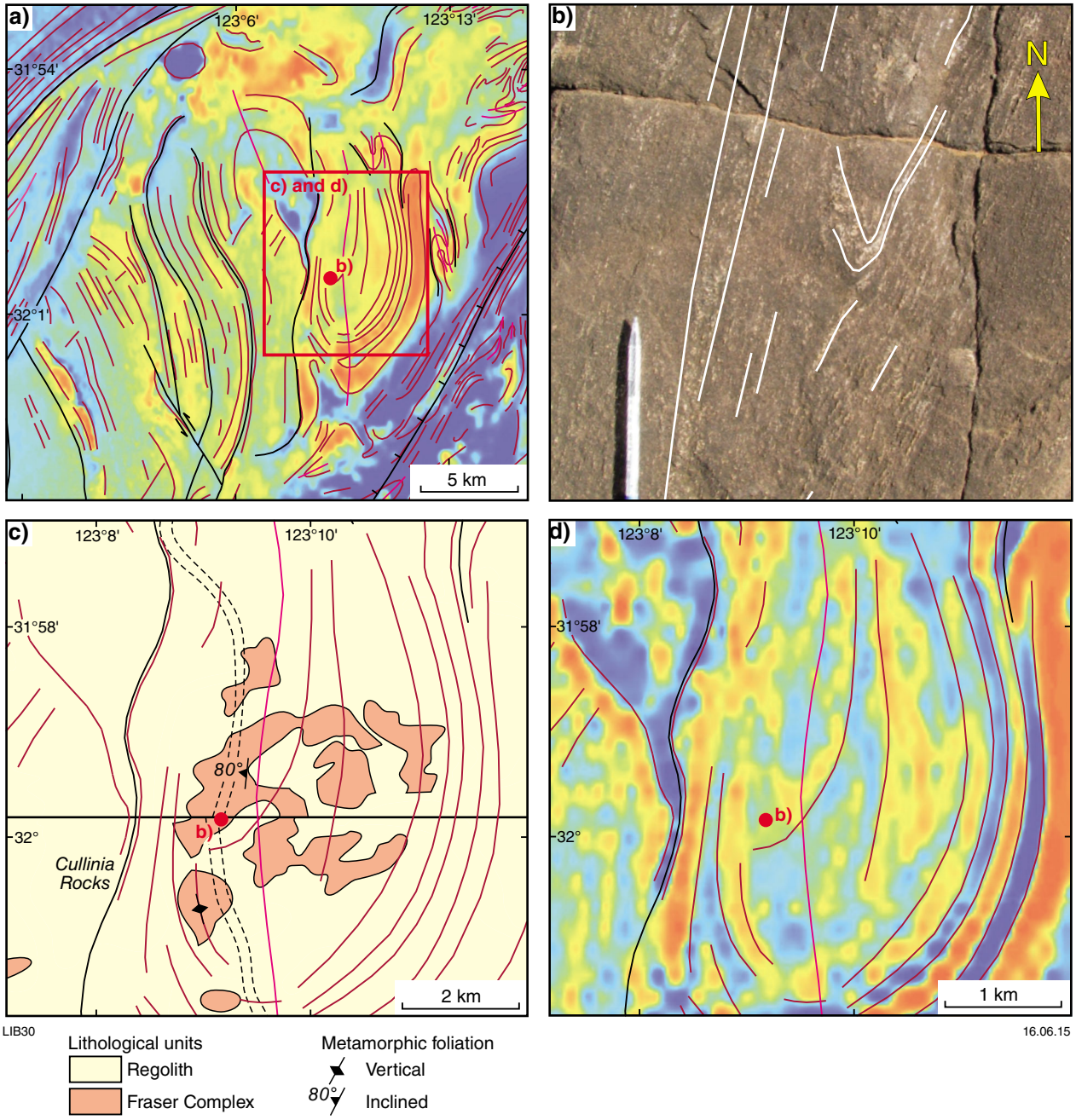

Figure 15. Subdomain 6 of the Fraser Zone: a) reduced to the pole first vertical derivative (RTP 1VD) aeromagnetic image showing north- and north-northwest-trending isoclinal folds; b) outcrop photograph showing north-trending foliation and intrafolial isoclinal folds (with folds outlined); c) 1:250 000 surface geology showing the subparallel magnetic horizons and foliation measurements; d) RTP 1VD aeromagnetic image showing north-trending magnetic horizons; key for a) and c) shown in Figure 11b

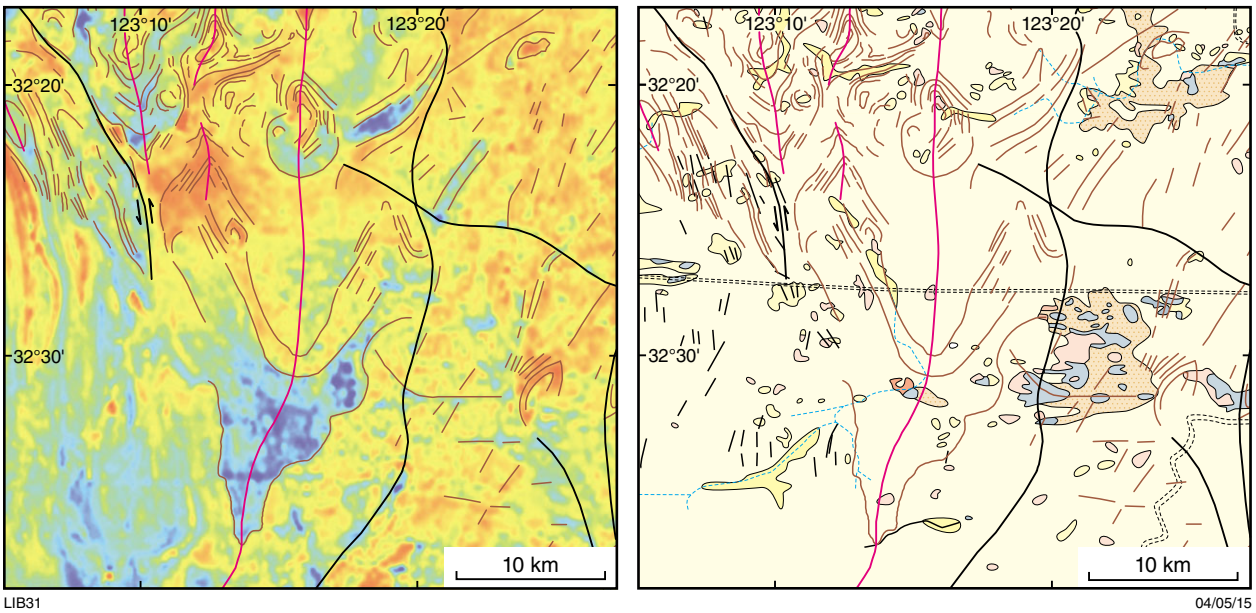

Figure 16. Domain 1 of the Nornalup Zone: a) reduced to the pole (RTP) aeromagnetic image showing the non-cylindrical, north-trending folds; b) 1:250 000 surface geology of the area shown in a); key to a) shown in Figure 11b

Domain 3 also includes variably magnetic, circular to subcircular anomalies that are not coincident with gravity highs (Fig. 19a,b). Given their low density, the subcircular magnetic anomalies are interpreted as felsic plutons, most likely of the Esperance Supersuite. Several of the variably magnetic plutons contain discrete regions of slightly higher density. In outcrop, felsic granitic rocks commonly contain mafic enclaves (Fig. 19c) and it is possible that the slight gravity highs in 1VD Bouguer gravity images are regions with more mafic enclaves. Domain 3 also contains a weakly foliated, K-feldspar porphyritic monzogranite dated at 1135 ± 56 Ma (GSWA 83667, Nelson, 1995) belonging to the Esperance Supersuite (Spaggiari and Pawley, 2012). This variety of the Esperance Supersuite has a weak susceptibility and no expression in magnetic images.

The basement into which these ?Esperance Supersuite plutons were emplaced include Paleoproterozoic to Mesoproterozoic magmatic rocks, metasedimentary rocks of the Arid Basin and Barren Basin, and magmatic rocks of the Recherche Supersuite that have undergone metamorphism and deformation during either or both Stage I and II of the Albany–Fraser Orogeny. In outcrop, many of the weak to moderately foliated granites, possibly of the Esperance or Recherche Supersuites, contain rafts of migmatitic gneiss, most likely from the basement (Fig. 19d).

Domain 4, southeast of the Tagon Shear Zone, has relatively low magnetic intensity and a smooth magnetic texture (Fig. 20a) with minor, northeast-trending, weakly magnetic horizons that are enhanced in the 1VD RTP image (Fig. 20b). Locally, magnetic horizons are interpreted as tightly folded, 2 to 4 km wide, and truncated by demagnetized northeast-trending shears. The isoclinal northeast-trending folds, which are truncated by the Tagon Shear Zone, are an example of folds that are well imaged in magnetic data (Fig. 20c,d). Domain 4 also contains subcircular magnetic features interpreted as intermediate intrusive rocks, although they are smaller and less common than in domain 3 (Fig. 20e,f). The only outcrop in domain 4 is a weakly foliated K-feldspar porphyritic monzogranite (?Esperance Supersuite) that has a weak susceptibility and no expression in magnetic images. The magnetic fabric of domains 3 and 4, including the intermediate intrusive rocks, is crosscut by a series of regionally extensive (up to 70 km), demagnetized, west-northwest-trending faults with apparent dextral offset (Fig. 20e,f). It is possible these structures are intruded by dykes of the c. 750 Ma Nindibillup Dyke Suite (Spaggiari et al., 2009). Dykes of this suite typically trend west-northwest and post-date Stage II of the Albany–Fraser Orogeny (Spaggiari et al., 2009, 2011).

Magnetic and gravity forward modelling

Method

Two crustal-scale, approximately 200 km-long magnetic and gravity forward models that traverse the east Albany–Fraser Orogen (Figs 6 and 21) were constructed in the Oasis Montage add-in GmSys (version 8.2) (<www.geosoft.com/products/gm-sys/>). Profile 2 traverses the length of the study area, including the Bouguer gravity high of the Fraser Zone and the long wavelength gravity high to the southeast of the Fraser Zone. Profile 1 traverses the orogen to the northwest of the study area, and was constructed primarily to model the geometry of the Fraser Zone independently of the long wavelength Bouguer gravity high (Fig. 21).

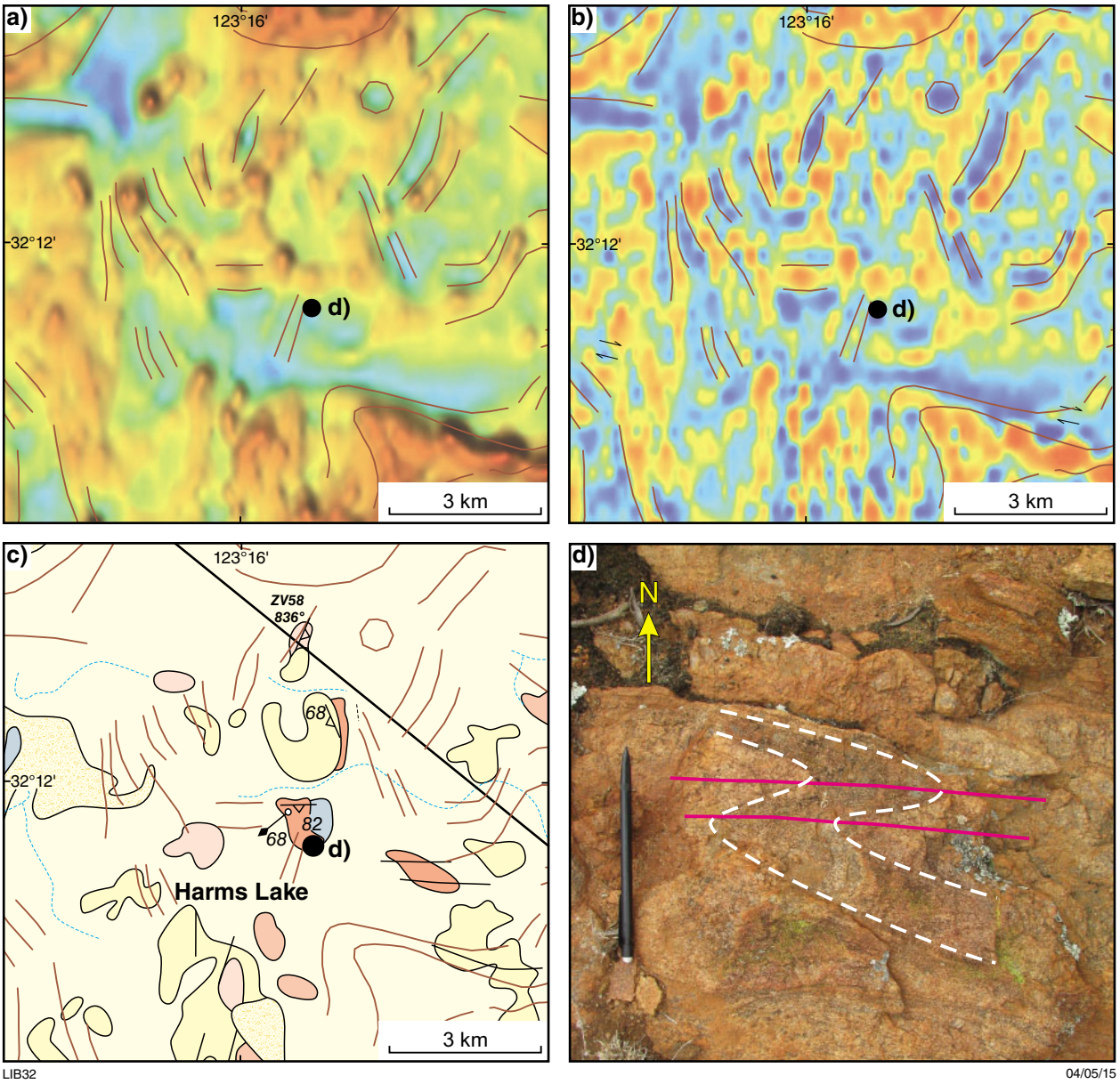

Figure 17. **Harms Lake area in domain 1 of the Nornalup Zone: a) reduced to the pole (RTP) aeromagnetic image showing the complex magnetic fabric; b) RTP first vertical derivative (1VD) aeromagnetic image of the region shown in a); c) 1:250 000 surface geology of the area shown in a); d) west-trending folds in a migmatitic gneiss; key shown in Figure 11b**

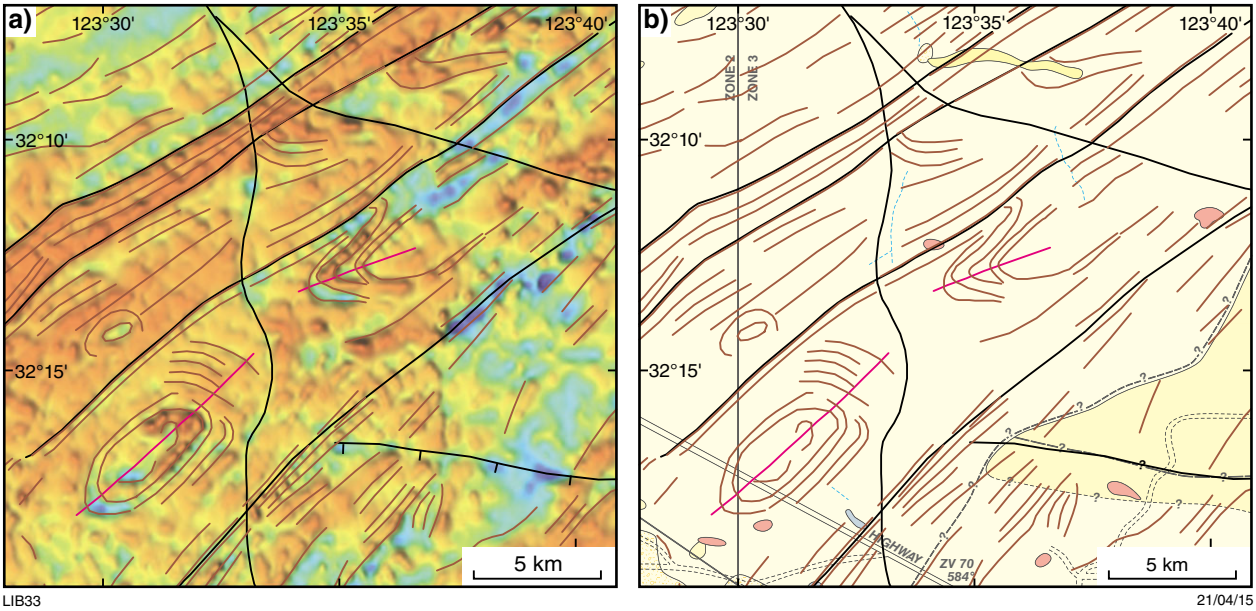

Figure 18. Domain 2 of the Nornalup Zone showing northeast-trending tight folds truncated by northeast-trending shears: a) reduced to the pole (RTP) aeromagnetic image, with aeromagnetic trend lines and interpreted structures; b) 1:250 000 surface geology, showing lack of outcrop; key to a) shown in Figure 11b

For the two profiles, RTP aeromagnetic and Bouguer gravity data were sampled from grids at 500 m spacing. Polygons representing the subsurface were then constructed and attributed with physical properties (magnetic susceptibility and density). The surface location and geometries of the modelled polygons were constrained using the available geological data, and the physical properties were constrained using the east Albany–Fraser Orogen petrophysical dataset. The geometries and physical properties of the polygons were then adjusted iteratively until a suitable match was achieved between the data and the magnetic and gravity responses of the model.

Other constraints on the forward models include the depth to the Moho, which was sampled from the AusMOHO model (Kennett et al., 2011). In this model the Moho is approximately 37 km deep and features a trough beneath the Fraser Zone that extends to a depth of 44 km (profile 1) and 42 km (profile 2). In both profiles the top of the lower crust is assumed at a depth of between 17 and 20 km and subparallel to the Moho. Following Christensen and Mooney (1995) the lower crust has been modelled with a density of 2.80 g/cm^3 and the upper mantle with a density of 3.20 g/cm^3. These variables were kept constant during modelling and zero magnetization in the lower crust is assumed. The thickness of the Eucla Basin is modelled according to Lowry (1970) although it is not visible at the scale of the models shown.

Profile 1

Profile 1 is approximately 20 km to the northwest of the study area and traverses the Northern Foreland, Biranup Zone, Fraser Zone, and Nornalup Zone (Fig. 6). The dominant features in the gravity data include a moderate wavelength trough in the Northern Foreland and a high-amplitude anomaly associated with the metagabbro-dominated Fraser Zone (Figs 21 and 22). One of the aims of modelling this profile, and in particular the gravity data, was to determine the most likely geometry of the Fraser Zone independently of the long wavelength gravity anomaly in profile 2. The magnetic data in the majority of profile 1 is of relatively low intensity with the exception of high-amplitude, high-frequency anomalies in the Fraser Zone, and the high-amplitude, moderate-frequency anomaly in the Nornalup Zone at the southeastern end of the profile (Fig. 22a).

In profile 1, the Northern Foreland is modelled as three southeast-dipping units that extend to the top of the lower crust (Fig. 22). This geometry is based on structural observations that suggest the Northern Foreland and the adjacent southeast margin of the Yilgarn Craton are dominated by northwest-vergent folding and thrusting. The polygons that comprise the Northern Foreland have been attributed low relative susceptibilities and low densities, with an increase in density from northwest to southeast. The source of the moderate wavelength gravity trough is interpreted as the two northwestern units of the Northern Foreland (modelled with densities of ~2.64 g/cm^3). The low densities of the two northwestern units suggest they are dominated by Archean granites (median specific gravity ~2.64 g/cm^3) or metasedimentary rocks, possibly of the Paleoproterozoic Woodline Formation, or both. The moderate density unit in the southeast of the Northern Foreland (~2.75 g/cm^3) may contain a greater proportion of higher density Archean greenstone or material from the higher density adjacent Biranup Zone (Biranup Zone median specific gravity is 2.75 g/cm^3).

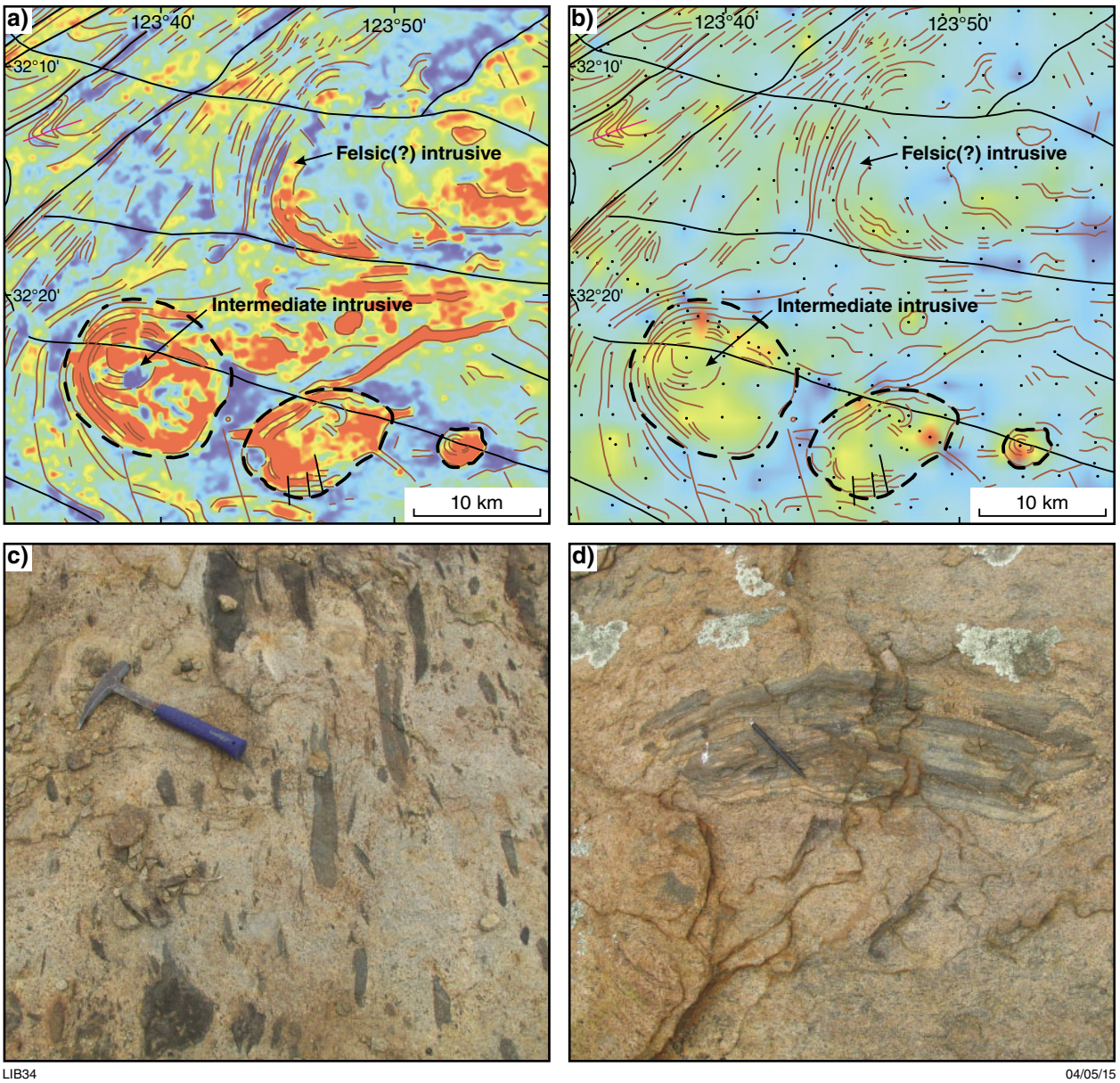

Figure 19. Domain 3 of the Nornalup Zone: a) reduced to the pole (RTP) aeromagnetic image showing the interpreted magmatic fabrics, and in dashed lines the intense magnetic anomalies, of the interpreted intermediate intrusives; b) first vertical derivative (1VD) Bouguer gravity image and gravity stations, showing in dashed lines the slight Bouguer gravity anomalies of the intermediate intrusives; c) mafic enclaves in a monzogranite about 5.5 km south-southeast of Nanambinia Rock (MGA 556665E 6380115N); d) gneissic raft in K-porphyritic monzogranite about 5 km south-southeast of Nanambinia Rock (MGA 559124E 6383367N); key to a) and b) shown in Figure 11b

Figure 20. (opposite) Domain 4 of the Nornalup Zone: a) reduced to the pole (RTP) aeromagnetic image, showing the subdued magnetic response to the southeast of the Tagon Shear Zone; b) RTP first vertical derivative (1VD) aeromagnetic image of the area shown in a); c) RTP 1VD aeromagnetic image, showing a northeast-trending tight fold truncated against the Tagon Shear Zone; d) RTP 1VD aeromagnetic image of the area shown in c); e) RTP 1VD aeromagnetic image showing the highly magnetic intermediate intrusives in dashed lines; f) 1VD of the Bouguer gravity data and gravity stations of the area shown in e); key shown in Figure 11b

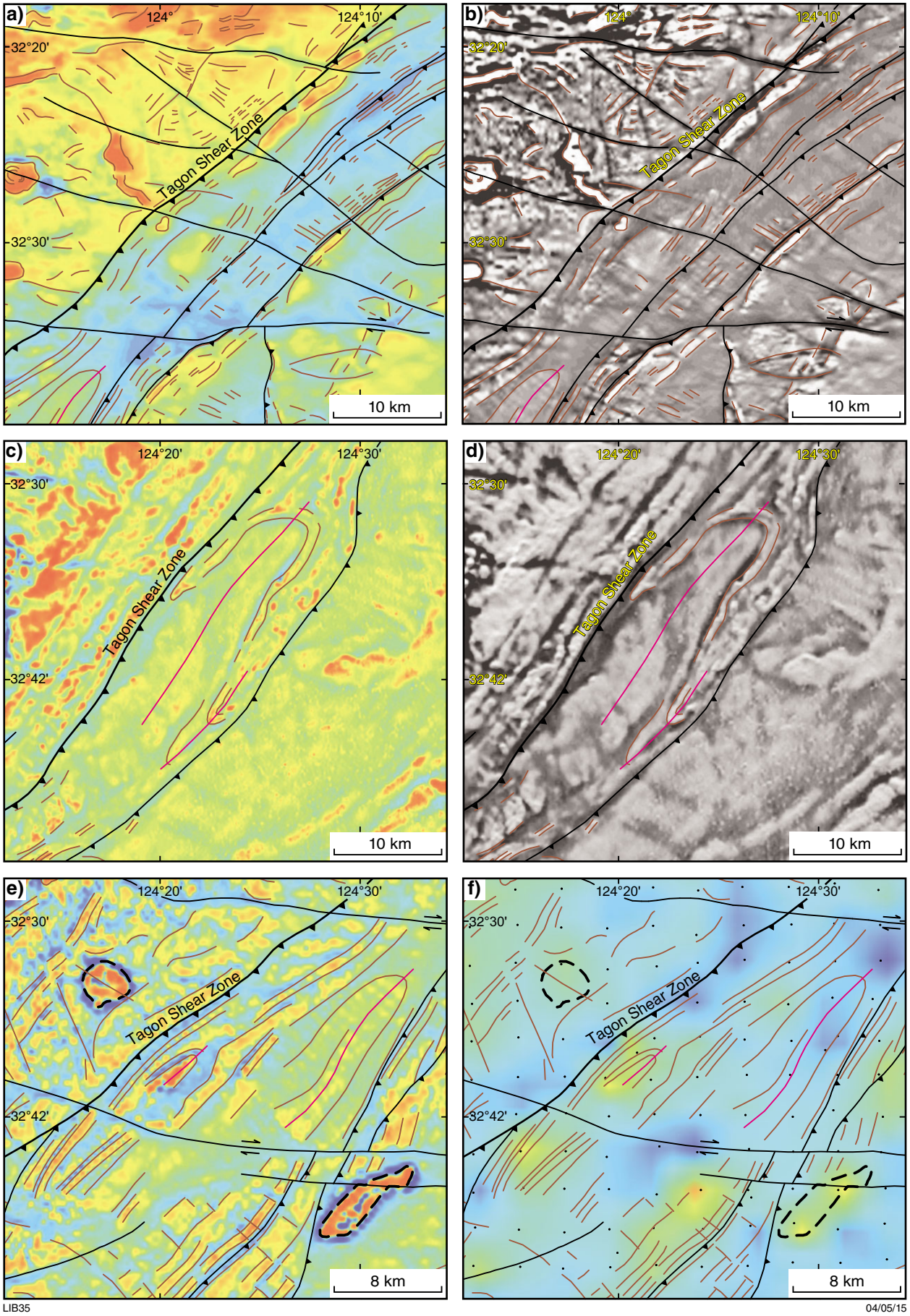
a)
124°
124°10'
32°20'
32°30'
Tagon Shear Zone
10 km
b)
124°
124°10'
32°20'
32°30'
Tagon Shear Zone
10 km
c)
124°20'
124°30'
32°30'
32°42'
Tagon Shear Zone
10 km
d)
124°20'
124°30'
32°30'
32°42'
Tagon Shear Zone
10 km
e)
124°20'
124°30'
32°30'
32°42'
Tagon Shear Zone
8 km
f)
124°20'
124°30'
32°30'
32°42'
Tagon Shear Zone
8 km
LIB35
04/05/15

To the southeast, the Northern Foreland is separated from the Biranup Zone by the Frog Dam Shear Zone. There is very little magnetization or gravity contrast across the Frog Dam Shear Zone, which prevents the orientation of this structure from being constrained using forward modelling. The Biranup Zone is modelled with a moderate density (2.75 g/cm^3) and a low relative susceptibility (–0.005 SI). Where it outcrops, the largely under cover Biranup Zone contains steeply southeast-dipping gneissic foliation. In profile 1 both the Frog Dam Shear Zone and Biranup Zone are modelled as southeast dipping, based on the structural measurements in the Biranup Zone, and the geometry of the adjacent Northern Foreland. The Fly Dam Formation and the Eddy Suite, interpreted as structurally interleaved with other units of the Biranup Zone (Spaggiari and Pawley, 2012), are also shown in profile 1.

Southeast of the Biranup Zone, the Fraser Zone is modelled in 2.5D (with an along-strike extent of 10 km to the southwest and 130 km to the northeast) and attributed a density of 3.00 g/cm^3 (the median specific gravity of the Fraser Zone). With these properties, and honouring the surface constraints, the Fraser Zone has been modelled as near-triangular and extending to a depth of 12.4 km (Fig. 22). Sensitivity testing of the Fraser Zone is discussed at the end of this section. The metasedimentary-dominated component of the Fraser Range Metamorphics (Snowys Dam Formation) lies along the northwest margin of the Fraser Zone and has been modelled with a slightly lower density of 2.95 g/cm^3. If the Snowys Dam Formation were modelled with an even lower density, which is possible if the proportion of metagabbro were lower, the northwestern margin of the Fraser Zone, and the Fraser Shear Zone, would steepen.

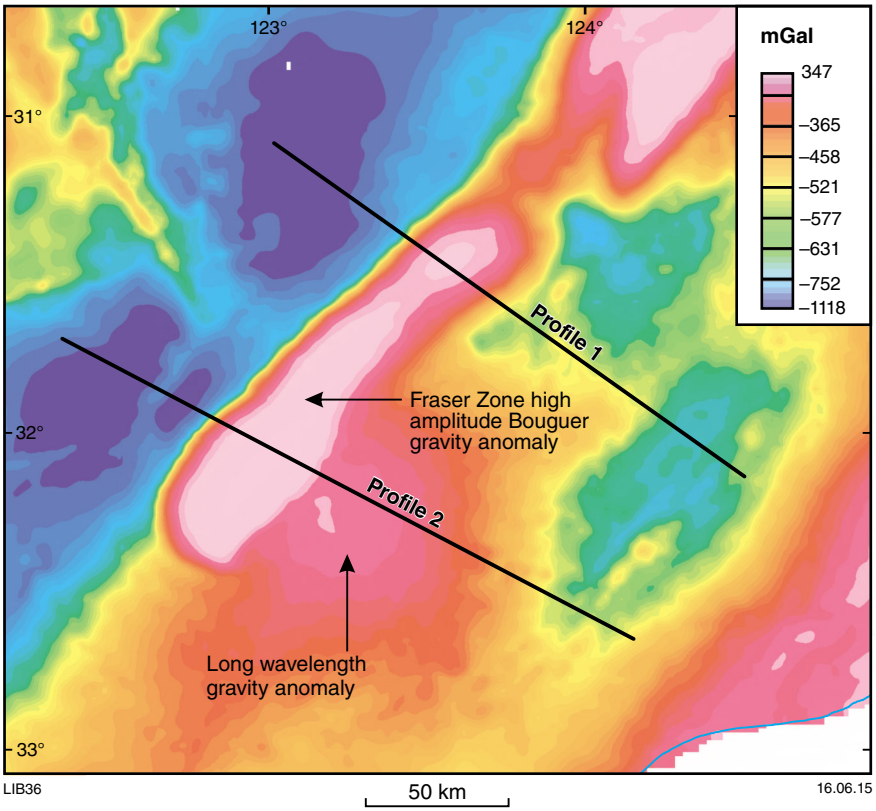

Figure 21. Location of forward modelled profiles 1 and 2 on Bouguer gravity data, showing gravity anomalies produced by the Fraser Zone and the long wavelength gravity anomaly to the southeast of the Fraser Zone in profile 2

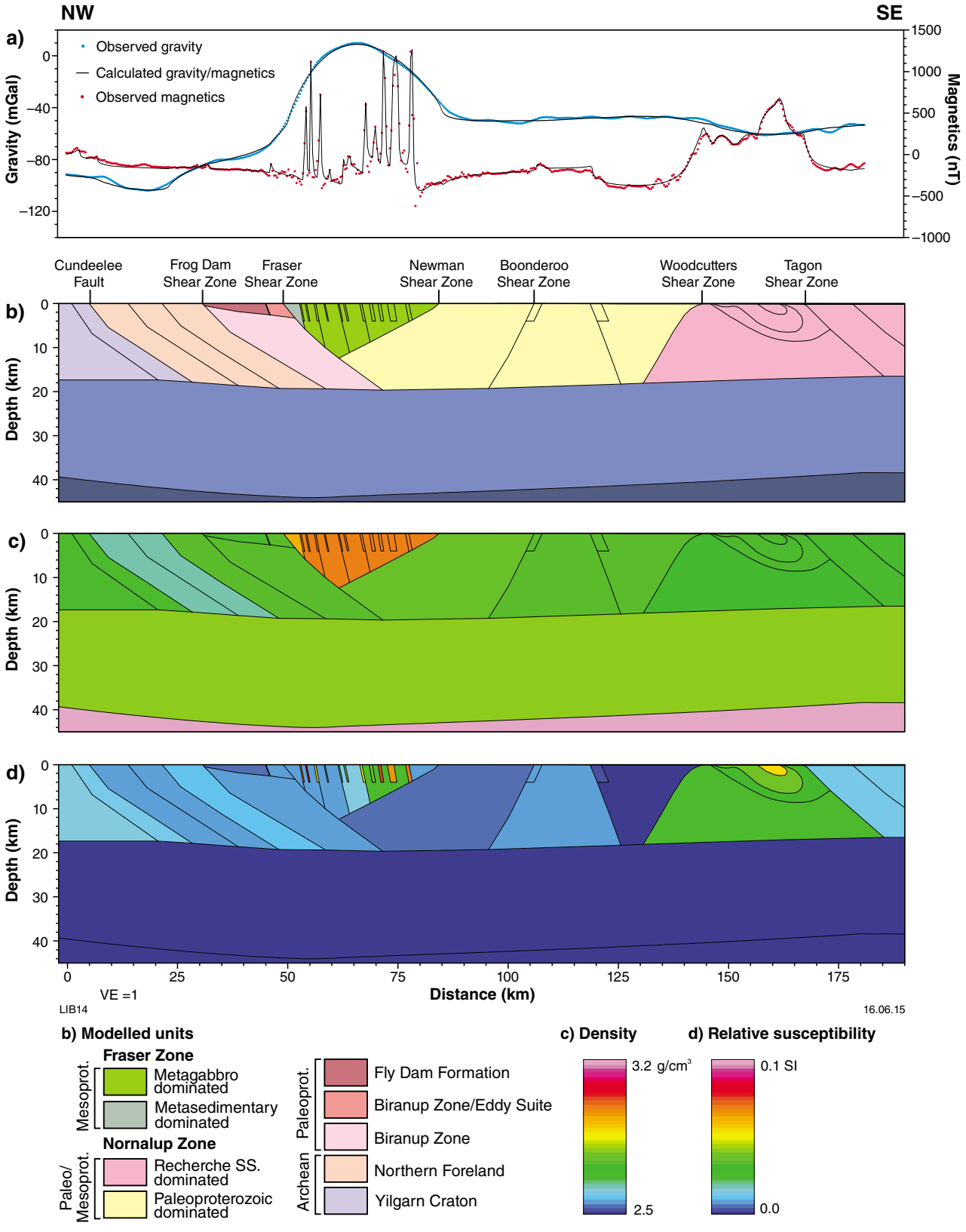

Figure 22. Forward model of profile 1: a) observed and calculated gravity and magnetic data; b) modelled units, showing major structures; c) density model; d) relative susceptibility model

The high-amplitude, high-frequency magnetic anomalies of the Fraser Zone (amplitude ~1500 nT relative to the Fraser Zone) are modelled as southeast-dipping units that extend to a depth of 4 km, below which sensitivity is low (Fig. 22d). In magnetic images these units are northeast-trending, highly magnetic horizons, some of which are isoclinally folded at a scale smaller than the resolution of the model. The southeast dip is based on the dominant asymmetry of the magnetic anomalies. The longer wavelength magnetic variations in the Fraser Zone are accounted for by units that extend to the base of the Fraser Zone (Fig. 22d). The boundaries of these units correspond to major shear zones (Spaggiari and Pawley, 2012).

To the southeast of the Fraser Zone, the geology is completely under cover and has been interpreted as Biranup-like Paleoproterozoic-dominated Nornalup Zone (Spaggiari and Pawley, 2012). This interpretation is based on the low magnetic intensity and smooth magnetic texture characteristic of the Biranup Zone rather than the typically higher susceptibility Recherche Supersuite dominated Nornalup Zone. The interpreted Paleoproterozoic-dominated crust is intersected by several major structures. One of these structures is the Boonderoo Shear Zone (Spaggiari and Pawley, 2012); however, because there is little magnetization contrast across this structure it is difficult to constrain its orientation with forward modelling. At the southeastern end of the profile, the Paleoproterozoic-dominated Nornalup Zone is interpreted as separated from the Recherche Supersuite – dominated Nornalup Zone by the Woodcutters Shear Zone (Spaggiari and Pawley, 2012). There is a strong magnetic and gravity contrast across the Woodcutters Shear Zone, and forward modelling suggests this structure can be modelled as northwest dipping and steepening with depth.

The part of the Nornalup Zone dominated by the Recherche Supersuite is interpreted to the southeast of the Woodcutters Shear Zone. The source of the high-amplitude magnetic anomaly and coincident gravity low in the Recherche Supersuite – dominated Nornalup Zone is modelled as a magnetically zoned pluton (Fig. 22d). To the southeast, the Tagon Shear Zone separates this highly magnetic pluton from lower magnetic intensity crust (Spaggiari and Pawley, 2012). Forward modelling of the strong magnetic contrast and slight gravity contrast across the Tagon Shear Zone suggest this structure dips to the southeast.

Profile 2

Profile 2 is 70 km to the southwest of profile 1 (Figs 6 and 21). Dominant features in the Bouguer gravity data include the high-amplitude anomaly above the Fraser Zone, and a long wavelength (~150 km) gravity high to the southeast of the Fraser Zone (Fig. 23a). One of the aims of modelling profile 2, and in particular the gravity data, was to suggest a source for this long wavelength Bouguer gravity anomaly. The aeromagnetic data in the Northern Foreland, Biranup Zone, and the northwest Fraser Zone are of low intensity and smooth texture. Aeromagnetic data in the southeast Fraser Zone and the Nornalup Zone, however, contain many high-frequency, high-amplitude anomalies (Fig. 23a). Because of the complex, overlapping nature of the magnetic anomalies, particularly above the Nornalup Zone, only broad peaks and troughs have been modelled in profile 2. Longer wavelength features in the aeromagnetic data above the Nornalup Zone include a low above the demagnetized Newman Shear Zone, a broad increase in magnetization to the southeast of the Newman Shear Zone, and a decrease towards the southeastern end of the profile (Fig. 23a).

The Northern Foreland, similar to profile 1, is interpreted to form three southeast-dipping units that extend to the top of the lower crust. This geometry, as in profile 1, is based on structural observations, which suggest the Northern Foreland and the adjacent southeast margin of the Yilgarn Craton are dominated by northwest-vergent folds and thrusts. The boundaries of these three southeast-dipping units correspond to major structures previously interpreted by Spaggiari and Pawley (2012). The Bouguer gravity data of the Northern Foreland and Yilgarn Craton margin contain a long wavelength low that extends along much of the Yilgarn Craton's southern margin. This long wavelength feature extends outside the limit of the model, making it difficult to constrain with the profiles modelled in this study. Superimposed on the long wavelength Bouguer gravity low are shorter wavelength peaks and troughs. The source of the short wavelength gravity trough is interpreted as the southeastern unit of the Northern Foreland. In profile 2, the density required to produce this short wavelength trough is lower (2.60 g/cm^3) than the median value for the Northern Foreland felsic intrusives (~2.64 g/cm^3) and lower than values obtained for granites of the Agnew–Wiluna belt (Williams, 2009). It is most likely that the southeastern unit of the Northern Foreland has a density greater than 2.60 g/cm^3 and the broad gravity trough is produced by a large low-density body at depth along the margin of the Yilgarn Craton. Based on a deep crustal seismic and gravity study, Tassell and Goncharov (2006) suggest that the source of this gravity low is a deep crustal root beneath the margin of the Yilgarn Craton and the Albany–Fraser Orogen.

To the southeast of the Northern Foreland, the Biranup Zone is modelled as a southeast-dipping unit that is narrower than in profile 1, although with a similar moderate density (2.75 g/cm^3) and low relative susceptibility (–0.007 SI). Like profile 1, the geometry of the Biranup Zone is based on sparse, steeply southeast-dipping foliations.

The Fraser Zone was modelled in 2.5D, with an along-strike length of 20 km to the southwest and 120 km to the northwest and a density of 3.00 g/cm^3. As in profile 1, the Fraser Zone is near-triangular although it extends to a greater depth of 15.4 km (Fig. 23). Aeromagnetic data in the northwest Fraser Zone are subdued, with high-frequency, although low-amplitude, magnetic anomalies. In map-view these magnetic anomalies correspond to the folded magnetic horizons of subdomains 2 and 3 of the Fraser Zone. The regional-scale synforms and antiforms in subdomains 2 and 3 of the Fraser Zone are shown in the northwest of profile 2. Unlike in the northwest, the southeast Fraser Zone contains many high-frequency, high-amplitude magnetic anomalies.

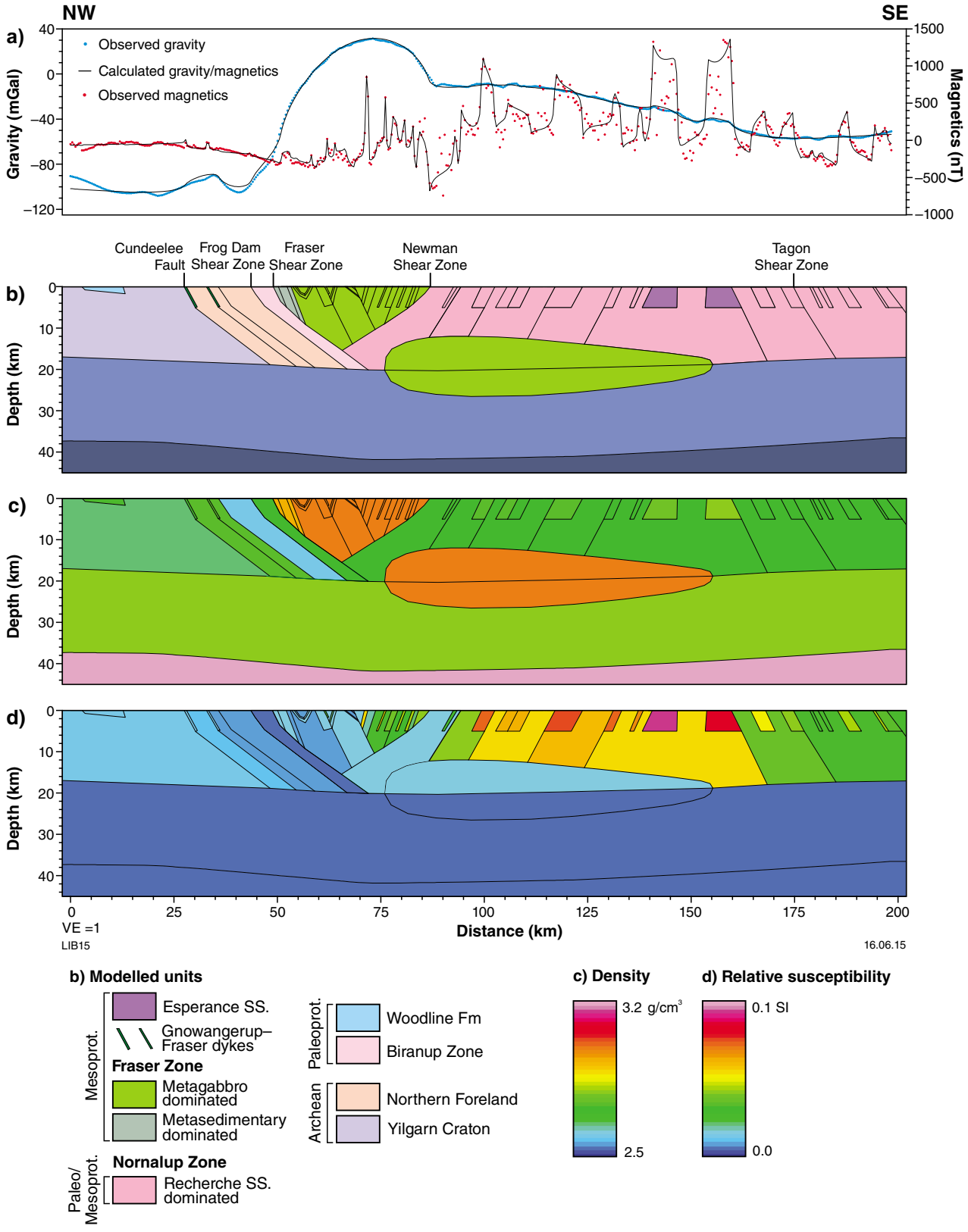

Figure 23. Forward model of profile 2: a) observed and calculated gravity and magnetic data; b) modelled units, showing major structures; c) density model; d) relative susceptibility model

In map-view these magnetic anomalies correspond to the magnetic horizons of subdomain 6 of the Fraser Zone, which are folded around an apparently north-trending fold axis (Fig. 15). Based on the asymmetry of the magnetic anomalies and structural observations from the 1:250 000 Balladonia map sheet (Doepel and Lowry, 1970a), these folded horizons are modelled as dipping to northwest (Fig. 23).

The internal architecture of the Nornalup Zone, which begins directly southeast of the Newman Shear Zone, is difficult to constrain. This is partly because the Nornalup Zone is almost entirely under cover, and partly because the magnetic data are dominated by numerous overlapping magnetic anomalies (Fig. 23a).

The Nornalup Zone crust, or the crust beneath the Nornalup Zone, contains a long wavelength (~150 km) Bouguer gravity high. This anomaly can be accounted for by a mid-crustal body, modelled in 2.5D with an along-strike extent of 20 km to the southwest and 10 km to the northeast, with a density of 3.00 g/cm^3 and maximum thickness of approximately 14.5 km (Fig. 23c). This long wavelength Bouguer gravity high appears symmetric and therefore the shape of the source is assumed to be subhorizontal. Sensitivity testing of this body is discussed in the following section. Superimposed on the long wavelength Bouguer gravity high are higher frequency gravity highs, most of which are at a scale smaller than can be represented on the model. Some of the high-frequency, high-density anomalies (modelled with densities of 2.78 and 2.80 g/cm^3) are coincident with intense magnetic anomalies and which are reported as shallow intermediate intrusions (Williams and Robertson, 2011).

The high-frequency magnetic anomalies of the Nornalup Zone have been modelled broadly to a depth of 5 km, beyond which sensitivity is limited. Constraining the dip of these anomalies is hindered by their complex overlapping nature. Aeromagnetic images of the Nornalup Zone show prominent, north- to northeast-trending, curvilinear demagnetized zones, several of which have been interpreted as major structures that separate domains with different structural and magmatic trends (Fig. 10). However, magnetic profiles of the Nornalup Zone are dominated by high-frequency, high-amplitude anomalies that make it difficult to determine whether demagnetized zones are major structures or not, and what their orientation is. Also interpreted in map-view in the Nornalup Zone are north- to northeast-trending folds (~3 to 10 km in width) truncated by northeast-trending shears. However, the complex overlapping magnetic anomalies (Fig. 23d) make it difficult to constrain the dip direction of shears or the axial plane and plunge of folds. This problem could be overcome by making multiple, along-strike profiles from upward continued data and trying to identify common longer wavelength features that may be associated with major structures.

Sensitivity testing

The Fraser Zone in profile 1 and the mid-crustal mafic body in profile 2 were sensitivity tested. Here, sensitivity testing refers to varying the density and geometry of bodies, within constraints of the specific gravity data and the surface geology, to test the range of possible geometries and physical properties. In profile 1, the Fraser Zone has been attributed densities of 2.95, 3.00, and 3.10 g/cm^3, and extends to maximum depths of approximately 19.4, 12.4, and 7.6 km, respectively (Fig. 24). Densities lower than 2.95 g/cm^3 are not possible if the surface location of the Fraser Zone is honoured and densities higher than 3.10 g/cm^3 are not likely given the specific gravity dataset. The models with a density of 2.95 g/cm^3 are Fraser Zone with a higher proportion of either or both metasedimentary rock and metagranite, and models with a density of 3.10 g/cm^3 are Fraser Zone with a higher proportion of metagabbro and possibly ultramafic rocks. Ultramafic intrusives do not commonly outcrop in the southwest Fraser Zone although they have been reported in drillcore from Nova–Bollinger (Smithies et al., 2013) and in the Fraser Zone to the northeast of the study area (Orion Gold NL, 2013).

The mafic body, interpreted as the source of the long wavelength Bouguer gravity high in profile 2, was also sensitivity tested. Although no petrophysical constraints are available, the specific gravity was varied within a range of values geologically reasonable for mafic and ultramafic rocks. The interpreted mafic body has been modelled in the mid-crust with densities of 2.95, 3.00, 3.10, and 3.20 g/cm^3, with the thickness of the body at 17.7, 14.5, 11.1, to 8.8 km, respectively (Fig. 25). The mafic body was been modelled in the lower crust, and with densities of 3.10 and 3.20 g/cm^3 the thickness of the body varies from 17.8 to 16.3 km, respectively (Fig. 26). Although possible, a lower crustal body with such a large thickness is considered less likely than a thinner mid-crustal body.

Discussion

Structural interpretation

Fraser Zone

The magnetic horizons in the Fraser Zone are interpreted as a combination of gneissic layering defined by lithological variations and subparallel structures (Fig. 27a). The sequence of deformation interpreted from aeromagnetic images includes the formation of the magnetic horizons and the subsequent folding and shearing of these horizons. This gneissic layering has been interpreted to have formed shortly after the emplacement of the Fraser Zone magmas during Stage I of the Albany–Fraser Orogeny (Kirkland et al., 2011a, b). Clark et al. (2014) suggest this foliation formed during Stage I of the Albany–Fraser Orogeny at c. 1290 Ma under peak metamorphic conditions of c. 850°C and 7–9 kbar. Magnetic horizons, if they represent this gneissic layering, may also have formed during Stage I.

Magnetic horizons have then been folded into regional-scale folds that vary between approximately 1 and 6 km in width. Regional-scale, northeast-trending tight to isoclinal folds (~6 km in width) have been interpreted

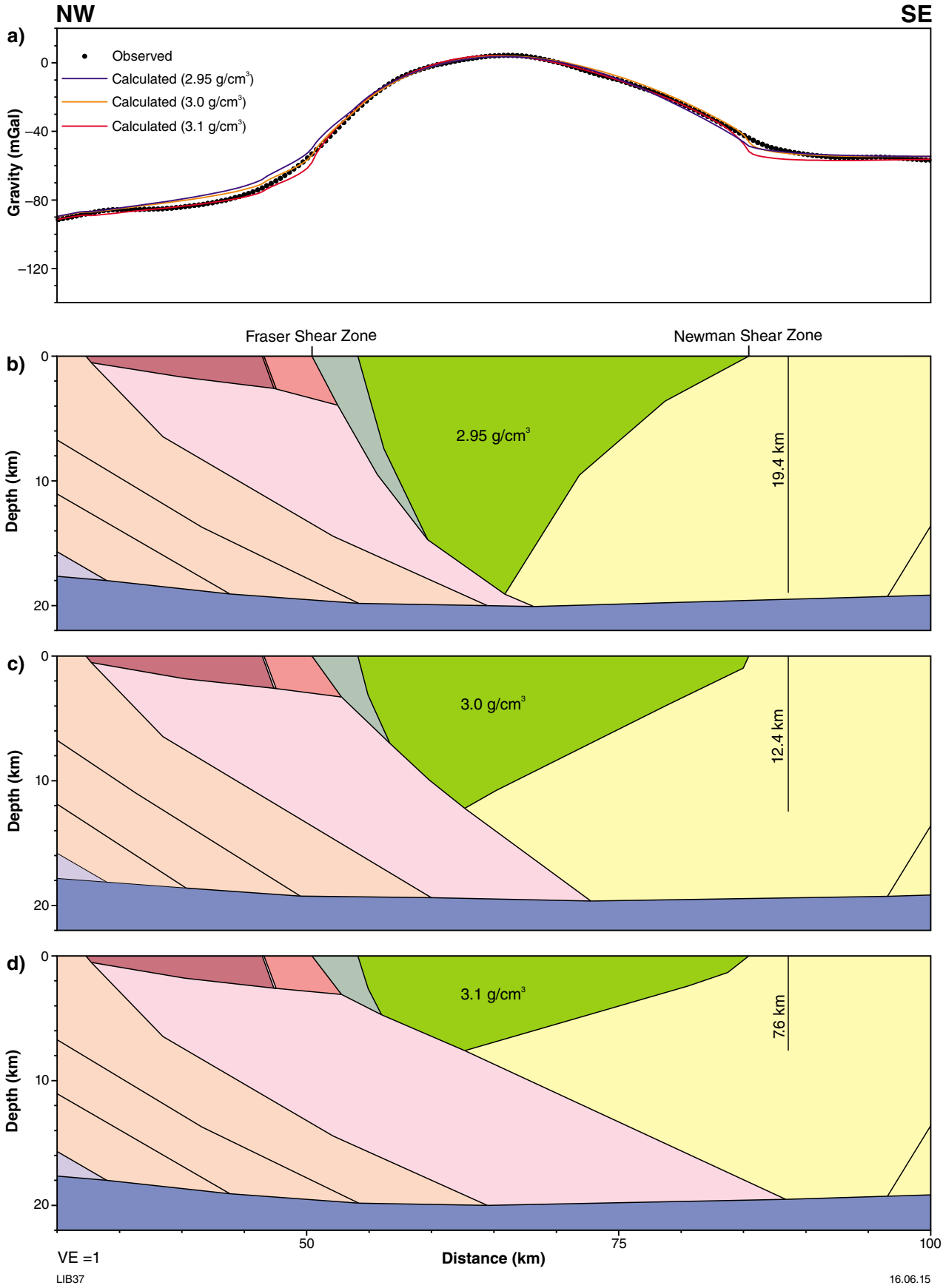

Figure 24. Profile 1 Fraser Zone density sensitivity test: a) observed gravity data and calculated gravity responses of the models. Fraser Zone modelled with a density of: b) 2.95 g/cm^3; c) 3.00 g/cm^3; d) 3.10 g/cm^3

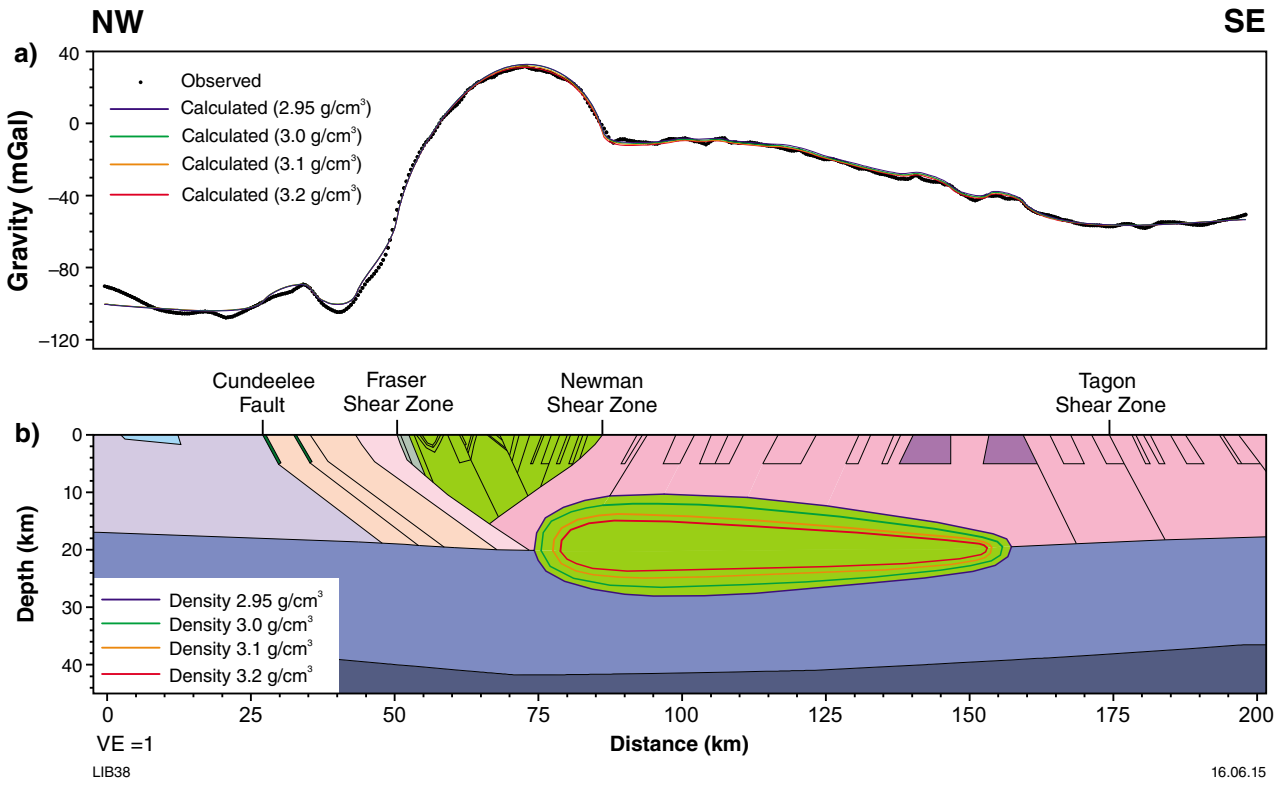

Figure 25. Profile 2 sill density sensitivity test: a) observed gravity data and the calculated gravity responses of the models in part b); b) mid-crust body modelled with densities of 2.95, 3.00, 3.10, and 3.20 g/cm³

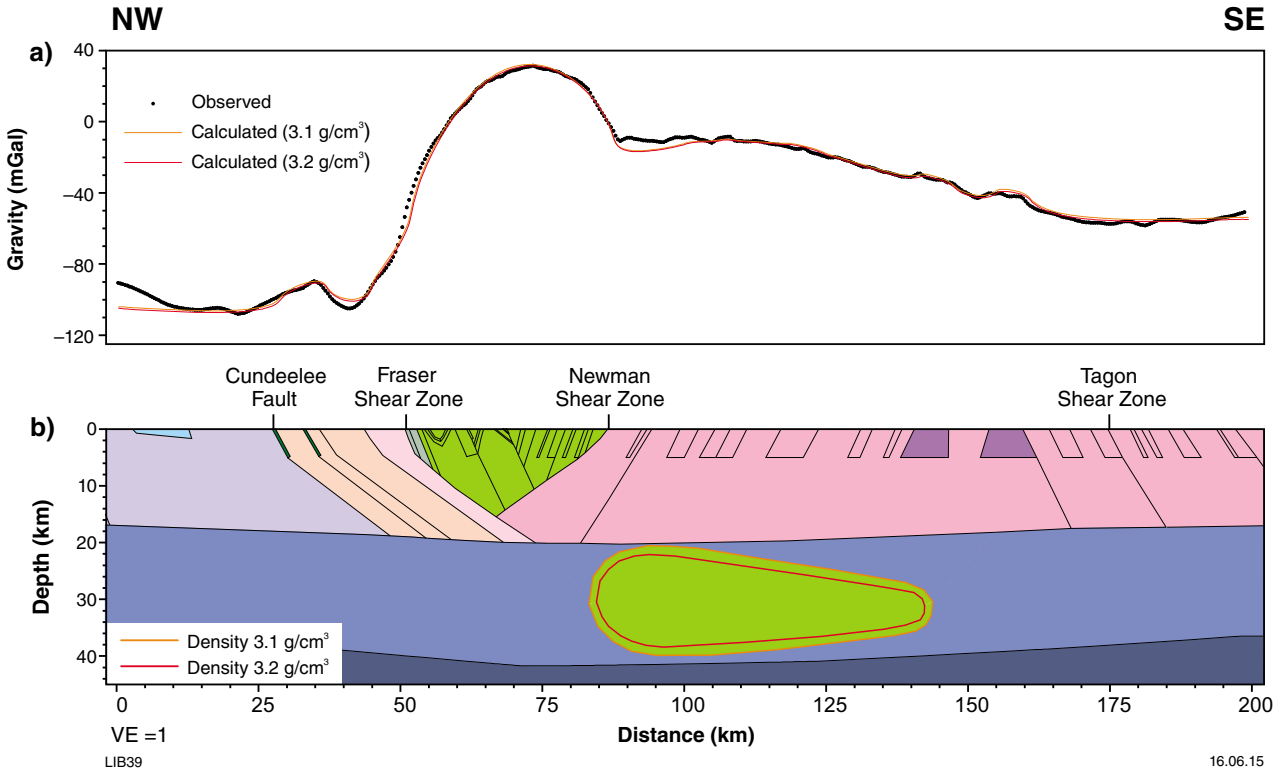

Figure 26. Profile 2 sill density sensitivity test: a) observed gravity data and the calculated gravity responses of the models in part b); b) lower crustal body modelled with densities of 3.10 and 3.20 g/cm³

previously in aeromagnetic images of the Fraser Zone (Spaggiari and Pawley, 2012). This work identifies more northeast-trending, isoclinal folds (~1 km in width) in the southwest Fraser Zone. Whether the larger (~6 km) and smaller (~1 km) regional-scale folds were produced during the same regional-scale folding event is not known. The age of the regional northeast-trending folding and shearing in the Fraser Zone is not known. There are several possible interpretations of the relationship between the tight to isoclinal regional-scale folds from aeromagnetic images and the outcrop-scale isoclinal intrafolial folds. First, the gneissic layering and intrafolial folds occurred as part of a progressive deformation event that culminated in the regional-scale folds. This interpretation is supported by folds having the same trend and geometry and would imply that regional-scale folding occurred during Stage I.

Second, the regional-scale folding and shearing may have formed during a later deformation event that overprints the gneissic foliation and intrafolial folds, possibly during Stage II of the Albany–Fraser Orogeny. The lack of preserved Stage II metamorphic ages in the Fraser Zone (Kirkland et al., 2011a, b) does not necessarily indicate a lack of deformation during Stage II; it may just indicate that prior to Stage II the Fraser Zone had been exhumed to shallow crustal levels, unfavourable for zircon growth (Kirkland et al., 2011a, b). Jones and Hall (2004) describe steep northeast-striking shear bands (D_{F2}) that overprint the gneissic layering (D_{F1}) (Fig. 27b). Given the differences in scale, it is not possible to directly correlate the structures in outcrop with structures in aeromagnetic images. The northeast-striking demagnetized shear zones in aeromagnetic images (Fig. 27a) could have formed during either the D_{F1} or D_{F2} event reported by Jones and Hall (2004) (Fig. 27b).

In subdomain 2 of the Fraser Zone, the along-strike width of the fold varies from approximately 2 to 6 km (Spaggiari and Pawley, 2012; this study), suggesting that one deformation event can produce folds of varying width. This variation in fold width may result from variations in stress, or differences in lithology. Higher strain zones may be dominated by either or both metasedimentary and metagranitic rocks, which are relatively less competent, whereas the lower strain zones may contain more relatively competent metagabbro.

The Fraser Zone also contains several eye-shaped aeromagnetic anomalies (Fig. 28a). Given the lack of outcrop above these anomalies, the interpretation of these features cannot be constrained using structural observations. One interpretation is that these features are doubly plunging antiforms or synforms of non-cylindrical folds (Fig. 28b). Alternatively, they could be large-scale proxies for sigma-mantled porphyroclasts (magnetic porphyroclasts; Fig. 28c) (after Betts et al., 2007). According to the porphyroclast model, magnetic horizons are interpreted as material dominated by either or both metagranite and metasedimentary rock, which wrap around relatively rigid metagabbro-dominated 'clasts'. The possible magnetic porphyroclasts in the study area appear to have a slight dextral asymmetry.

There is some field-based structural evidence near the eye-shaped anomalies for dextral movement on northeast-trending shears. In the northwest of the Fraser Zone, a northeast-trending, gneissic foliation is associated with a weakly developed, northeast-plunging lineation and asymmetric tails on augen that suggest a component of dextral shear (Jones and Hall, 2004). Approximately 35 km to the north-northeast of the eye features, structural measurements from the ZANTHUS map sheet show

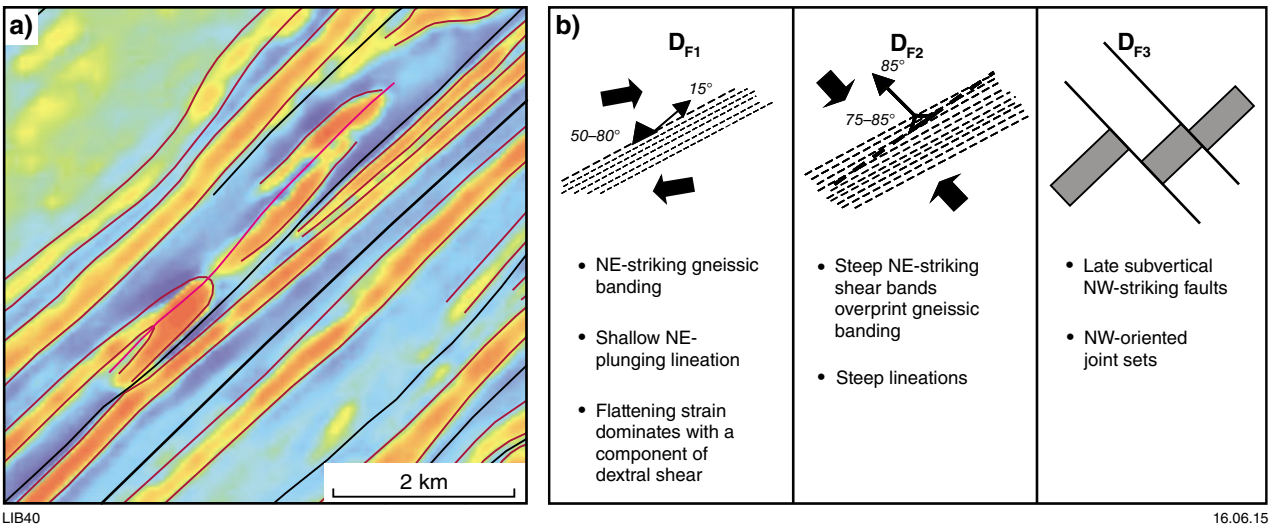

Figure 27. a) Northeast-trending high- and low-intensity magnetic horizons in the Fraser Zone (key shown in Fig. 11b); b) sequence of deformation events described in outcrop in the northwest Fraser Zone (figure from Jones and Hall, 2004); northeast-striking magnetic horizons are parallel to both the gneissic layering and northeast-striking shears (D_{F1} and D_{F2}, respectively, of Jones and Hall, 2004).

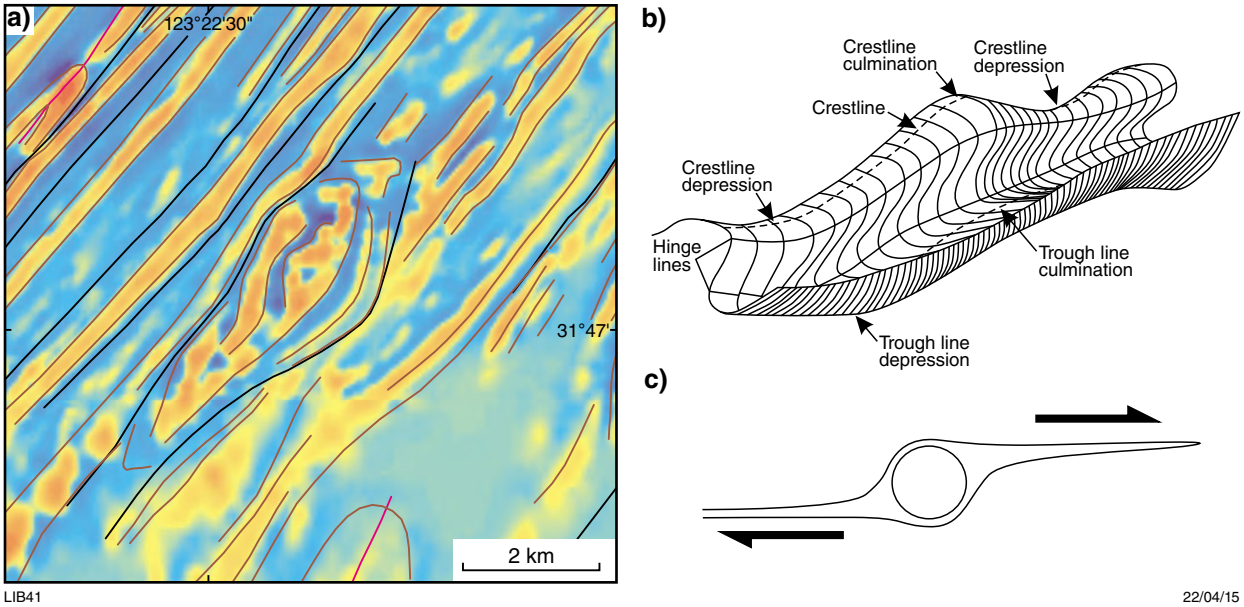

Figure 28. a) Eye-shaped aeromagnetic anomaly, shown in reduced to the pole first vertical derivative (RTP 1VD image) (key shown in Fig. 11b). Possible interpretations of this anomaly include: b) doubly plunging antiforms and synforms of non-cylindrical folds (from Twiss and Moores, 1992); c) large-scale proxies for porphyroclasts (from Passchier and Trouw, 1996).

northeast-trending, steeply dipping foliation and mineral lineations that plunge gently to moderately to the northeast. However, this dextral movement in the northwest of the Fraser Zone may be associated with the dextral movement reported on and near the Fraser Shear Zone (Myers, 1985; Spaggiari et al., 2011) and not within the Fraser Zone. The interpretation of the eye-shaped magnetic anomalies as non-cylindrical folds is perhaps more consistent with the regional-scale folds observed in aeromagnetic data (Spaggiari and Pawley, 2012; this study).

Subdomain 6 of the Fraser Zone also contains high- and low-intensity magnetic horizons that are tightly folded around north-northwest-trending fold axial traces. The north-northwest-trending folds correspond to the central and eastern parts of 'Unit 5' (Myers 1985), a region described as containing largely undeformed metabasic rocks (Fig. 29). This region is also covered by the Balladonia map sheet, which shows relatively good exposure, and restricted north- and northwest-striking, steeply dipping foliations that are roughly parallel to the magnetic horizons described in this study. As suggested above, the source of the magnetic horizons may be compositional variations in the bedding-parallel gneissic layering, or demagnetized shear zones. The regional-scale north-northwest-trending fold axial traces could be the non-cylindrical fold geometry of an overall northwest-vergent folding event. This interpretation is more consistent with other northeast-trending folds shown in outcrop and aeromagnetic data in the Fraser Zone. Alternatively, these fold traces may be north-trending axial planes, and preserve an episode of east–west compression. Given that the northeast magnetic horizons wrap around the north-trending magnetic horizons, north–west compression most likely occurred earlier than the southeast–northwest compression. The unusual trend of the axial trace in this region may result from lithological variations in the Fraser Zone, possibly a dominance of relatively competent metagabbro in this region.

Nornalup Zone

Regional-scale, tight to isoclinal northeast-trending folds and northeast-trending shear zones are the dominant structures observed in aeromagnetic data in the northwestern part of the Nornalup Zone. The shear zones and axial planes of folds trend northeast, although the dip direction of the axial planes, plunge of fold axes, and dip direction of the shear zones are not constrained. The structures described here have geometries consistent with a northwest-directed fold and thrust belt (Fig. 30). Alternatively, it is possible that the folds, rather than having an upright axial plane and non-cylindrical fold axis, have a vertical axial plane and steeply plunging fold axis. Field-based structural observations are needed to determine which of these models is more likely.

The Recherche Supersuite, in the eastern Albany–Fraser Orogen, is reported to include northeast-trending southeast side-up thrust zones that have been reactivated by dextral shearing under greenschist to amphibolite facies conditions (Clark et al., 2000). It is possible that the northeast-trending folds and shears described in the Nornalup Zone in this study are similar to the northeast-side-up thrust structures reported by Clark et al. (2000). Further fieldwork is needed to determine whether the northeast-trending shear zones have been reactivated by dextral shearing.

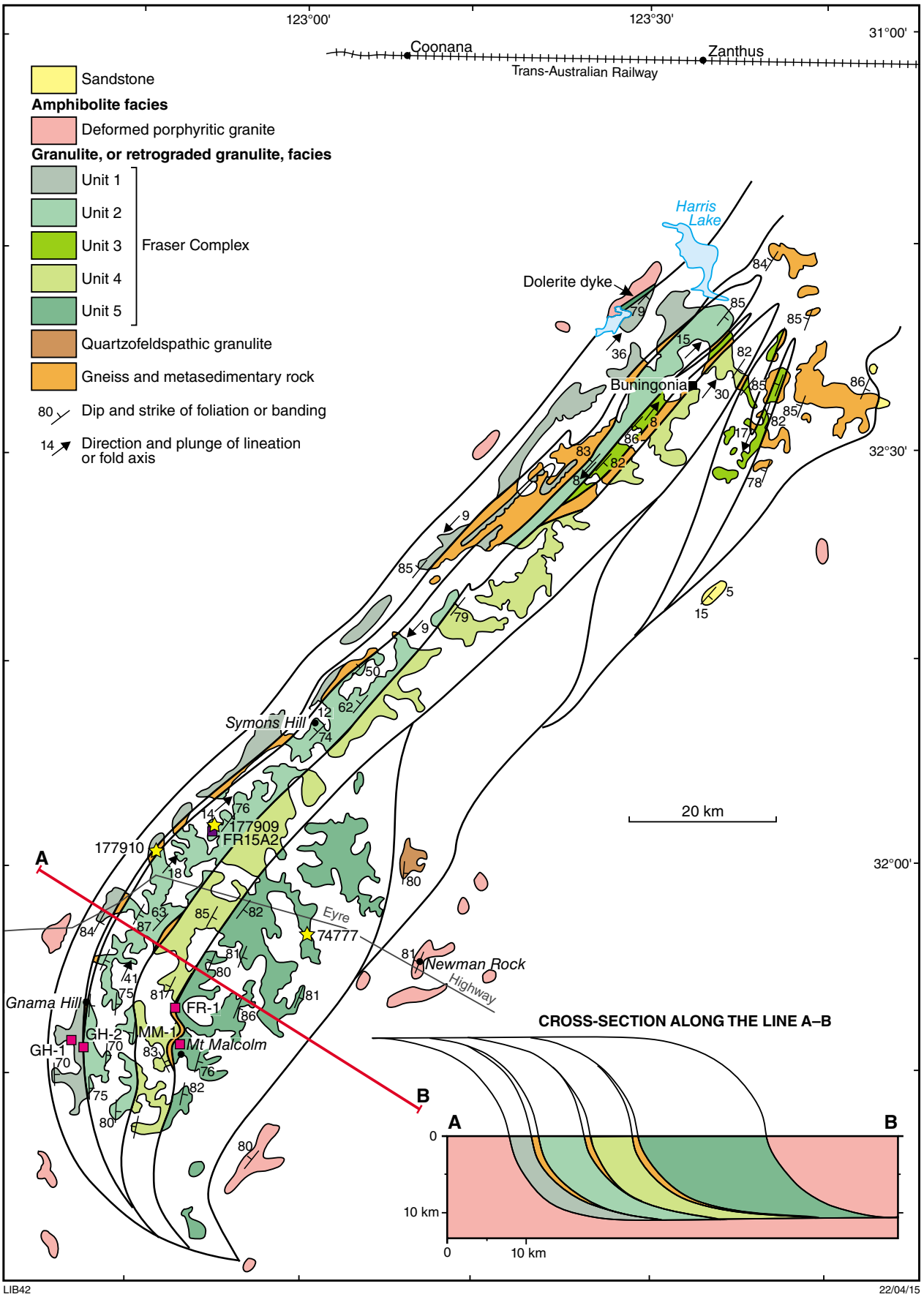

Figure 29. Map and interpreted section across the Fraser Zone, showing interpreted southeast-dipping thrust faults (Myers, 1985)

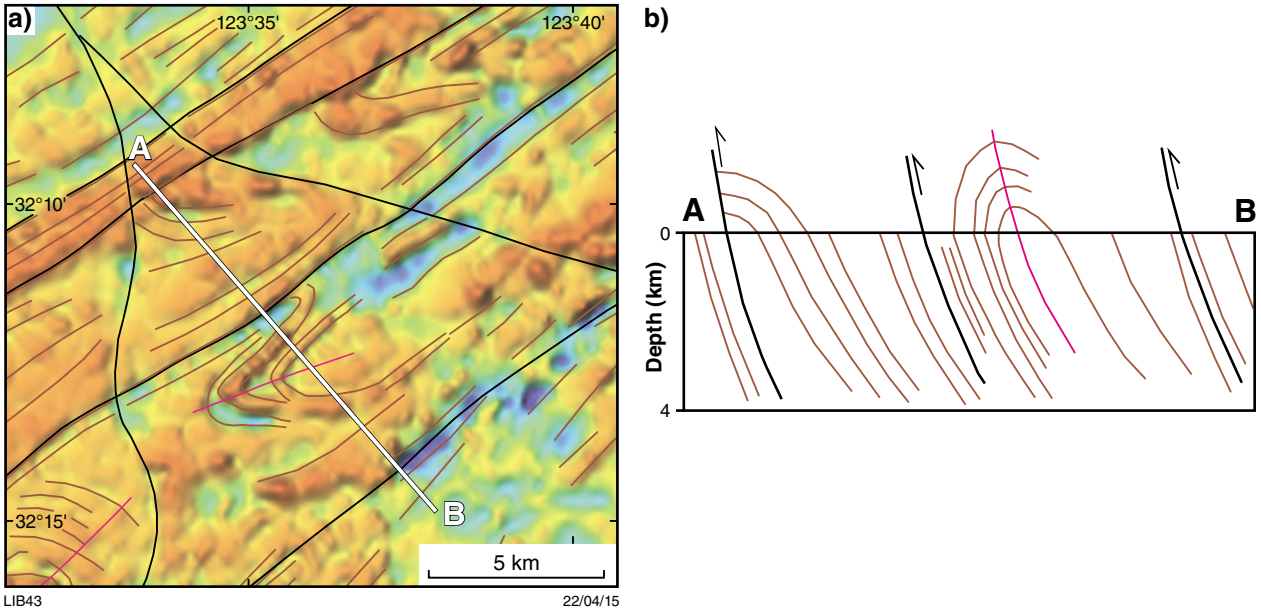

Figure 30. Nornalup Zone showing: a) possible northwest-directed fold and thrust system interpreted from reduced to the pole (RTP) aeromagnetic image; b) cross-section along profile A–B; key shown in Figure 11b

Domain 2 of the Nornalup Zone contains two lithologies, which have been dated, indicating metamorphism during Stage II of the Albany–Fraser Orogeny (Fig. 31). Near an interpreted north-trending shear, the protolith to a granitic gneiss with an irregular migmatitic fabric is dated at 1809 ± 8 Ma and yields a metamorphic date of 1198 ± 11 Ma, coincident with Stage II and interpreted as the age of migmatization (Kirkland et al., 2014). The trend of this migmatitic fabric is parallel to the north-northeast-trending, discontinuous magnetic trends near the geochronology sample. Approximately 4.7 km to the south of this sample, the protolith to a monzogranitic gneiss has a magmatic crystallization date of 1320 ± 8 Ma (Recherche Supersuite) and a metamorphic date of 1198 ± 7 Ma (GSWA 194786; MTD Wingate, 2015, written comm., 13 May), coincident with Stage II. The fabric of the monzogranitic gneiss is migmatitic, and trends to the north-northeast and dips steeply to the east. The north to northeast-trending magnetic fabrics and the regional-scale folding events most likely developed during Stage II of the Albany–Fraser Orogeny. However, further fieldwork is needed to resolve the age of migmatization in relation to the age of regional-scale folding.

Given the prevalence of Stage II metamorphic ages in the Nornalup Zone (Kirkland et al., 2011a, b) and the Stage II metamorphic age near the north-trending fold, it is likely that folding occurred during Stage II of the Albany–Fraser Orogeny. In the eastern Nornalup Zone, Clark et al. (2000) report northeast-trending, southeast side-up thrust zones, reactivated by dextral shearing under greenschist to amphibolite facies. Similar Stage II kinematics have been reported within the Coramup Shear Zone in the central Nornalup Zone, where dextral transpression is compartmentalized into pure shear, characterized by subvertical, southeast-dipping fold axial planes, and dextral simple shear, characterized by subvertical, southeast-dipping shear zones parallel to fold axial planes (Bodorkos and Clark, 2004). Resolving whether the northeast-trending folds and shears observed in aeromagnetic images in this study are equivalent to the structures described by Clark et al. (2000) and Bodorkos and Clark (2004) requires further structural and geochronology studies.

Magnetic and gravity forward modelling

Northern Foreland and Biranup Zone

The lack of density or magnetization contrasts within the Northern Foreland and the Biranup Zone, and between the Northern Foreland and the Biranup Zone, makes it difficult to constrain the geometries of these units at depth. However, the northwest-vergent fold and thrust geometry in the Northern Foreland (Jones and Ross, 2005; Spaggiari and Pawley, 2012) and in the Yilgarn Craton adjacent to the Northern Foreland were used to constrain the southeast-dipping geometry of the Northern Foreland and Biranup Zone in the forward models (Figs 22 and 23).

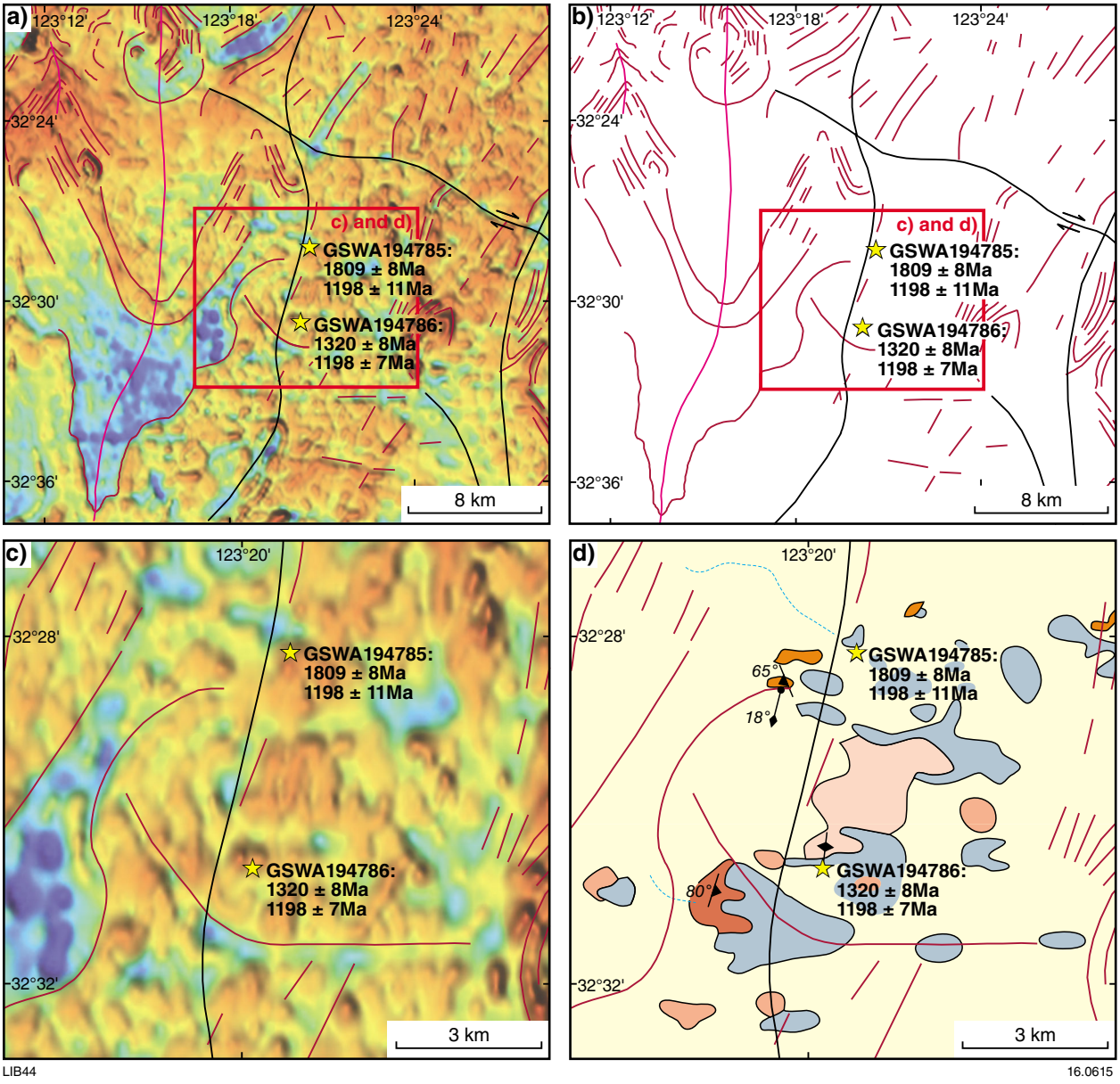

Figure 31. Domains 1 and 2 of the Nornalup Zone: a) reduced to the pole (RTP) aeromagnetic image, showing the north-trending fold of domain 1, discontinuous north-trending magnetic fabric of domain 2, and GSWA geochronology data; b) RTP aeromagnetic data at geochronology sites; c) RTP aeromagnetic image of geochronology sites; d) 1:250 000 mapped geology at geochronology sites

Fraser Zone

In this study, forward modelling of the magnetic and gravity fields suggests that the Fraser Zone, in section-view, is triangular and extends to a depth of approximately 14 km. This geometry is similar to previous results (Gee, 1979; Fig. 32). Gee (1979) used geologically constrained gravity modelling, along a profile similar to profile 2, to suggest that the Fraser Zone has a bowl-shaped geometry and extends to a depth of approximately 15 km.

In other early work, Myers (1985) divided the southwest Fraser Zone into five units (Fig. 29). In cross-section, the units of the Fraser Zone are bounded by major thrust faults that are interleaved with slivers of basement gneiss and metasedimentary rock, and interpreted to dip to the southeast (Myers, 1985). More recent interpretations of the section-view geometry of the Fraser Zone, interpreted primarily from structural observations, are presented on the Balladonia and Yardilla map sheets. The Balladonia 1:250 000 scale map sheet includes a section to approximately 6 km depth that traverses the southeastern margin of the Fraser Zone (Doepel and Lowry, 1970a). In this section the southeastern margin of the Fraser Zone, and the bounding Newman Shear Zone, are interpreted to dip steeply to the southeast.

The Yardilla 1:100 000 scale map sheet includes a cross-section to 4 km depth that traverses the northwestern margin of the Fraser Zone (Jones and Ross, 2005). In this section, the northwestern margin of the Fraser Zone, and the bounding Fraser Shear Zone, are interpreted as steeply northwest dipping, subparallel to the dominant foliations in the Fraser Zone.

The Fraser Zone is interpreted to be bounded by the Fraser Shear Zone and the Newman Shear Zone. In profile 2, the northwestern margin of the Fraser Zone dips about 40–65°SE and the Newman Shear Zone dips about 32°NW (Fig. 33a). In the Fraser Shear Zone, metamorphic foliations typically dip moderately to the southeast (e.g. Zanthus; Doepel and Lowry, 1970c) although there are also steeper southeast-dipping foliations. The dips of foliations in the Fraser Shear Zone are similar to the dip of the northwestern margin of the Fraser Zone in the forward models (Fig. 33a).

In the Newman Shear Zone, at Newman Rocks, foliations and mylonite zones dip steeply to the southeast and northwest (e.g Balladonia; Doepel and Lowry, 1970a) (Fig. 33b,c).The steep dip of the foliation in outcrop is different from the approximately 32°NW dip of the southeast margin of the Fraser Zone in the forward models (Fig. 33). One explanation is that the proto-Newman Shear Zone was originally a shallow structure and has been overprinted by steeper structures.

A triangular or bowl-shaped geometry for the Fraser Zone (Gee, 1979; this study) has also been suggested in recent magnetotelluric (MT) and deep crustal seismic surveys. The MT survey traverses the Fraser Zone along a very similar profile to profile 2 of this study (Dentith et al., 2010). In MT images, the Fraser Zone has been interpreted as a highly resistive, triangular feature (Kirkland et al., 2011b; Fig. 34). In Albany–Fraser Orogen deep crustal seismic line 12GA-AF3, which traverses the Fraser Zone to the northeast of profile 1, the Fraser Zone has been interpreted to have a bowl-shaped geometry (Spaggiari et al., 2014b; Fig. 35).

Mid-crustal mafic body

In the geologically constrained gravity model (Gee, 1979), the source of the long wavelength gravity anomaly is interpreted as an offset in a layer of lower crustal ?pyroxene granulite (Fig. 32). The lower crustal pyroxene granulite is interpreted as uplifted to the southeast of the Newman Shear Zone by normal movement on the northwest-dipping Newman Shear Zone. In this study, the source of the long wavelength gravity anomaly is interpreted as a subhorizontal mafic to ultramafic body in the middle crust. Although Gee (1979) suggested that the layer of lower crustal pyroxene granulite is present at depth along the entire length of the profile, in this study, the mafic–ultramafic body is interpreted to exist only beneath the gravity anomaly.

The Stage I mafic intrusive event that formed the Fraser Zone gabbros is also interpreted as the source of the subhorizontal mid-crustal body for several reasons. First, the Stage I event is the only known large mafic intrusive event in the Albany–Fraser Orogen. Second, the presence of primitive Nova–Bollinger magmas and more fractionated Fraser gabbros in the Fraser Zone (Smithies et al., 2013) suggests that the fractionation required to produce the Fraser gabbros from the Nova–Bollinger magmas would leave residual olivine and pyroxene. The interpreted mid-crustal sill may be a residual body of very dense pyroxene–olivine cumulate material. The geometry of the mid-crustal sill of mafic material, which is possibly a feeder of the Fraser Zone, may have been controlled by flat-lying extensional structures, along which they intruded.

Contribution to the tectonic evolution of the Fraser Zone

Having suggested a gross geometry for the Fraser Zone, it is possible to speculate how this geometry evolved. Based on its bowl-shaped geometry, Gee (1979) suggested that the geometry of the Fraser Zone is consistent with a northeast-plunging synform. It is possible that the regional-scale tight to isoclinal folds, observed in both aeromagnetic images and outcrop in the Fraser Zone, may reflect the larger scale geometry of the Fraser Zone.

It is also likely that the current geometry of the Fraser Zone is, to some extent, controlled by the precursors of the Fraser and Newman Shear Zones. It is possible that the southeast-dipping proto-Fraser Shear Zone and the northwest-dipping proto-Newman Shear Zone may have been major graben-forming faults. The graben formed by the proto-Fraser and Newman Shear Zones may have been a depocentre for the Arid Basin sedimentary rocks, and these structures may have also been a conduit for Fraser Zone magmas. Alternatively, the Fraser Zone magmas may have intruded into a half-graben

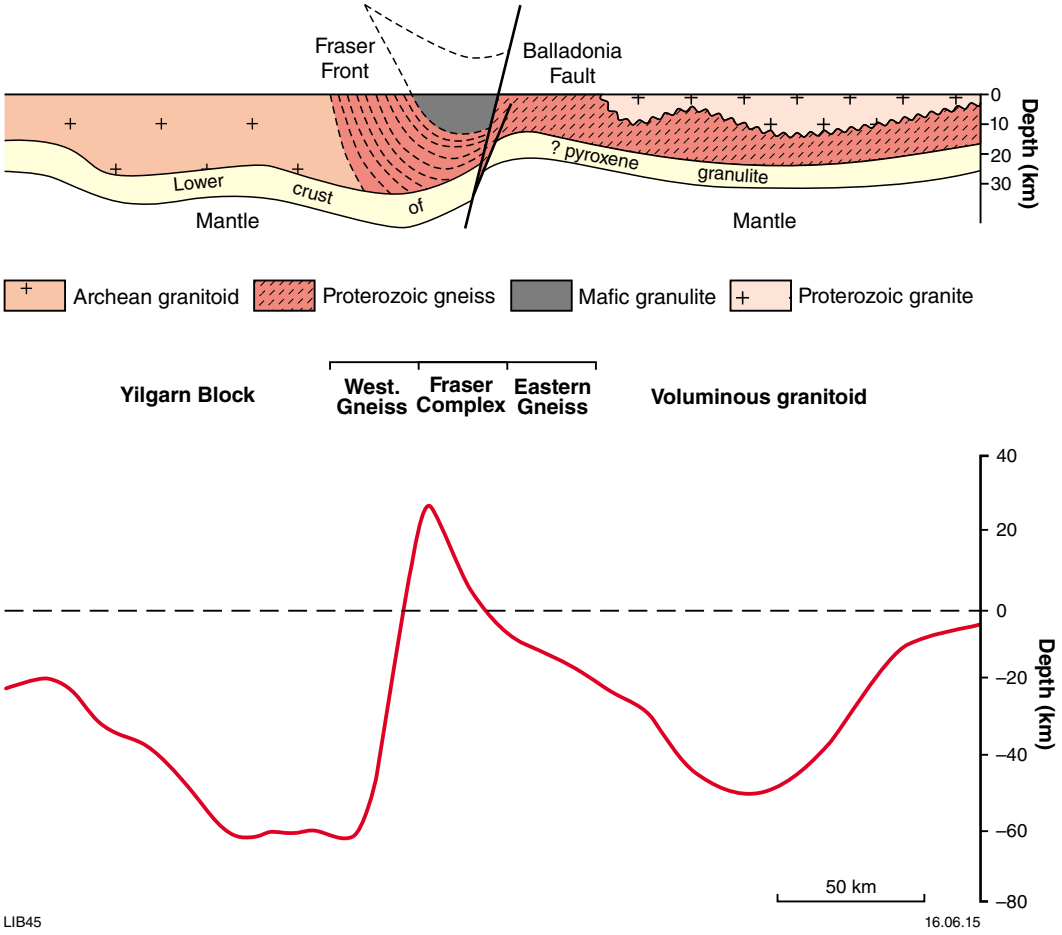

Figure 32. Geologically constrained density model of the Fraser Zone, showing the bowl-shaped geometry (Gee, 1979)

formed by normal movement on the Fraser Shear Zone. A graben or half-graben model is consistent with interpretations of the Fraser Zone metagabbro geochemistry, which suggests that the gabbros formed in an upwelling beneath an intracontinental rift or back-arc (Smithies et al., 2013), and other studies that suggest the Fraser Zone formed in the back-arc of west-dipping subduction to the east of the accreted Loongana arc (Spaggiari et al., 2014a).

Newman Rocks, within the demagnetized zone of the Newman Shear Zone, contain steeply northwest-dipping mylonite zones that have a southeast side-up, normal sense of movement (Gee, 1979; Spaggiari et al., 2011). The date of this movement is not known although it must post-date the 1297 ± 12 Ma Recherche Supersuite in which these structures exist (Kirkland et al., 2012). It is possible that the normal sense of movement in the mylonite zones in the Newman Shear Zone represents a Stage I extensional event. Alternatively, normal shearing may be part of a Stage II event. Structural evidence for extension has not been observed in the Fraser Shear Zone, although if it had occurred, it may have been overprinted by later shortening events.

The Fraser Zone terminates just southwest of the study area in a region informally called the ‘S-bend’, and which describes the shape of the joined Fraser and Newman Shear Zones (Spaggiari et al., 2011; Fig. 36). If the Fraser Zone intruded into an extensional tectonic setting with northeast-trending, basin-controlling normal faults, the southwest termination of the Fraser Zone may originally have been a major northwest-trending basin bounding structure (Fig. 36). During either or both Stage I and II, this northwest structure would have undergone a component of northwest–southeast shortening that possibly resulted in the folding of this structure around a northeast-trending fold axial trace (Fig. 36).

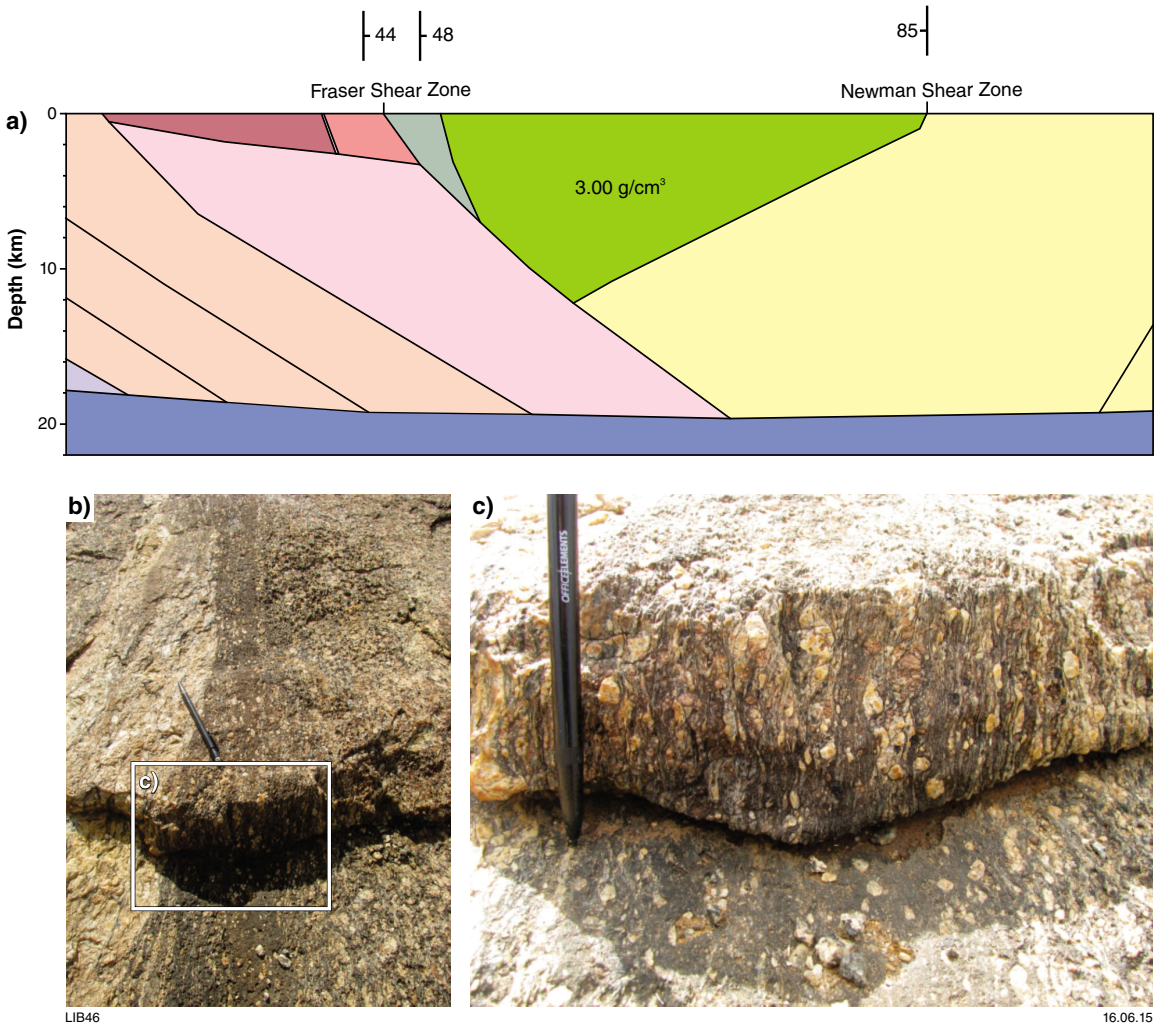

Figure 33. **a) Geometry of the Fraser Zone determined from magnetic and gravity forward modelling; b) northeast-trending mylonite zone at Newman Rocks in the Newman Shear Zone, pen points north; c) steeply dipping mylonite zones at Newman Rock in the Newman Shear Zone**

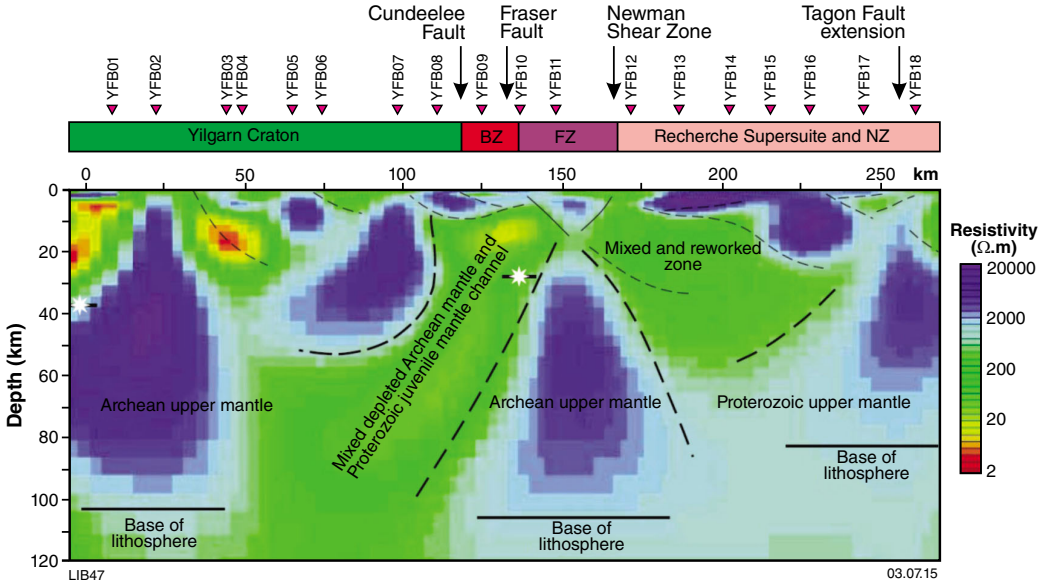

Figure 34. **Interpreted east Albany–Fraser Orogen magnetotelluric survey, showing the high-resistivity, triangular Fraser Zone (figure from Kirkland et al., 2011b). BZ, Biranup Zone; FZ, Fraser Zone; NZ, Nornalup Zone; star, the Moho; YFB, station numbers**

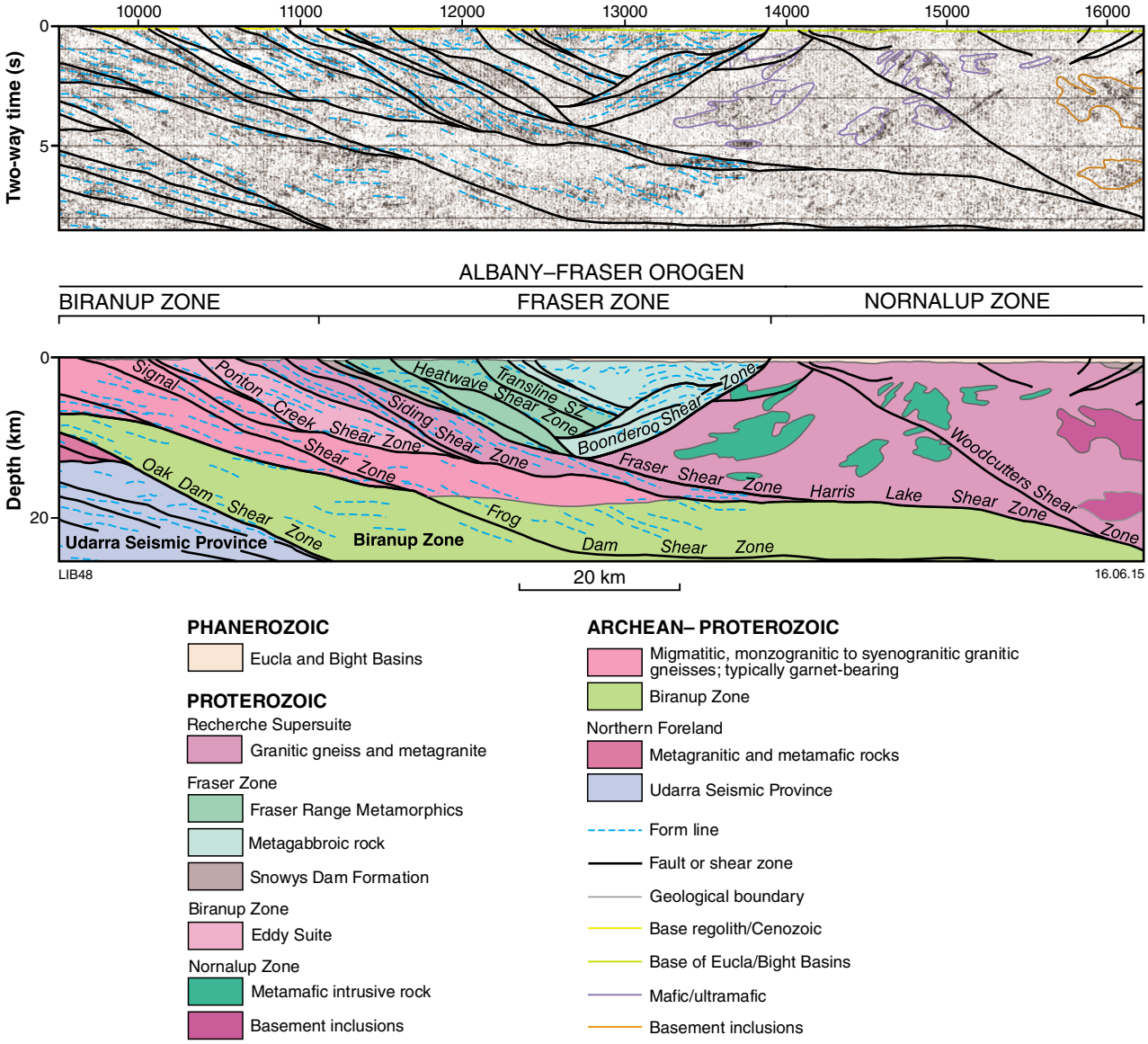

Figure 35. Geological interpretation of the Albany–Fraser Orogen deep crustal seismic line 12GA-AF3, showing the interpreted geometry of the Fraser Zone (figure from Spaggiari et al., 2014b)

Conclusion

Structural interpretation, based primarily on aeromagnetic image interpretation, suggests that the Mesoproterozoic Fraser Zone contains structural domains that can be characterized by: (1) regional-scale, northeast-trending tight to isoclinal folds (~1.6 to 4.5 km in width); (2) isoclinal folds (~500 m in width) truncated by northeast-trending shear zones and eye-shaped magnetic features, interpreted as either doubly plunging antiforms or synforms of non-cylindrical folds, or as 'magnetic porphyroclasts'; and (3) regional-scale, north- to north-northwest-trending, tight to isoclinal folds (~6 km in width). The Paleoproterozoic to Mesoproterozoic Nornalup Zone is divided into four structural domains that are characterized by: (1) north- and northeast-trending folds (~10 km in width); (2) north- and northeast-trending magnetic horizons, locally with northeast-trending tight folds (~3 km); (3) variably magnetic subcircular anomalies interpreted as plutons of the 1200–1140 Ma Esperance Supersuite; and (4) weakly magnetic northeast-trending horizons that locally are folded by isoclinal northeast-trending folds.

Geologically and petrophysically constrained forward modelling of the distinct Bouguer gravity high associated with the Fraser Zone suggests that the Fraser Zone is near-triangular and extends to depths of 12.4 and 15.4 km in profiles 1 and 2, respectively. The geometry of the Fraser Zone is likely controlled by the precursors of the Fraser and Newman Shear Zones, which may have formed a graben or half-graben structure that was a depocentre for Arid Basin sedimentary rocks. The proto-Fraser or proto-Newman Shear Zones may have also formed a conduit

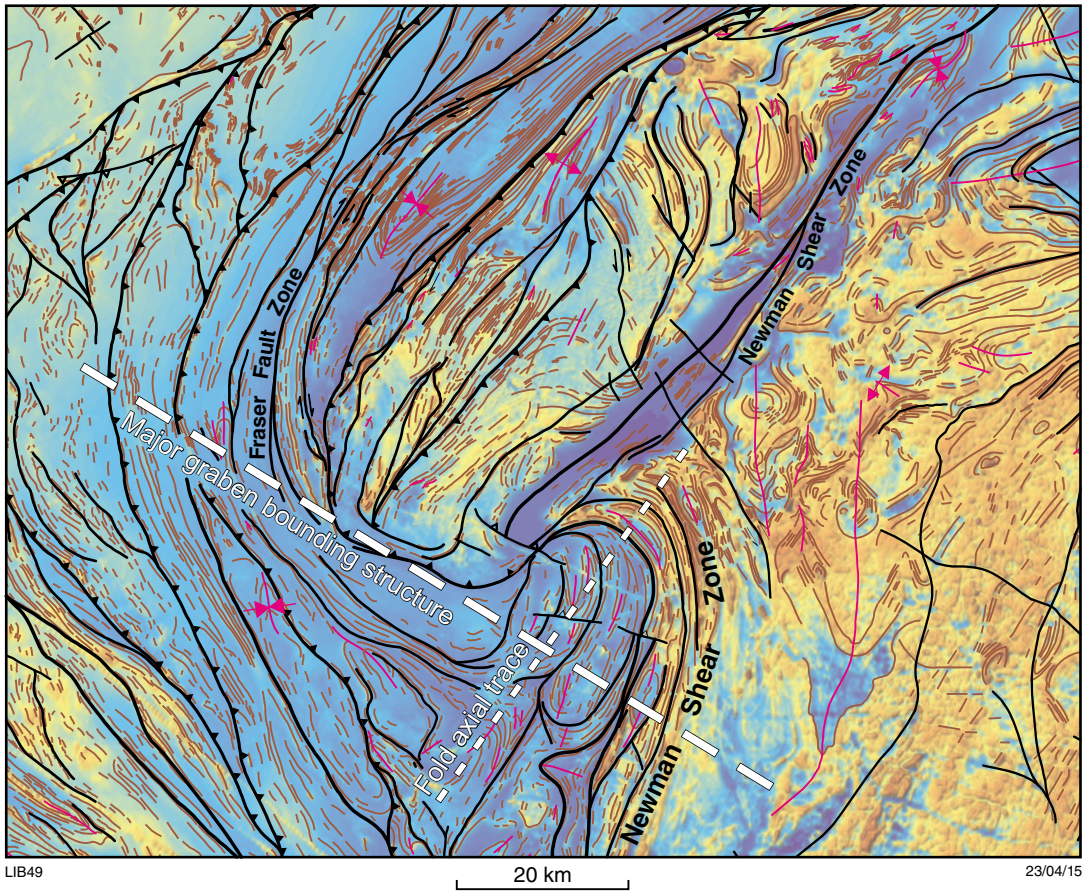

Figure 36. Reduced to the pole (RTP) aeromagnetic image of the 'S-bend' at the southwest margin of the Fraser Zone (aeromagnetic trend lines and structures outside the study area are from Spaggiari and Pawley, 2012); key shown in Figure 11b

for the Fraser Zone magmas. In the crust to the southeast of the Fraser Zone, Bouguer gravity data show a long wavelength (~150 km) gravity high. This long wavelength gravity anomaly can be accounted for by a subhorizontal, mid-crustal body of mafic–ultramafic composition. If attributed a specific gravity of 3.00 g/cm^3 this mid-crustal body will have a maximum thickness of about 14.5 km. Given the intrusion of the mafic–ultramafic rocks of the Fraser Zone is the only voluminous mafic intrusive event recorded in the Albany–Fraser Orogen, it is likely that the mid-crustal mafic body may have also formed during Stage I of the Albany–Fraser Orogeny.

References

Baranov, V 1957, A new method for interpretation of aeromagnetic maps: pseudo-gravimetric anomalies: Geophysics, v. 22, p. 359–383.

Barquero-Molina, M 2010, Kinematics of bidirectional extension and coeval NW-directed contraction in orthogneisses of the Biranup Complex, Albany Fraser Orogen, southwestern Australia: Geological Survey of Western Australia, Report 109, 205p.

Betts, PG, Valenta, RK and Finlay, J 2003, Evolution of the Mount Woods Inlier, northern Gawler Craton, Southern Australia: an integrated structural and aeromagnetic analysis: Tectonophysics, v. 366, no. 1–2, p. 83–111.

Betts, P, Williams, H, Stewart, J and Ailleres, L 2007, Kinematic analysis of aeromagnetic data: looking at geophysical data in a structural context: Gondwana Research, v. 11, p. 582–583.

Bodorkos, S and Clark, DJ 2004, Evolution of a crustal-scale transpressive shear zone in the Albany Fraser Orogen, SW Australia: 2. Tectonic history of the Coramup Gneiss and a kinematic framework for Mesoproterozoic collision of the West Australian and Mawson cratons: Journal of Metamorphic Geology, v. 22, no. 8, p. 713–731, doi: 10.1111/j.1525-1314.2004.00544.x.

Christensen, NI and Mooney, WD 1995, Seismic velocity structure and composition of the continental crust: A global view: Journal of Geophysical Research: Solid Earth, v. 100, no. B6, p. 9761–9788.

Clark, C, Kirkland, CL, Spaggiari, CV, Oorschot, C, Wingate, MTD and Taylor, RJ 2014, Proterozoic granulite formation driven by mafic magmatism: an example from the Fraser Range Metamorphics, Western Australia: Precambrian Research, v. 240, p. 1–21.

Clark, DA 1997, Magnetic petrophysics and magnetic petrology: aids to geological interpretation of magnetic surveys: AGSO Journal of Australian Geology and Geophysics, v. 17, no. 2, p. 83–103.

Clark, DJ, Hensen, BJ and Kinny, PD 2000, Geochronological constraints for a two-stage history of the Albany–Fraser Orogen, Western Australia: Precambrian Research, v. 102, no. 3, p. 155–183.

Clark, DJ, Kinny, PD, Post, NJ and Hensen, BJ 1999, Relationships between magmatism, metamorphism and deformation in the Fraser Complex, Western Australia: constraints from new SHRIMP U–Pb zircon geochronology: Australian Journal of Earth Sciences, v. 46, no. 6, p. 923–932, doi:10.1046/j.1440-0952.1999.00753.x.

Dentith, M, Evans, S, Ferguson, I, Gallardo, L, Joly, A, Cawood, PA, McCuaig, C and Tyler, IM 2010, Magnetotelluric surveys across major Precambrian tectonic boundaries in southern Western Australia, *in* ASEG Extended Abstracts: Australian Society of Exploration Geophysicists and Petroleum Exploration Society of Australia; ASEG 2010 21st International Geophysical Conference and Exhibition, Sydney, NSW, Preview 147, 4p.

Doepel, JJG and Lowry, DC (compilers) 1970a, Balladonia, Western Australia: Geological Survey of Western Australia, 1:250 000 Geological Series Explanatory Notes, 17p.

Doepel, JJG and Lowry, DC 1970b, Explanatory notes on the Balladonia 1:250 000 geological sheet, Western Australia: Geological Survey of Western Australia, Record 1970/11, 20p.

Doepel, JJG and Lowry, DC (compilers) 1970c, Zanthus, Western Australia: Geological Survey of Western Australia, 1:250 000 Geological Series Explanatory Notes, 17p.

Fletcher, IR, Myers, JS and Ahmat, AL 1991, Isotopic evidence on the age and origin of the Fraser Complex, Western Australia: a sample of Mid-Proterozoic lower crust: Chemical Geology: Isotope Geoscience, v. 87, p. 197–216.

Gee, RD 1979, Structure and tectonic style of the Western Australian Shield: Tectonophysics, v. 58, p. 327–369.

Geological Survey of Western Australia 2014, 1:500 000 State interpreted bedrock structural lines, 2014: Geological Survey of Western Australia.

Grant, FS 1985, Aeromagnetics, geology and ore environments, I. Magnetite in igneous, sedimentary and metamorphic rocks: an overview: Geoexploration, v. 23, p. 303–333.

Hall, CE, Jones, SA and Bodorkos, S 2008, Sedimentology, structure and SHRIMP zircon provenance of the Woodline Formation, Western Australia: implications for the tectonic setting of the West Australian Craton during the Paleoproterozoic: Precambrian Research, v. 162, p. 577–598, doi:10.1016/j.precamres.2007.11.001.

Isles, DJ and Rankin, LR 2013, Geological interpretation of aeromagnetic data: The Australian Society of Exploration Geophysicists, Perth, Western Australia, 357p.

Jones, SA and Hall, CE 2004, Archaean and Proterozoic geology of the southeastern margin of the Yilgarn Craton — a field guide: Geological Survey of Western Australia, Record 2004/18, 37p.

Jones, SA and Ross, AA 2005, Yardilla, WA Sheet 3434: Geological Survey of Western Australia, 1:100 000 Geological Series.

Kennett, BLN, Salmon, M, Saygin, E and AusMoho Working Group 2011, AusMoho: the variation of Moho depth in Australia: Geophysical Journal International, v. 187, no. 2, p. 946–958, doi:10.1111/j.1365-246X.2011.05194.x.

Kirkland, CL, Spaggiari, CV, Pawley, MJ, Wingate, MTD, Smithies, RH, Howard, HM, Tyler, IM, Belousova, EA and Poujol, M 2011a, On the edge: U–Pb, Lu–Hf, and Sm–Nd data suggests reworking of the Yilgarn Craton margin during formation of the Albany–Fraser Orogen: Precambrian Research, v. 187, p. 223–247.

Kirkland, CL, Spaggiari, CV, Wingate, MTD, Smithies, RH, Belousova, EA, Murphy, R and Pawley, MJ 2011b, Inferences on crust–mantle interaction from Lu–Hf isotopes: a case study from the Albany–Fraser Orogen: Geological Survey of Western Australia, Record 2011/12, 25p.

Kirkland, CL, Wingate, MTD and Spaggiari, CV 2012, 194783: metamonzogranite, Newman Rock; Geochronology Record 1027: Geological Survey of Western Australia, 4p.

Kirkland, CL, Wingate, MTD and Spaggiari, CV 2014, 194785: metatonalite, east of Boingaring Rocks; Geochronology Record 1161: Geological Survey of Western Australia, 4p.

Lowry, DC 1970, Geology of the Western Australian part of the Eucla Basin: Geological Survey of Western Australia, Bulletin 122, 201p.

Myers, JS 1985, The Fraser Complex: a major layered intrusion in Western Australia, *in* Professional papers for 1983: Geological Survey of Western Australia, Report 14, p. 57–66.

Myers, JS 1990a, Albany–Fraser Orogen, *in* Geology and mineral resources of Western Australia: Geological Survey of Western Australia, Memoir 3, p. 255–263.

Myers, JS 1990b, Yilgarn Craton — mafic dyke swarms, *in* Geology and mineral resources of Western Australia: Geological Survey of Western Australia, Memoir 3, p. 126–127.

Myers, JS 1995, Geology of the Esperance 1:1 000 000 sheet (2nd edition): Geological Survey of Western Australia, 1:1 000 000 Geological Series Explanatory Notes, 10p.

Myers, JS, Shaw, RD and Tyler, IM 1996, Tectonic evolution of Proterozoic Australia: Tectonics, v. 15, p. 1431–1446.

Nelson, DR 1995, 83667: porphyritic biotite granite, Balladonia Rock; Geochronology Record 76: Geological Survey of Western Australia, 4p.

Nelson, DR, Myers, JS and Nutman, AP 1995, Chronology and evolution of the Middle Proterozoic Albany–Fraser Orogen, Western Australia: Australian Journal of Earth Sciences, v. 42, p. 481–495, doi:10.1080/08120099508728218.

Oorschot, CW 2011, P–T–t evolution of the Fraser Zone, Albany–Fraser Orogen, Western Australia: Geological Survey of Western Australia, Record 2011/18, 101p.

Orion Gold NL 2013, Phase 1 drilling completed at Peninsula Ni–Cu Project, WA: Report to Australian Securities Exchange, 19 December 2013, 12p.

Passchier, C and Trouw, R 1996, Microtectonics: Springer-Verlag, Berlin, 289p.

Smithies, RH, Spaggiari, C, Kirkland, CL, Howard, HM and Maier, WD 2013, Petrogenesis of gabbros of the Mesoproterozoic Fraser Zone: constraints on the tectonic evolution of the Albany–Fraser Orogen: Geological Survey of Western Australia, Record 2013/5, 29p.

Smithies, R, Spaggiari, C, Kirkland, C and Maier, W 2014, Geochemistry and petrogenesis of igneous rocks in the Albany–Fraser Orogen, *in* Albany–Fraser Orogen seismic and magnetotelluric (MT) workshop: extended abstracts *compiled by* CV Spaggiari and IM Tyler: Geological Survey of Western Australia, Perth, WA, Report 2014/6, p. 77–88.

Spaggiari, CV, Bodorkos, S, Barquero-Molina, M, Tyler, IM and Wingate, MTD 2009, Interpreted bedrock geology of the south Yilgarn and central Albany–Fraser Orogen, Western Australia: Geological Survey of Western Australia, Record 2009/10, 84p.

Spaggiari, CV, Kirkland, CL, Pawley, MJ, Smithies, RH, Wingate, MTD, Doyle, MG, Blenkinsop, TG, Clark, C, Oorschot, CW, Fox, LJ and Savage, J 2011, The geology of the east Albany–Fraser Orogen — a field guide: Geological Survey of Western Australia, Record 2011/23, 97p.

Spaggiari, C, Kirkland, C, Smithies, R, Occhipinti, S and Wingate, W 2014c, Geological framework of the Albany–Fraser Orogen, *in* Albany–Fraser Orogen seismic and magnetotelluric (MT) workshop: extended abstracts *compiled by* CV Spaggiari and IM Tyler: Geological Survey of Western Australia, Perth, WA, Record 2014/6, p. 12–27.

Spaggiari, CV, Kirkland, CL, Smithies, RH and Wingate, MTD 2012, What lies beneath — interpreting the Eucla basement, *in* GSWA 2012 Extended Abstracts: promoting the prospectivity of Western Australia: Geological Survey of Western Australia, Record 2012/2, p. 25–27.

Spaggiari, CV, Kirkland, CL, Smithies, RH and Wingate, MTD 2014a, Tectonic links between Proterozoic sedimentary cycles, basin formation and magmatism in the Albany–Fraser Orogen, Western Australia: Geological Survey of Western Australia, Report 133, 63p.

Spaggiari, CV, Occhipinti, SA, Korsch, RJ, Doublier, MP, Clark, DJ, Dentith, MC, Gessner, K, Doyle, MG, Tyler, IM, Kennett, BLN, Costelloe, RD, Fomin, T and Holzschuh, J 2014b, Interpretation of Albany–Fraser seismic lines 12GA-AF1, 12GA-AF2 and 12GA-AF3: implications for crustal architecture, *in* Albany–Fraser Orogen seismic and magnetotelluric (MT) workshop 2014: extended abstracts *compiled by* CV Spaggiari and IM Tyler: Geological Survey of Western Australia, Record 2014/6, p. 28–43.

Spaggiari, CV and Pawley, MJ 2012, Interpreted pre-Mesozoic bedrock geology of the east Albany–Fraser Orogen and southeast Yilgarn Craton, *in* The geology of east Albany–Fraser Orogen — a field guide *edited by* CV Spaggiari, CL Kirkland, MJ Pawley, RH Smithies, MTD Wingate, MG Doyle, TG Blenkinsop, C Clark, CW Oorschot, LJ Fox and J Savage: Geological Survey of Western Australia, Record 2011/23, Plate 1.

Tassell, H and Goncharov, A 2006, Geophysical evidence for a deep crustal root beneath the Yilgarn Craton and Albany–Fraser Orogen, Western Australia, *in* Conference abstracts: Geological Society of Australia; Australian Earth Sciences Convention 2006, Melbourne, Victoria, 2 July 2006, 6p.

Twiss, RJ and Moores, EM 1992, Structural geology (1st edition): WH Freeman, New York, 532p.

Williams, NC 2009, Mass and magnetic properties for 3D geological and geophysical modelling of the southern Agnew–Wiluna greenstone belt and Leinster nickel deposits, Western Australia.: Australian Journal of Earth Sciences, v. 56, no. 8, p. 1111–1142.

Williams, VA and Robertson, W 2011, Final report, Eucla Project E69/2603 for the period 14th May, 2010 to 13th May, 2011; Enterprise Metals Limited: Geological Survey of Western Australia, Statutory mineral exploration report, A90741.

Wingate, MTD, Campbell, IH and Harris, LB 2000, SHRIMP baddeleyite age for the Fraser Dyke Swarm, southeast Yilgarn Craton, Western Australia: Australian Journal of Earth Sciences, v. 47, p. 309–313.

Appendix 1

Detailed description of petrophysical data

Northern Foreland

Specific gravity

Northern Foreland specific gravity samples include mafic and felsic intrusives and two metasedimentary rocks. Felsic intrusives of the Northern Foreland (n = 13) are dominantly granitic gneisses and metagranites and have a unimodal, positively skewed distribution with a low mean specific gravity typical of granitic rocks (Table 1; Fig. 3a). The small sample of mafic intrusives (n = 9) is dominated by metagabbros and metadolerites and has a broad distribution with a high mean specific gravity typical of mafic rocks (Fig. 3a). An outlier in the distribution of mafic intrusives is a serpentinized ultramafic schist of low specific gravity. This sample also has a moderate susceptibility, which in serpentinized rocks is commonly inversely proportional to density (Clark, 1990). A metamorphic iron formation, included in the metasedimentary rocks, has a high specific gravity.

Magnetic susceptibility

Felsic intrusives (n = 21) of the Northern Foreland are dominantly granitic gneisses and metagranites and have an approximately bimodal susceptibility distribution with a subpopulation of non-susceptible samples and a broad subpopulation of moderately susceptible samples (Fig. 3b). Non-susceptible samples include metamonzogranites and metasyenogranites. Moderately susceptible samples include migmatitic and gneissic granites and one sample of metagranodiorite. The four metasedimentary rocks include two samples of conglomerate and a meta-iron formation of moderate susceptibility (Fig. 3b). The small sample of mafic intrusives (n = 10) comprises metagabbros and metadolerites that are dominantly non-susceptible (Fig. 3b). Two samples, a metagabbro and a serpentinized ultramafic schist (of low specific gravity), have moderate susceptibilities (Fig. 3b).

Barren Basin

Specific gravity

Specific gravity data were collected for a small sample of Barren Basin metasedimentary rocks (n = 16) including samples of Woodline Formation, Fly Dam Formation, and undivided Barren Basin metasedimentary rocks. Woodline Formation samples comprise quartz arenites with low specific gravity. Fly Dam Formation samples include semipelitic and psammitic gneisses that have a broad range of specific gravities. Semipelitic gneisses typically have higher specific gravity. The undivided Barren Basin metasedimentary rocks include diverse rock types comprising migmatitic gneiss, metamorphosed iron formation, psammitic gneiss, and a siliciclastic schist. Of these samples, the metamorphosed iron formation and a metasandstone show high specific gravities, with values equivalent to the mafic intrusives. Collectively, the Barren Basin metasedimentary rocks have a broad specific gravity distribution with a moderate mean specific gravity (Fig. 3c).

Magnetic susceptibility

Barren Basin susceptibility samples (n = 30) have a bimodal susceptibility distribution with a population of non-susceptible samples and a broad population of susceptible samples. Samples from the Woodline Formation and the Eddy Suite are non-susceptible. Samples from the Fly Dam Formation and undivided Barren Basin metasedimentary rocks have non-susceptible and susceptible populations (Fig. 3d). The psammitic and quartzofeldspathic gneisses of the Fly Dam Formation have moderate susceptibilities and the semipelitic gneisses are non-susceptible, suggesting the susceptibility of Barren Basin metasedimentary rocks is not determined by the original iron content of the unconsolidated sediments. Of the undivided Barren Basin metasedimentary rocks, samples with moderate susceptibility include both migmatitic gneisses and the metamorphosed iron formation (also with a high specific gravity).

Eastern Biranup Zone

Specific gravity

Eastern Biranup Zone specific gravity samples include felsic, intermediate, and mafic intrusives. The felsic intrusives (n = 40) comprise metamonzogranites, metasyenogranites, and metagranodiorites. Felsic intrusives have a positively skewed distribution with a low mean specific gravity typical of felsic rocks (Fig. 4a). The mafic intrusives (n = 26) are dominated by metagabbros, metadolerites, and metagabbronorites. Mafic intrusives have an approximately normal distribution with a high mean specific gravity typical of mafic rocks (Fig. 3e). The small sample of intermediate intrusives (n = 7), most of which are metadiorites, have a normal distribution with a moderate specific gravity.

Magnetic susceptibility

Eastern Biranup Zone susceptibility samples include felsic, intermediate, and mafic intrusives. Felsic intrusives (n = 67), which include metamonzogranites, metasyenogranites, and metagranodiorites, contain a dominant subpopulation of non-susceptible samples and a

smaller subpopulation of moderately susceptible samples (Fig. 3f). Felsic intrusives of the eastern Biranup Zone cannot be discriminated by susceptibility.

Mafic intrusives (n = 33) include metagabbros, metadolerites, and gabbronorites. Like the felsic intrusives, they also show a bimodal susceptibility distribution dominated by the subpopulation of non-susceptible samples. Moderately susceptible samples are dominantly metadolerites, although they also include a serpentinite and two mafic gneisses (an amphibolitic gneiss and a mafic gneiss). In this dataset, samples of metagabbro and metagabbronorite are non-susceptible. The small sample of intermediate intrusives (n = 7) is dominantly diorites; all, except for one sample, are non-susceptible (Fig. 3g,h).

The relatively small numbers of felsic and mafic samples that are susceptible show similar distributions and similar peak susceptibilities. Given this similarity it is not possible to discriminate moderately susceptible felsic intrusives from moderately susceptible mafic intrusives.

Nornalup Zone and Recherche Supersuite

Specific gravity

Nornalup Zone samples (including Paleoproterozoic granitic gneisses and Recherche Supersuite samples) are dominated by felsic and intermediate intrusives. Felsic specific gravity samples (n = 21) form a normal distribution with a low mean specific gravity (Fig. 3i). The upper tail of the specific gravity distribution is occupied by mafic intrusives and migmatitic gneisses (including samples from Afghan and Nanambinia Rock).

Magnetic susceptibility

Nornalup Zone and Recherche Supersuite susceptibility samples include felsic intrusives (n = 62), intermediate intrusives (n = 23), and mafic intrusives (n = 4). Felsic intrusive samples include metamonzogranites, metagranodiorites, and granitic gneisses and show a bimodal susceptibility distribution dominated by a subpopulation of highly susceptible samples (Fig. 3j). Because highly susceptible samples dominate, felsic intrusives have a high mean susceptibility (Table 1). This dataset contains two samples of known Paleoproterozoic age; both are migmatitic gneisses with moderate and high susceptibilities.

Fraser Zone

Specific gravity

Fraser Zone specific gravity samples are dominantly mafic intrusives although they also include felsic intrusives and metasedimentary rocks. Felsic intrusives (n = 10) are dominated by metasyenogranites and metamonzogranites and have a low mean specific gravity typical of granites (Fig. 3k). Metasedimentary rocks (n = 18), dominantly psammitic and semipelitic gneisses, form an approximately normal distribution with large variability and a moderate mean specific gravity, higher than mean specific gravity for felsic intrusives (Fig. 3k). Mafic intrusives (n = 60) are dominantly metagabbro although they also include amphibolite and mafic granulite, and form a negatively skewed distribution with a high mean specific gravity typical of mafic rocks (Fig. 3l). The lower tail of the distribution is occupied by hybridized mafic intrusives and the upper tail by amphibolites.

Magnetic susceptibility

Felsic intrusive samples (n = 20) include metagranites, metasyenogranites, and metamonzogranites. Susceptibility is bimodally distributed with a small subpopulation of non-susceptible samples and a larger subpopulation of moderately susceptible samples (Fig. 3m). Because susceptible samples dominate, felsic intrusives have a moderate mean susceptibility, higher than felsic intrusives of the eastern Biranup Zone (Table 1).

Metasedimentary rock samples (n = 26) comprise psammitic and pelitic gneisses, undivided metasedimentary rocks and minor calc-silicate gneisses. Metasedimentary rock susceptibilities are bimodally distributed with a subpopulation of non-susceptible samples and a dominant subpopulation of moderately susceptible samples (Fig. 3m). Because moderately susceptible samples dominate, metasedimentary rocks have a moderate mean susceptibility (Table 1). Interestingly, semipelitic and psammitic gneisses both contain similar numbers of susceptible and non-susceptible samples. Semipelitic samples, because of their higher original iron content, which is a major control on the capacity of sedimentary rocks to produce magnetite, might be expected to have a higher susceptibility than psammitic gneisses (Grant, 1985).

Mafic intrusives (n = 101) are dominated by metagabbroic rocks and include samples of amphibolite and mafic granulite. Mafic intrusives form a bimodal distribution with a population of non-susceptible samples and a slightly larger population of moderately susceptible samples (Fig. 3n). Amphibolite to granulite facies metamorphism of metagabbro samples has likely had a significant influence on the magnetic properties. Amphibolite facies metamorphism of mafic rocks typically produces heterogeneous magnetic properties and granulite facies metamorphism typically produces secondary magnetite (Clark, 1997).

The magnetically susceptible subpopulations of mafic and felsic intrusives and metasedimentary rocks show considerable overlap. Susceptible mafic intrusives show a broader distribution and slightly higher susceptibility than felsic intrusives, possibly caused by an increase in susceptibility with the increase in mafic, iron-bearing minerals (Clark, 1997). Susceptible metasedimentary rocks also have a slightly higher susceptibility than felsic intrusives. These differences, however, are not sufficient to discriminate susceptible mafic, felsic, and metasedimentary rocks.

Esperance Supersuite

Specific gravity

The felsic intrusives sampled from the Esperance Supersuite (n = 3) show low mean specific gravities that range from 2.613 to 2.722 (Fig. 3o).

Magnetic susceptibility

Esperance Supersuite susceptibility samples are dominantly felsic intrusives although they also include a small number of intermediate and mafic intrusive samples. Felsic intrusives, dominantly monzogranites, have a unimodal distribution with a high mean susceptibility (Fig. 3p). Mafic and intermediate intrusives occupy the upper end of the felsic intrusive distribution and include an intensely susceptible diorite intersected by Enterprise Metals NL at their Balladonia prospect. Intensely magnetic, circular anomalies in the southeast of the study area are interpreted as diorite.

Appendix 2

Details of aeromagnetic surveys used in this study

Survey name	*Data source*	*Line spacing (m)*	*Line direction (°)*
Heron–Karonie	Open file	50	90
Fraser Range Area 2	Open file	100	90
Fraser Range Area 1	Open file	100	90
Balladonia West Tempest	Open file	200	50
Naretha Eucla Basin 3	Government	200	90
Area_h-Fraser Range	Open file	200	90
Southern Hills	Open file	200	116
Norseman	Open file	200	135
Eucla Basin 6 Onshore	Government	200	180
Yardilla	Open file	250	138
Lake River	Open file	250	140
Central Fraser	Open file	300	90
Southern Fraser	Open file	300	90
Balladonia	Government	400	90
Yilgarn compilation	Government	200	90
Balladonia	Confidential	100	90

This study uses the integrated analysis of aeromagnetic, gravity and geological data to suggest map and section-view interpretations of the crustal architecture in the Proterozoic east Albany–Fraser Orogen. The diverse magnetic properties in the study area, in particular in the Fraser and Nornalup Zones, allow the regional structural trends in the Fraser Zone and the regional structural and magmatic trends in the Nornalup Zone, to be mapped from aeromagnetic images. The Fraser Zone forms a distinct Bouguer gravity high making it possible to determine the section-view geometry of this zone using gravity and magnetic forward modelling. Two crustal-scale forward models, constrained by aeromagnetic and gravity image interpretation, and petrophysical and outcrop data, were constructed along northwest-trending profiles that traverse the east Albany–Fraser Orogen. The Fraser Zone was modelled with the median specific gravity of the Fraser Zone petrophysical samples (3 g/cm^3) and is interpreted as near-triangular and extending to depths of 12.4 km in profile 1 and 15.4 km in profile 2. The long wavelength Bouguer gravity anomaly to the southeast of the Fraser Zone, in profile 2, is interpreted as a subhorizontal body of mafic–ultramafic material located in the middle crust. When attributed the same density as the Fraser Zone (3 g/cm^3), this body has a maximum thickness of 14.5 km. This mid-crustal body is possibly associated with the intrusion of the Fraser Zone gabbros and granites (1305–1290 Ma) during Stage I of the Albany–Fraser Orogeny, given that this is the only regional mafic intrusive event recognized in the Albany–Fraser Orogen.

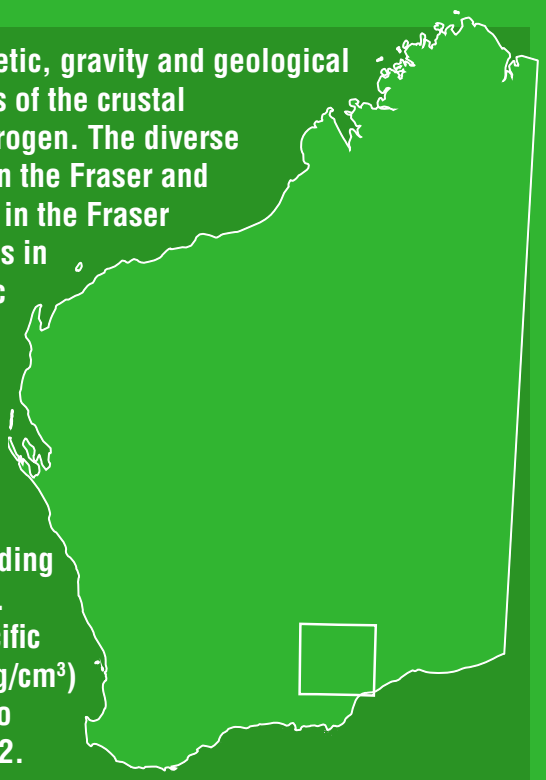

Further details of geological products and maps produced by the Geological Survey of Western Australia are available from:

Information Centre
Department of Mines and Petroleum
100 Plain Street
EAST PERTH WA 6004
Phone: (08) 9222 3459 Fax: (08) 9222 3444

www.dmp.wa.gov.au/GSWApublications

BRISBOUT

DETERMINING CRUSTAL ARCHITECTURE IN THE EAST ALBANY–FRASER OROGEN FROM GEOLOGICAL AND GEOPHYSICAL DATA

REPORT 152